Recirculatory Modeling in Man using Indocyanine Green

Marije Reekers

The studies described in this thesis were performed at the Department of Anesthesiology of the Leiden University Medical Center, Leiden, The Netherlands.

Cover photo by Chris Goodroe
Cover design by Jan Ketting
Layout by Ad Vletter
Printed by Mostert & van Onderen, Leiden
ISBN: 978-90-9026477-6

The printing of this thesis was financially supported by the Department of Anesthesiology of the Leiden University Medical Center, Leiden, The Netherlands

Recirculatory Modeling in Man using Indocyanine Green

PROEFSCHRIFT

ter verkrijging van
de graad van Doctor aan de Universiteit Leiden,
op gezag van Rector Magnificus prof. mr. P.F. van der Heijden,
volgens besluit van het College voor Promoties
te verdedigen op donderdag 19 januari 2012
klokke 16:15 uur

door

Marije Reekers
geboren te Oegstgeest
in 1971

Promotiecommissie:

Promotor:	Prof. dr. A. Dahan
Co-promotores:	Dr. F. Boer Dr. J. Vuyk
Overige leden:	Prof. dr. L.P.H.J. Aarts Prof. dr. M. Weiss, Martin Luther University Halle-Wittenberg, Halle (Saale), Germany Prof. dr. C.A.J. Knibbe

The unknown

As we know,
There are known knowns.
There are things we know we know.
We also know
There are known unknowns.
That is to say
We know there are some things
We do not know.
But there are also unknown unknowns,
The one's we don't know
We don't know.

February 12, 2002
Department of defense news briefing.
Donald Rumsfeld, minister of defense, USA

Aan mijn ouders Joke en Paul
Voor Paul, Birgit en Floris

Contents

1

Introduction and Outline of the Thesis

Introduction

In the clinical field of anesthesia, the sciences of physiology and pharmacology are almost touchable. With knowledge of the mechanisms involved in the behavior of anesthetic agents in a continuously changing environment, the anesthesiologist provides the best possible conditions for the performance of therapeutic and diagnostic procedures while safeguarding the patient.

The dose-concentration relationship of a drug, known as pharmacokinetics (PK), can be expressed in terms of bioavailability, absorption, distribution, metabolism and elimination. In anesthesia the preferred route of administration of a drug is intravenous, thus bypassing processes involved in the transfer of drug from the intestinal tract into the bloodstream. As a result, the reported pharmacokinetic profiles of anesthetic agents typically include the drug's distribution and elimination half-lives, volumes of distribution, and metabolic and distributional clearances. The importance of these pharmacokinetic parameters varies with the different phases of the anesthetic procedure. For example, during induction of anesthesia the initial distribution is affected by cardiac output and pulmonary uptake, while drug clearance may be less important. During maintenance of anesthesia, especially for prolonged procedures, drug elimination may gain clinical importance with time.

The studies in this thesis focus on the pharmacokinetics and pharmacodynamics (PD, the concentration-effect relationship) of anesthetic agents during induction of anesthesia. Since the pharmacology of the induction of anesthesia is still poorly understood, this translates in an often troubled induction phase. Induction of anesthesia is associated with frequent underdosing causing insufficient analgesia or awareness, but also undesirable overdosing causing hemodynamic and respiratory depression. In general the pharmacology of induction of anesthesia is described using compartmental modeling, despite the knowledge that this methodology describes the dose-concentration relationship at induction inaccurately.

In this thesis we looked for better ways to describe the early phase PK and PD of agents used in anesthesia through recirculatory modeling. As indocyanine green plays an important role in recirculatory modeling, the first chapters deal with the analysis and modeling of ICG in blood. The last chapters of this thesis deal with the recirculatory PK and PD of rocuronium, a muscle relaxant, and propofol, a hypnotic agent.

Outline of the thesis

The studies presented in this thesis were aimed at answering the following questions;

1. Is it possible to adequately measure ICG transcutaneously for determination of hemodynamic parameters?
2. Is it possible to adequately determine the plasma disappearance rate of ICG in a non-invasive manner and what is the range of this parameter in a “normal” population?
3. Is it possible to determine a circulatory model for rocuronium in humans, based on intravascular and diffusion kinetics, using ICG as a marker?
4. Can a recirculatory model based on ICG be developed for propofol in humans and what can be said about the role of the lung in the disposition and elimination of propofol?
5. How does the implementation of a recirculatory PK model for propofol reflect on the k_{e0} of propofol and BIS in the early phase after bolus administration, using PK-PD modeling?

In **chapter 2** a review is provided on pharmacokinetic modeling of anesthetic drugs. Besides a general overview of the various methods of pharmacokinetic modeling, the recirculatory model which has been described by Kuipers et al. for the muscle relaxant rocuronium, using ICG as intravascular marker, is discussed in detail.

In **chapter 3** a study is presented in which the accuracy of the non-invasive transcutaneous measurement of ICG by the DDG-2001 is discussed. Two different probes were used to determine the concentration of ICG and the derived hemodynamic parameters cardiac output, central blood volume and total blood volume. These measurements were compared to the simultaneous measurements of ICG in arterial blood, and the derived hemodynamic parameters based on arterial measurements, acquired by rapid sampling.

In **chapter 4** the findings are presented concerning the accuracy of the non-invasive measurement of the ICG-PDR versus arterial measurement of ICG, studied in the population described in chapter 3. As data on ICG-PDR measured transcutaneously in a population without liver failure is scarce, this has been explored. The implication of these findings upon clinical decision making in the treatment of patients, subject to imminent liver failure is discussed.

In **chapter 5** a circulatory pharmacokinetic model for rocuronium is presented, based on intravascular and diffusion kinetics. The data upon which this model is based were the same as used for the model described in chapter 2. The model applying diffusion kinetics further explores the distribution into the interstitial space and its relationship with cardiac output.

In **chapter 6** a recirculatory pharmacokinetic model for propofol in humans is presented. The model describes the distribution, recirculation and elimination of propofol, based on ICG pharmacokinetics, after the administration of an induction bolus dose. The role of the lung in the distribution and elimination of propofol is discussed.

In **chapter 7** the recirculatory PK model for propofol is implemented in a PK-PD model for propofol. Effect is measured by BIS, which is transferred at high frequency from the A-2000 monitor. Two different PD models are implemented in the PK-PD model to explore the effect on the k_{e0} and its correlation with flow.

2

Basic Concepts of Recirculatory Pharmacokinetic Modeling

Marije Reekers, Fred Boer and Jaap Vuyk

Department of Anesthesiology, Leiden University Medical Center, Leiden, The Netherlands

Advances in Experimental Medicine and Biology. 2003;523:19-26.

Introduction

The science of pharmacokinetic analysis embodies the description of the time-dependant concentration changes of a drug. Pharmacokinetic models may be used to predict the behavior of the drug in individuals, preferably under various circumstances. In the practice of anesthesia pharmacokinetics can be studied on the work floor. Differences in pharmacokinetics between individuals are observed on a daily basis. Factors responsible for the inter-individual variability are being studied extensively and more data become available in time. From these data the significance of demographic factors such as age and gender become increasingly apparent. Other factors like weight or lean body mass may substitute parameters for physiologically based variations in pathways of distribution and elimination. Obesity e.g. may be considered as a disproportionate increase of adipose tissue mass. Peripheral blood flow must increase to supply this extra tissue. As organ-specific blood flow remains equal, cardiac output will increase. The surplus of fatty tissue will act as an extra depot for lipid-soluble drugs like thiopental. As a consequence, peak-concentrations are expected to decrease, whereas the terminal half-life and steady state volume of distribution may increase.[1] Physiological parameters such as cardiac output, flow and tissue distribution have a more direct relationship with pharmacokinetic parameters like distribution volumes and clearances. Inclusion of a parameter like cardiac output into a pharmacokinetic model may improve the accuracy of the model, especially with respect to fast acting drugs like intravenous anesthetics. The influence of changes in cardiac output on the pharmacokinetics of anesthetic agents is under research. The largest impact of a change in the cardiac output on the behavior of drugs can be expected in compounds showing a flow-limited distribution and/or clearance such as thiopental[1], lidocaine[2], alfentanil[3] and propofol.[4] Pulmonary uptake may also be of influence on the early-phase distribution of a substance. These influences will be described in more detail further on in this chapter.

Another factor of influence on drug behavior is the method of administration. A rapid intravenous bolus injection will be best characterized by a set of pharmacokinetic parameters different from parameters derived after a prolonged intravenous infusion, as is used in devices for target controlled infusion (TCI).[5,6] Prolonged infusion of a drug with a rapid clearance and extensive distribution, such as propofol, may be better characterized by a 3-compartment model, whereas for a bolus injection a 2-compartment model may suffice. In a study published by Schnider and colleagues, is shown that propofol concentrations after a bolus injection were not adequately described

by the pharmacokinetics derived from blood samples taken during a propofol infusion in the same patients.[7] The drug concentrations during the first 10 minutes after a bolus injection were significantly biased with an overestimation at minute 2 and 4 followed by a subsequent underestimation of the actual propofol concentration. Selecting the right pharmacokinetic model for the right type of administration and phase of interest (early-phase or steady-state) is important.

Selecting a pharmacokinetic model

A large variety of pharmacokinetic models exists ranging from very abstract to naturalistic.[8] The commonly used models are linear and time-invariant (Figure 1). Empirical models describe the relationship between input, the drug dose, and output, the plasma concentration, in a mathematical form without reference to a physiological or pharmacological explanation. Empirical models treat the human body as a black box. The key to this method is the fitting procedure. Compartmental models are most frequently applied, consisting of 2- or 3-compartments. These compartments may have a physiological (plasma, tissue) basis but are derived purely mathematically.

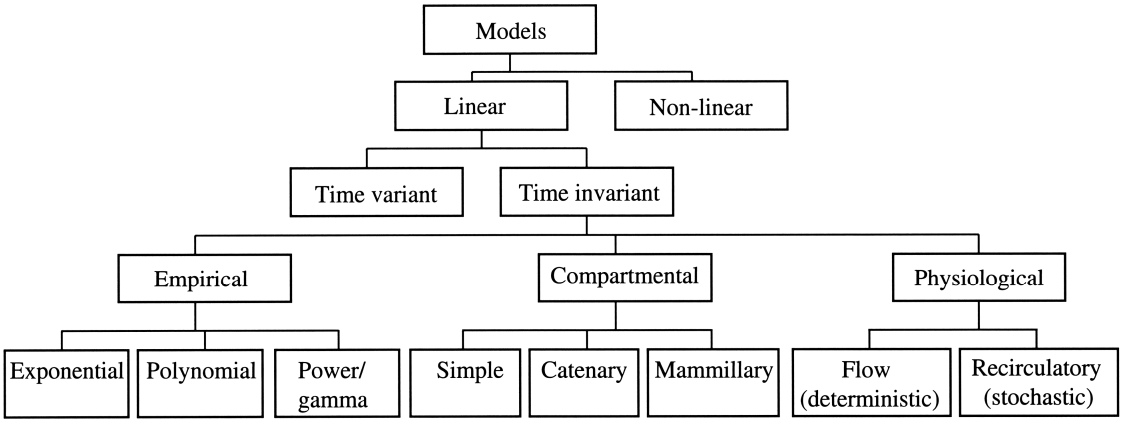

Figure 1 A taxonomy of pharmacokinetic models. Reproduced from J. Kuipers, Pharmacokinetic modelling of anaesthetics: The role of cardiac output. PhD thesis, with permission.

Compartmental models are based on the assumption of instantaneous mixing of the drug after a bolus injection within the central compartment. Distribution and elimination occur solely from the central compartment. Other

compartments serve as “peripheral” compartments, with “slow” equilibration constants, from which the drug is redistributed. By assuming complete initial mixing within the central compartment, which is actually not the case, the compartmental model becomes inaccurate when pulmonary uptake or the process of initial mixing in the first minutes after injection are studied.

The development of recirculatory models

In the process of the pharmacokinetic evaluation of concentration-time data, analysis is frequently performed by fitting data to a 2- or 3-compartment model. However, for some anesthetic agents this may not be the best model suited. More and more drugs are introduced that exhibit a very rapid initial distribution, resulting in the propagation of a clinical effect before complete mixing has occurred. Ignoring the mechanism of initial mixing may lead to significant deviations in the estimation of the volume of the central compartment.[9] Other drugs such as fentanyl, meperidine[10], sufentanil[11], propofol[12,13], ketamine[14] and lidocaine[15,16] are known to undergo substantial pulmonary uptake. Furthermore, in fast acting compounds the distribution appears to be flow dependant.[17] Including a flow parameter such as cardiac output into the model is therefore strongly desired.[1] Taking these factors into consideration, one may suggest that the examination of early phase pharmacokinetics based exclusively on conventional compartment modeling, may be insufficient[18] and provide inaccurate data.

One solution to the issues mentioned is the system dynamics approach as described by van Rossum.[19] This approach provides a different method of modeling by calculation of so-called body transfer functions. The transport function of the body (closed loop) is considered a stochastic process characterized by a density function of total body residence times. The relationship between the body transit time distribution and the body residence distribution is determined by the feedback-loop arrangement, the cardiac output and the extraction ratio. The cardiac output is included as an important hemodynamic variable in this model.[20]

Other models allowing recirculation have been introduced, constructed as catenary compartmental models with different compartments linked in a serial manner. In a study by Avram and colleagues, this model of concurrent disposition of ICG and thiopental allowed to analyze intravascular mixing by computing the recirculation of the intravascular marker ICG, combined with a

peripheral compartment for thiopental.[21] Further development led to recirculatory models using ICG as a marker for the intravascular compartment.[22] Finally, a combination of recirculatory compartments and peripheral slow and fast tissue compartments was developed that made the recirculatory model more physiologically based.[23]

For any drug the complete recirculatory model can be built on the basis of a model for ICG. Since the distribution of ICG is limited to the intravascular space, the ICG model describes the passage through the central and peripheral blood compartments. The central compartments are by definition located between the venous point of injection and the arterial point of sampling. The central intravascular part of the model, representing the flow through the heart and lungs, is best described by two compartments. Hereby, modeling of pulmonary uptake and redistribution is allowed. Since the mean transit time of one compartment is shorter that that of the other compartment, they are identified as the fast central and the slow central compartment. Peripheral compartments are described similarly. The compartments for ICG are considered to represent the effect of dispersion of ICG in the vascular tree. In the model this dispersion is simulated by so-called tanks-in-series, being very small consecutive compartments from which the drug is cleared exponentially. Parallel pathways can differ in the number of tanks in series and the proportion of the blood flow to the respective compartments.

For the test drug peripheral tissue compartments are added to the ICG model. These tissue compartments are similar to the compartments of other catenary models. The tissue compartments are coupled to the peripheral vascular compartments such that the slow vascular compartment is coupled to the slow tissue compartment. If the drug undergoes significant pulmonary uptake a pulmonary tissue compartment may be added[21] (see figure 2).

Recirculatory modeling in practice

Recirculatory models for different compounds such as thiopental[21], halothane[24], alfentanil[3,25], propofol[12], and rocuronium[26] have been described. As a marker for the intravascular compartment ICG was used. To adequately measure the recirculation of ICG the sampling frequency must be high; the process of initial mixing is complete within 5 minutes. The quality of model fitting is therefore highly dependent on the amount of blood samples taken within the first minutes after the bolus dose administration. From these samples the first-pass

concentration curve of ICG can be determined, described by two parallel pathways consisting of Erlang functions, represented by a number of tanks in series. A representation of such a model is depicted in figure 2.

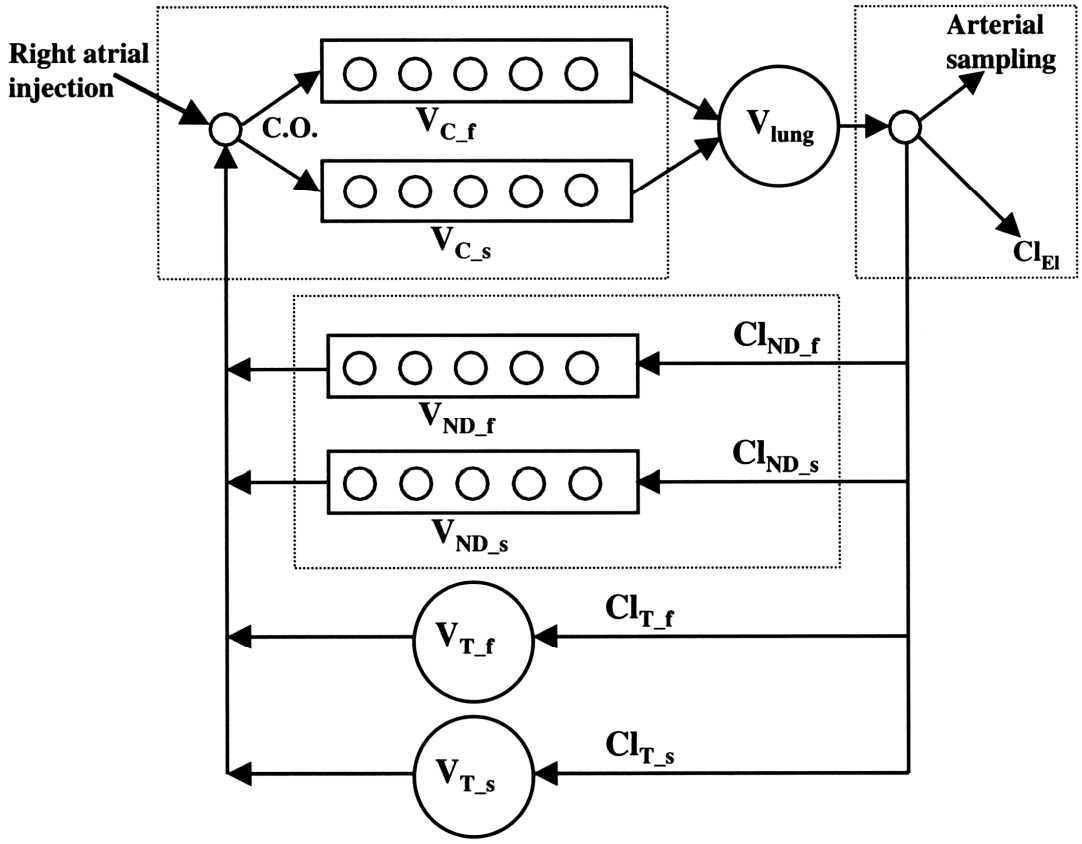

Figure 2. Recirculatory pharmacokinetic model used for analysis of indocyanine green and simultaneously injected drug (modified from Krejcie et al.[23]). The parts in the dashed boxes represent the recirculatory model for indocyanine green, the intravascular part of the model. These intravascular compartments are represented by a rectangle with five compartments, but the actual number of compartments may vary and has no physiological background. The intravascular model consists of a central part, receiving all of the cardiac output, divided in a slow (V_{C_s}) and a fast (V_{C_f}) central compartment and a peripheral part, divided in a slow (V_{ND_s}) and a fast (V_{ND_s}) peripheral compartment. The simultaneously injected drug distributes into organs and therefore, 3 tissue compartments are added to the intravascular indocyanine green model; the lung compartment (V_{lung}), a slow (V_{T_s}) and a fast (V_{T_f}) peripheral tissue compartment. The sum of the peripheral clearances equals the cardiac output. Reproduced from J. Kuipers, Pharmacokinetic modelling of anaesthetics; The role of cardiac output. PhD thesis, with permission.

The parameters derived from this model can now be combined with peripheral compartments to represent distribution and elimination as described above. Constructing such a model is possible using the SAAM II program (SAAM institute, University of Washington, Seattle, USA). It consists of a numerical mode and compartmental mode. The latter allows for the construction of a model on a canvas where the program attaches the formulas. The solver function of the program computes the parameters in an iterative way with fixed or relative weights (SAAM II manual). The statistics performed on the parameters are calculation of the standard deviation, fractional standard deviation and representation of a correlation matrix, covariance matrix or the residual sum of squares, including the Akaike criterion. Other statistical tests described are the one sample runs test to check for random scatter around the fit. The group of Krejcie uses the IDENT2 program to check for identifiability and estimability of the parameters.[27]

Results

As an example of differences in pharmacokinetic outcome using conventional 2-compartment modeling compared to recirculatory modeling, a short representation will be given of the results from a study performed by Kuipers and colleagues regarding the pharmacokinetics of rocuronium in patients.[26] In this study a recirculatory model has been used based on arterial ICG concentrations collected with a rapid sampling device. In addition, cardiac output was determined by dividing the dose of ICG by the area under the first-pass ICG concentration-time curve. Rocuronium had been selected as a model drug because of its fast onset of action. The effect of rocuronium could be quantified easily and reliably and be expected to be linked to cardiac output based on its dependency on the blood flow through the muscles. In addition, the effect measurements were included in a PK-PD model to determine the k_{e0} of rocuronium using compartmental modeling parameters and recirculatory modeling parameters. The recirculatory model, used to analyze indocyanine green and rocuronium pharmacokinetics and the rocuronium pharmaco-dynamics, was built like the model in figure 2, with the exclusion of the lung compartment and with the addition of an effect compartment placed after the arterial sampling site. The effect compartment was not included in the recirculatory system. The sum of the clearances through the parallel fast and slow non-distributive circuits for ICG equals the cardiac output. Rocuronium data were evaluated by addition of a fast and slow peripheral distributive compartment to the ICG model. The ratio between fast and slow peripheral

clearances was set equal for ICG and rocuronium, but the absolute values were allowed to differ. The pharmacokinetic data could well be fitted using recirculatory pharmacokinetics, whereas the two-compartment model showed large uncertainty regarding the drug behavior in the first minutes. A pharmacokinetic-pharmacodynamic analysis could be done using recirculatory pharmacokinetics as well. Some of the parameters determined by the recirculatory model and the two-compartment model can be seen in table 1.

Table 1 Pharmacokinetic and pharmacokinetic-dynamic parameters of rocuronium determined by a recirculatory model and 2-compartment model (mean and SD). For abbreviations see legend of figure 2. The unit of k_{e0} is (min^{-1}), of EC_{50} is ($\mu g.L^{-1}$)

	V_C	V_{ss}	V_T	Cl_{EL}	V_1	V_2	Cl_{12}	K_{e0}	EC_{50}
Recirculatory									
Mean	1.52	17.29	14.77	0.45				0.129	876
SD	0.40	4.82	4.85	0.11				0.036	118
2-compartment									
Mean		10.50		0.50	6.76	3.73	0.43	0.239	684
SD		3.54		0.14	1.69	1.98	0.20	0.104	97

Reproduced from J. Kuipers, Pharmacokinetic modelling of anaesthetics: the role of cardiac output. PhD thesis, with permission.

The results showed correlation between cardiac output and the central volume of ICG and rocuronium. The clearances correlated significantly with cardiac output as well. The values of k_{e0} and EC_{50} obtained with the compartmental model were significantly different from the values estimated with the recirculatory model. The k_{e0} determined using the compartmental model was nearly double and the EC_{50} approximately 22% lower compared to those determined on the basis of the recirculatory approach. The k_{e0} of rocuronium showed correlation with cardiac output, although the correlation estimated from the recirculatory model was much stronger. This could well be explained by the difference in accuracy of fitting in the first minutes. It is known that by selecting a model, i.e. a 2- or 3-compartment model, the initial drug concentration may be either seriously underestimated or overestimated. In contrast, the recirculatory model was capable of accurately describing the front-end kinetics.[28] The correlation between cardiac output and effect site-equilibration time could be observed clinically as well. The patient with the lowest cardiac

output (2.4 $L.min^{-1}$) showed 90% twitch depression after 2.5 minutes, whereas the patient with the highest cardiac output (5.0 $L.min^{-1}$) needed only 1.5 minutes for near-complete relaxation. In the context of a rapid sequence induction, this means that not only the dose of muscle relaxant, but also the physiological status of the patient needs consideration. This supports the need for more accurate characterization of pharmacokinetic and pharmacodynamic parameters in the early phase when using fast-acting agents.

Conclusion

With the introduction of an increasing number of compounds exhibiting a rapid, flow dependant distribution and a rapid onset of effect before complete mixing, it becomes increasingly important to look at alternatives in pharmacokinetic modeling. At present, the most frequently used approach is the conventional 2- or 3- compartment model. This model is based on the assumption of complete mixing in the central compartment upon bolus-injection of the compound. In this model recirculation, flow-dependant distribution or pulmonary uptake are not taken into account. The introduction of recirculatory modeling as described by Krejcie et al.[23] provides a tool to model data in these situations. Disadvantages of recirculatory modeling are innate to the small time frame in which the processes take place. First of all, it is necessary to administer a marker for the intravascular space (ICG) in combination with the compound of interest. Secondly, in order to have sufficient data to model the first-pass circulation of ICG, the sampling frequency must be high; every few seconds. Besides the practical implications of this methodology, it implies that the quality of the fit is highly dependant on the number of data points within the first 3 minutes. Accurate modeling of early-phase pharmacokinetics is very important, since the better the understanding of the behavior of a drug in a "standard" situation (read "healthy subject"), the easier to predict the outcome when parameters change. Extending the knowledge in this field may lead to a better prediction of drug behavior in e.g. elderly patients or in patients with an altered cardiovascular state. The development of techniques to measure cardiac output in a non- or minimal invasive way, preferably on a beat-to-beat basis, may lead to fine-tuning of the pharmacokinetics of intravenous anesthetics on a patient-basis. In addition, it has also been shown that recirculatory modeling can be used in pharmacokinetic-pharmacodynamic modeling. This may lead to differences in the estimation of k_{e0} and EC_{50} compared to conventional approaches, as has been shown in the paragraph above.

In conclusion, recirculatory modeling may produce a more accurate prediction of actual blood and tissue drug concentrations, especially for rapid acting agents during rapid changes in concentration.

References

1. Wada DR, Bjorkman S, Ebling WF, et al. Computer simulation of the effects of alterations in blood flows and body composition on thiopental pharmacokinetics in humans. Anesthesiology 1997;87:884-99.

2. Kuipers JA, Boer F, de Roode A, et al. Modeling population pharmacokinetics of lidocaine: should cardiac output be included as a patient factor? Anesthesiology 2001;94:566-73.

3. Henthorn TK, Krejcie TC, Avram MJ. The relationship between alfentanil distribution kinetics and cardiac output. Clin Pharmacol Ther 1992;52:190-6.

4. Ludbrook GL, Upton RN. A physiological model of induction of anaesthesia with propofol in sheep. 2. Model analysis and implications for dose requirements. Br J Anaesth 1997;79:505-13.

5. Vuyk J, Engbers FH, Burm AG, et al. Performance of computer-controlled infusion of propofol: an evaluation of five pharmacokinetic parameter sets. Anesth Analg 1995;81:1275-82.

6. Gepts E, Camu F, Cockshott ID, Douglas EJ. Disposition of propofol administered as constant rate intravenous infusions in humans. Anesth Analg 1987;66:1256-63.

7. Schnider TW, Minto CF, Gambus PL, et al. The influence of method of administration and covariates on the pharmacokinetics of propofol in adult volunteers. Anesthesiology 1998;88:1170-82.

8. Tucker GT. Pharmacokinetic models - different approaches. In: Stoeckel H, ed. Quantitation, Modelling and Control in Anaesthesia, Stuttgart: Georg Thieme Verlag, 1985:54-63.

9. Chiou WL. Potential pitfalls in the conventional pharmacokinetic studies: effects of the initial mixing of drug in blood and the pulmonary first-pass elimination. J Pharmacokinet Biopharm 1979;7:527-36.

10. Roerig DL, Kotrly KJ, Vucins EJ, et al. First pass uptake of fentanyl, meperidine, and morphine in the human lung. Anesthesiology 1987;67:466-72.

11. Boer F, Bovill JG, Burm AG, Mooren RA. Uptake of sufentanil, alfentanil and morphine in the lungs of patients about to undergo coronary artery surgery. Br J Anaesth 1992;68:370-5.

12. Kuipers JA, Boer F, Olieman W, et al. First-pass lung uptake and pulmonary clearance of propofol: assessment with a recirculatory indocyanine green pharmacokinetic model. Anesthesiology 1999;91:1780-7.

13. He YL, Ueyama H, Tashiro C, et al. Pulmonary disposition of propofol in surgical patients. Anesthesiology 2000;93:986-91.

14. Henthorn TK, Krejcie TC, Niemann CU, et al. Ketamine distribution described by a recirculatory pharmacokinetic model is not stereoselective. Anesthesiology 1999;91:1733-43.

15. Krejcie TC, Avram MJ, Gentry WB, et al. A recirculatory model of the pulmonary uptake and pharmacokinetics of lidocaine based on analysis of arterial and mixed venous data from dogs. J Pharmacokinet Biopharm 1997;25:169-90.

16. Post C, Lewis DH. Displacement of nortriptyline and uptake of 14C-lidocaine in the lung after administration of 14C-lidocaine to nortriptyline intoxicated pigs. Acta Pharmacol Toxicol (Copenh) 1979;45:218-24.

17. Upton RN, Huang YF. Influence of cardiac output, injection time and injection volume on the initial mixing of drugs with venous blood after i.v. bolus administration to sheep. Br J Anaesth 1993;70:333-8.

18. Vaughan DP, Hope I. Applications of a recirculatory stochastic pharmacokinetic model: limitations of compartmental models. Journal of Pharmacokinetics and Biopharmaceutics 1979;7:207-25.

19. van Rossum JM, de Bie JE, van Lingen G, Teeuwen HW. Pharmacokinetics from a dynamical systems point of view. J Pharmacokinet Biopharm 1989;17:365-92.

20. Weiss M. Hemodynamic influences upon the variance of disposition residence time distribution of drugs. J Pharmacokinet Biopharm 1983;11:63-75.

21. Avram MJ, Krejcie TC, Henthorn TK. The relationship of age to the pharmacokinetics of early drug distribution: the concurrent disposition of thiopental and indocyanine green. Anesthesiology 1990;72:403-11.

22. Krejcie TC, Henthorn TK, Shanks CA, Avram MJ. A recirculatory pharmacokinetic model describing the circulatory mixing, tissue distribution and elimination of antipyrine in dogs. J Pharmacol Exp Ther 1994;269:609-16.

23. Krejcie TC, Henthorn TK, Niemann CU, et al. Recirculatory pharmacokinetic models of markers of blood, extracellular fluid and total body water administered concomitantly. J Pharmacol Exp Ther 1996;278:1050-7.

24. Avram MJ, Krejcie TC, Niemann CU, et al. The effect of halothane on the recirculatory pharmacokinetics of physiologic markers. Anesthesiology 1997;87:1381-93.

25. Kuipers JA, Boer F, Olofsen E, et al. Recirculatory and compartmental pharmacokinetic modeling of alfentanil in pigs: the influence of cardiac output. Anesthesiology 1999;90:1146-57.

26. Kuipers JA, Boer F, Olofsen E, et al. Recirculatory pharmacokinetics and pharmacodynamics of rocuronium in patients: the influence of cardiac output. Anesthesiology 2001;94:47-55.

27. Jacquez JA, Perry T. Parameter estimation: local identifiability of parameters. Am J Physiol 1990;258:E727-E736.

28. Krejcie TC, Avram MJ. What determines anesthetic induction dose? It's the front-end kinetics, doctor! Anesth Analg 1999;89:541-4.

3

Cardiovascular Monitoring by Pulse Dye Densitometry or Arterial Indocyanine Green Dilution

Marije Reekers, Mischa J.G. Simon, Fred Boer, René A.G. Mooren, Jack W. van Kleef, Albert Dahan, and Jaap Vuyk

Department of Anesthesiology, Leiden University Medical Center, Leiden, The Netherlands

Anesthesia & Analgesia 2009:109: 441-6.

Introduction

Noninvasive cardiac output (CO) monitoring has gained increasing clinical attention in recent years. Various methods have been developed, based on different techniques, with variation in reliability and clinical applicability. Pulse Dye Densitometry (PDD) uses the indicator dilution technique and requires only intravenous access. The indicator Indocyanine Green (ICG) is confined to the intravascular space due to its hydrophilic character and binding to plasma proteins and is cleared from the blood through the liver.[1] ICG has been used frequently to determine cardiovascular parameters such as cardiac output[2,3], cardiac index, blood volume[4-8], liver blood flow[9-11], and lung-uptake of drug components like lidocaine[12] through dye dilution. With the introduction of PDD, an adaptation of pulse spectrophotometry, it became possible to measure ICG noninvasively by means of transcutaneous spectrophotometry using a finger or nose probe.[13]

Three validation studies of the measurement of the arterial blood ICG concentration versus pulse dye densitometry have been published so far.[13-15] In these studies, blood samples were taken after recirculation had taken place. However, the phase of initial mixing, before recirculation of the dye, is the period in which the data are gathered for the estimation of cardiac output and central blood volume (CBV), since the area under the first pass curve is needed for the calculation of these parameters. In the study published by Sakka and colleagues, intravascular measurement of ICG using a fiberoptic device showed good agreement with transcutaneous measurement of ICG for the determination of total blood volume (TBV), moderately for CBV and could not be performed for CO, due to inaccurate detection of the first-pass curve.[16] Consequently, validation of transcutaneous measurement of ICG by PDD versus ICG concentration measurements in arterial blood during the initial mixing phase is not available.

To evaluate the noninvasive measurement of ICG using pulse dye densitometry, we compared in a group of patients the ICG data measured using the PDD finger or nose probe to the ICG concentrations in arterial blood, and compared the cardiovascular parameters derived by these 2 methodologies.

Methods

Study design and subjects

The ICG concentrations determined noninvasively by PDD and invasively in arterial blood were taken from patients who participated in either of two yet unpublished pharmacological studies. In 10 patients ICG concentrations were measured using the PDD finger probe, in 10 other patients the nose probe was used. The studies were performed after obtaining approval from the Medical Ethics Committee of the Leiden University Medical Centre and the patients' written informed consent. The patients were ASA physical status I or II and participated in the study prior to elective surgery. Exclusion criteria included a medical history of severe cardiovascular, respiratory, renal, hepatic, neurological or psychiatric disease, use of anti-hypertensive or anti-arrhythmic medication, pregnancy or lactation, and a history of hypersensitivity to amide local anesthetics or ICG.

Prior to the measurements a large venous cannula was inserted in the fossa cubiti and the radial artery was cannulated for gathering blood samples with a 22 G cannula. Placement of the finger probe was on the index finger and the nose probe on the right nasal wing. Cooling of the extremities was prevented to maintain signal quality. An experimental session only started when the PDD indicated a sufficient signal quality as measured by the finger or nose probe. Sufficient was judged a minimum of two out of five units as indicated on the DDG-2001. Each session started with the intravenous administration of 10 mg ICG (Infracyanine®), followed by a rapid bolus of 20 ml of saline. A computer-controlled syringe pump with fraction collector drew arterial blood samples at 3 sec intervals for the first min, and at 10 sec intervals for the second minute. Eight more samples were drawn manually up to 15 min after administration of the ICG bolus dose. The sampling system consists of a disposable sampling set, an automatic sampler and a carrousel with test tubes. The automatic sampler is a custom made device that can move a syringe plunger to a set volume and moves a stopcock in coordination with sampling. The sampler is connected to a computer that times the sampling. Because of limitations in blood flow in the radial artery the sampling rate is maximally 1 per 3 sec. The carrousel moves synchronous to the sampling. The disposable sampling system consists of a syringe with a stopcock, extension tubing between the patient and the sampling syringe, and extension tubing to the test tubes mounted on the carrousel. The extension tubing to the patient is connected with a stopcock to the intra-arterial catheter. The volumes in the extension tubes with the stopcocks have a dead space volume of 1.8 ml. The sampling

volume was set to 1.8 ml and is thus identical to the dead space in the extension tubes. Each sampling cycle consisted of drawing the sample from the patient, turning the stopcock on the syringe and then ejecting the content of the syringe to the extension tube to the test tubes. Since the movement of blood in the system is fully controlled, mixing of samples in the tubing is unlikely and each sample represents the concentration at the sampling time. The blood samples were collected in heparinized glass tubes and processed immediately.

The patients in whom the finger probe was used for determination of ICG concentrations underwent up to 3 repeated measurements in the same session separated by a time period of at least 15 min to allow for dye excretion. During each measurement patients were awake and in a hemodynamically stable condition. In the patients in whom the nose probe was used for the determination of ICG concentrations, single measurements were performed, as patients were studied during induction of anesthesia.

Measurements of ICG in blood

The concentrations of ICG were determined in whole blood using High Performance Liquid Chromatography (HPLC) (Separations analytical instruments, Hendrik-Ido-Ambacht, The Netherlands; column: Ultrasphere ODS 4.6 x 7.5 cm 244254, Beckman Coulter, Mijdrecht, The Netherlands) with ultraviolet and fluorescence detection. For each patient a calibration curve was constructed, using the patients own blood prior to injection of ICG. The fluorescence settings were as follows; excitation at a wavelength of 780 nm and the emission wavelength at 810 nm with a gain of 100. ICG was also measured at 777 nm, its peak in the spectrum. Both ICG and its degradation product were identified by a diode array (Photodiodedetector PDA 100, Dionex, Amsterdam, The Netherlands). The detection limit of the whole blood assay for ICG was at 0.15 or 0.2 $mg.L^{-1}$. The coefficient of variation was less than 6 % over the range from 0.5 to 10.45 $mg.L^{-1}$.

Data collection and processing

Pulse Dye Densitometry was performed using the DDG-2001 A/K (Nihon Kohden, Tokyo, Japan). Data were transferred to a laptop-computer and imported into a spreadsheet program (Excel 2000, Microsoft Corporation, Seattle, U.S.A.). Arterial blood concentrations were imported in the same spreadsheet program to undergo further analysis.

Cardiac output was calculated by dividing the administered ICG dose by the area under the first-pass concentration-time curve (A_1+A_2; see below). The

shape of the first pass concentration-time curve, including all data before evidence of ICG recirculation, was log-linearly described by the sum of two Erlang functions, each representing the convolution of n 1-compartment models connected in series [17]

$$C(t) = A_1 * \frac{k_1^{n_1} t^{n_1-1}}{(n_1-1)!} + A_2 * \frac{k_2^{n_2} t^{n_2-1}}{(n_2-1)!}$$

where n_1 and n_2 are the number of compartments in series in the central delay elements; k_1 and k_2 are the rate constants between the compartments in series; n_1/k_1 and n_2/k_2 are the mean transit times (MTT) of the central delay elements; A_1 and A_2 are the areas under the first pass concentration time curves. The two Erlang functions were fitted to the data using the solver function in Excel (Microsoft Corporation, Seattle, U.S.A.), whereby data were uniformly weighted.

Total blood volume was estimated as $TBV=D/C_0$, in which D is the dose administered and C_0 is the log-linearly back-extrapolated concentration at mean transit time, when first mixing but no elimination of ICG has occurred during the first circulation. The intrathoracic or central blood volume is determined as the product of CO and MTT.

Statistical analysis

Comparison of the two methods in both groups (nose and finger probe) was done by Bland-Altman analysis[18], reporting mean difference (bias) and Limits of Agreement (LOA, bias ± 2 SD). In the group using the finger probe, the total variance due to intra- and interindividual differences has been taken into account using additional oneway analysis of variance.[19] Comparison of ICG peak concentrations using the finger or nose probe versus the arterial blood ICG concentration was performed by a paired T-test (SPSS, version 14.0).

Results

Patients

Patient characteristics of both groups are represented in table 1.

Table 1 Patient characteristics (data presented as median and range).

	Finger probe group	**Nose probe group**
Patients (n)	10	10
Sessions (n)	26	10
Gender (M/F)	4 / 6	2 / 8
Age (yr)	56 (21-86)	44.5 (23-53)
Weight (kg)	67 (63-92)	65.5 (55-95)
Height (m)	1.70 (1.56-1.87)	1.71 (1.58-1.97)
Body mass index (kg m-2)	23.5 (21.2-29.3)	23.2 (18.9-25.1)

ICG concentration curves

In both sets of patients, it regularly proved difficult to obtain an adequate signal quality.

In two sessions performed with the finger probe the generated ICG curves consisted of a small-based concentration peak, generating CBV of 22.7 and 26.8 L and an accordingly high CO of 35 and 47.3 $L.min^{-1}$. Since these figures were far beyond physiologically acceptable values, the results for CO and CBV were excluded from the Bland-Altman analysis.

Due to the rapid arterial blood sampling it was possible to obtain an adequate number of data points to define the peak in the arterial ICG concentration, including recirculation of the dye**.** In each experiment, on average, 32 arterial blood samples for blood ICG concentration determination were taken, of which 20 were in the first minute. In both groups, the peak blood ICG concentration measured by PDD was generally higher than in the arterial blood. The average difference of +29% $\pm$ 36% (mean ± SD) using the finger probe (n=24, $p<0.001$) and +34.2% $\pm$ 46.5% (mean ± SD) using the nose probe (n=9, $p=0.079$). Furthermore, the peak concentration of ICG measured by PDD lagged behind the arterial blood ICG peak concentration. The average time shift between the noninvasively and invasively measured ICG concentration was 9.6 sec $\pm$ 9 (SD) in the finger probe group. In the nose probe group this time shift did not occur. Examples of ICG concentration curves showing a marked difference in MTT between invasive and noninvasive ICG measurements using the finger probe are shown in figure 1. The data were obtained from the same patient in

successive sessions. In this case no clear differences in peak concentrations were observed.

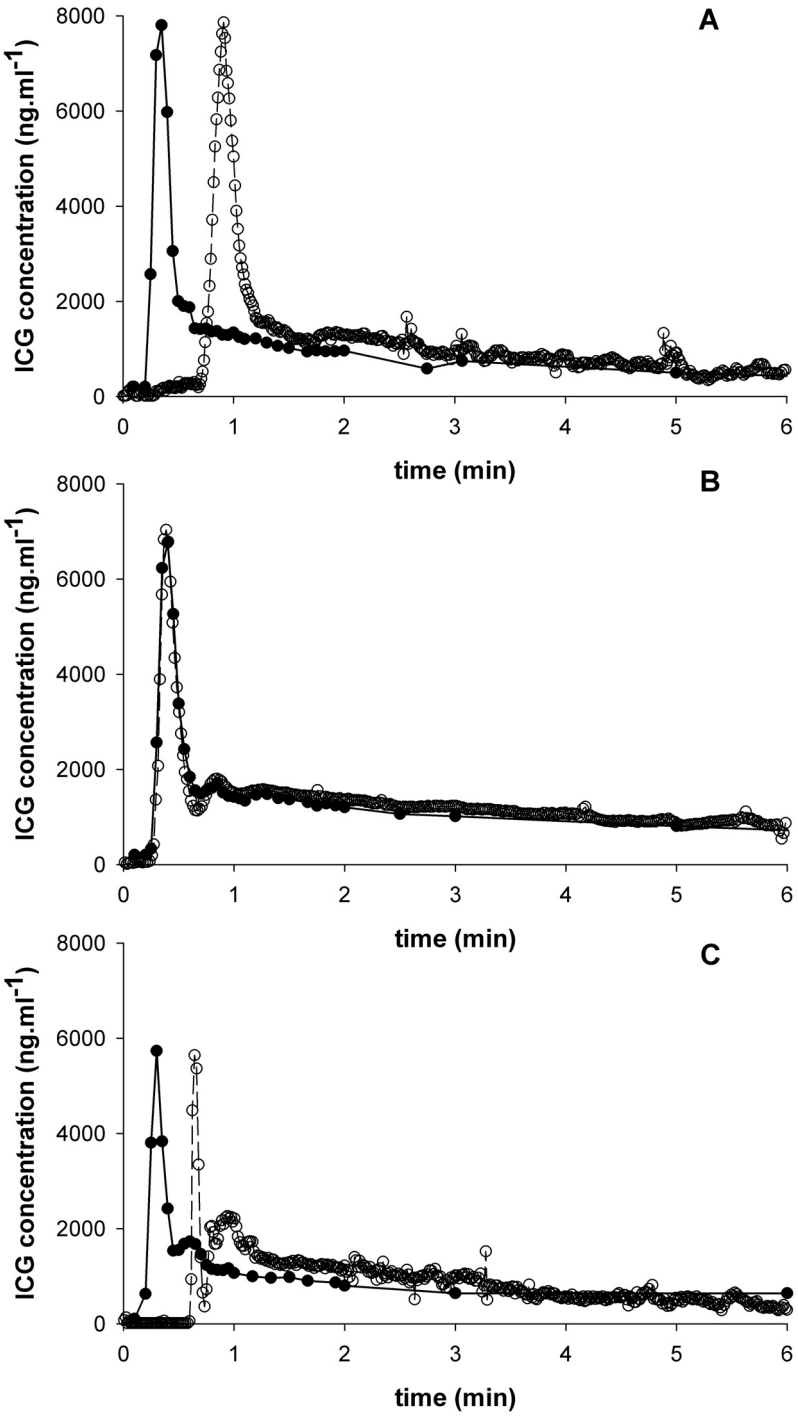

Figure 1 Indocyanine Green (ICG) concentration-time data of 3 sessions in a single patient, determined by the pulse dye densitometry (PDD) finger probe (open markers) and from arterial blood (closed markers). Note the time shift in the first experiment (panel A) and the difference in first circulation in the third experiment (panel C).

Hemodynamic parameters using the finger probe

In 24 datasets the cardiac output (CO) and central blood volume (CBV) and in 26 datasets total blood volume (TBV) were calculated and compared. TBV was recalculated from the raw data, using a spreadsheet with the algorithms as described in the methods section, to correct for major noise artifacts by adjusting the interval of the curve used for back-extrapolation to C_0. The Bland-Altman analysis revealed a mean absolute difference and limits of agreement between PDD and invasive measurements for CO of -0.43 $L.min^{-1}$ (-4.76 and 3.90 $L.min^{-1}$); for CBV of 0.76 L (-2.45 and 3.97 L) and for TBV of -1.42 L (-3.88 and 1.03 L) (Figure 2). The Bland-Altman analysis revealed a mean relative difference and LOA between PDD and invasive measurements for CO of -5% (-56% and 47%); for CBV of 21% (-54% and 96%) and for TBV of -15% (-38% and 8%).

Hemodynamic parameters using the nose probe

In all data sets (n = 10) the CO, central blood volume (CBV) and total blood volume (TBV) were compared. The Bland-Altman analysis revealed an absolute bias and LOA between PDD and invasive measurements for CO of 2.26 $L.min^{-1}$ (-4.67 and 9.20 $L.min^{-1}$); for CBV of 0.79 L (-2.08 and 3.66 L) and for TBV of -0.73 L (-3.48 and 2.01 L) (Figure 3). The Bland-Altman analysis revealed a mean relative difference and LOA between PDD and invasive measurements for CO of 30% (-67% and 127%); for CBV of 48% (-98% and 193%) and for TBV of -10% (-47% and 27%).

Discussion

Various studies on the comparison of PDD derived cardiovascular parameters versus intravascular measurements by e.g. a pulmonary artery catheter have been published: on cardiac output (CO)[3,20-23], central (or intrathoracic) blood volume (CBV)[4], total blood volume (TBV)[13], and hepatic blood flow.[24] The noninvasively derived dye dilution curve was not validated in any of these publications, yet the derived parameters were compared to results obtained by other methods of measurement. In other words, no study so far accurately compared frequently gathered arterial ICG concentrations before complete mixing had occurred with the noninvasive ICG data by PDD and evaluated the derived cardiovascular parameters based on these invasive and noninvasive ICG dilution methodologies.

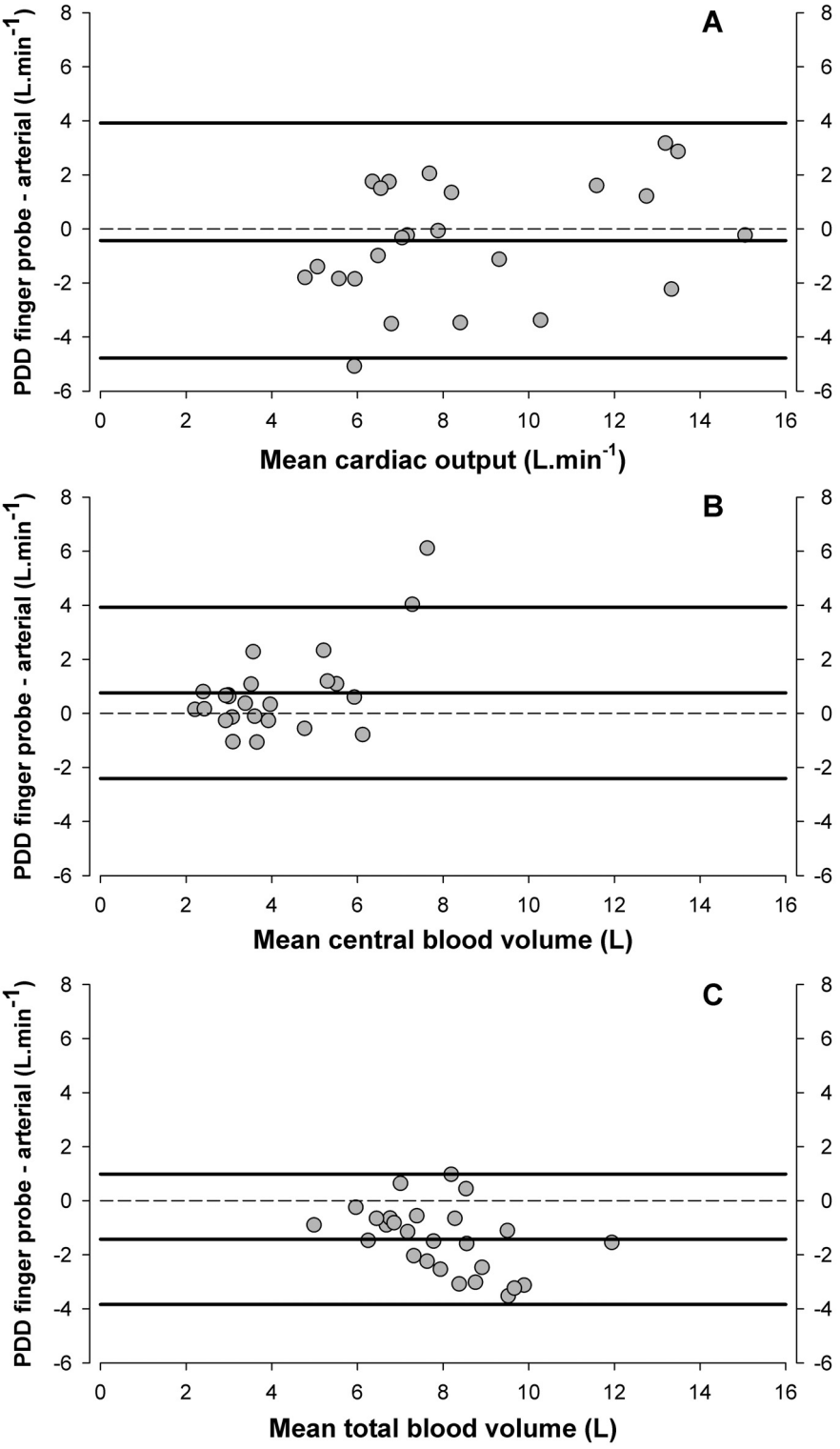

Figure 2 The bias (PDD-arterial) and limits of agreement (± 2 SD) for cardiac output (A), central blood volume (B) and total blood volume (C), measured by the pulse dye densitometry (PDD) finger probe.

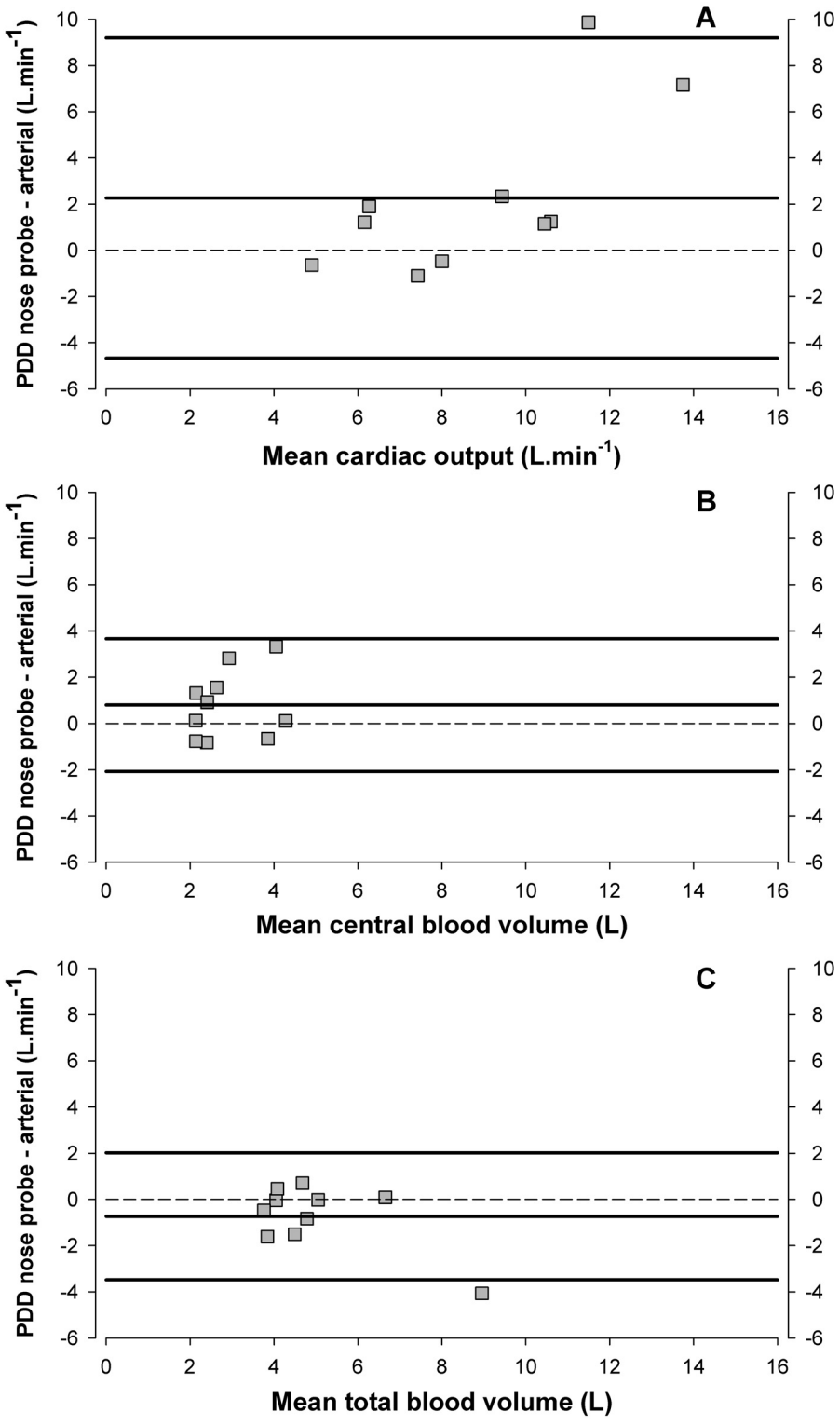

Figure 3 The bias (PDD-arterial) and limits of agreement (± 2 SD) for cardiac output (A), central blood volume (B) and total blood volume (C), measured by the pulse dye densitometry (PDD) nose probe.

In this study we evaluated the hemodynamic parameters based on noninvasive ICG measurements by pulse dye densitometry, using a finger or nose probe, and compared them to those based on invasive ICG measurements in the arterial blood.

Arterial measurement of ICG concentrations is not considered to be the gold standard for the determination of cardiovascular parameters. On the other hand, comparison of these two methods is the most accurate way to evaluate the underlying technique used in PDD. Hence, Bland-Altman analysis of the results is the only allowed method for comparison of the results. The data in the first part of this study were gathered using the finger probe; initially this probe was chosen because the anatomical proximity of the two sample sites (the radial artery and the index finger) was likely to improve the comparability of the data. To improve the comparison, we included a second patient group using the nose probe. For determination of TBV and the ICG plasma disappearance rate (ICG-PDR), both probes generally are considered equally reliable.[5,6,14] Some studies, however, suggest that the nose probe may be more reliable for determination of cardiac output[21], whereas other studies do not favor either probe for CO determination.[13,15] Our results show an overestimation of CO by the nose-probe and underestimation by the finger probe. Providing physio-pathological support for this finding is difficult. One can speculate that the influence of vasoconstriction in the microvasculature, tissue volume at the probe site and the proportion of mixed tissue absorption in the digits is more elaborate then in the nasal wing.

We conclude that transcutaneous measurements by PDD result in higher (finger and nose probe) and postponed (finger probe) ICG concentrations compared to arterial ICG concentration measurements of the same bolus of ICG. Any difference in detection of ICG peak concentration has influence on both CO and CBV calculation, as it affects the AUC. The phase shift is of consequence in the calculation of CBV, since it directly affects the MTT. Therefore, the PDD-derived hemodynamic parameters cardiac output and central blood volumes are inaccurate. As a consequence of the wide limits of agreement, in an individual patient with a CO of 6 $L.min^{-1}$, PDD could measure a CO of 3 $L.min^{-1}$ or 9 $L.min^{-1}$. This huge uncertainty significantly limits the use of PDD for the monitoring of CO in the individual patient.

The measurements of total blood volume correlated better. This can be explained by the fact that TBV is less influenced by a time shift in the first circulation curve, as long as the elimination curve compares well between the two methods. Before accepting a PDD generated TBV value, we recommend

taking the complete concentration curve into consideration: when (motion) artifacts occur in the interval used for back-extrapolation, estimation of the down slope may be highly affected and manual adjustment of the interval is necessary.

The clinical conditions, under which the two probes were tested, varied between subjects in the two studies. At higher ranges of the parameters determined, the relative differences between the methods did not show an increase. The magnitude of the bias is therefore not related to the range of cardiac output or TBV in our study.

Study limitations

Ideally, the comparison of the two probes would have been performed in a randomized cross-over manner, but due to the separate protocols and pre-operative character of the experiments, this was not possible. Unfortunately it was not possible to use both probes simultaneously.

Underestimation of the peak ICG concentration by arterial sampling may in part be explained by the lower sample frequency. However, even when smoothing of the curve by a moving average is assumed, the influence on the AUC should be minimal. Furthermore, the gathering of 6-8 arterial blood samples during the first circulation of ICG (usually 12-20 sec) is the maximum achievable in practice. Variability in the ICG measurements in blood was low; in some cases however, it was more difficult to fit the first circulation. This could occur in patients with a high cardiac output, generating less data points in the first circulation of the dye.

In our study two sessions performed with the finger probe were excluded in the Bland-Altman analysis for CO and CBV. The detected PDD concentration curves showed a small based peak during the first circulation, generating a very small AUC. The results for CO and CBV were over 20 L (per min) and clearly wrong. Incorrect detection of the PDD may lie in the signal:noise ratio being influenced by motion or low pulsatility of the signal due to constriction of the microvasculature in the digit. The signal may even be merely a reflection of a mixed tissue level, due to the passage of the indicator through small arterioles, capillaries and small veins. There was however no obvious reason for the findings in these sessions. Bremer et al. report an average of 5 performed measurements by PDD to collect 3 apparently valid recordings[20], Haruna and colleagues excluded 3 out of 10 volunteers due to motion artifacts and/or low signal:noise ratio.[6] Secondly, in cases where the declining part of

the concentration peak is not smooth, the PDD device may generate an inadequate fit of the first circulation. This cannot be adjusted manually.

We recommend the (future) user of the PDD method to pay attention to the following aspects: optimize signal quality by guarding the temperature of the probe site, avoid vasoconstriction, avoid excess light at the probe site, avoid motion of the patient or probe, check the signal quality during the measurement (aim for a minimum of 2 out of 5 units on the display), observe the concentration curve for adequacy of fit of the first circulation, adjust the interval for back-extrapolation if necessary.

Conclusion

In conclusion, the results of this study significantly question the reliability of pulse dye densitometry by Nihon Kohden for cardiac output and central blood volume measurement in the individual patient. The nose and finger probe were equally unreliable. Given the wide limits of agreement, pulse dye densitometry could misinform the clinician about the actual hemodynamic status of the patient. Despite the need for less invasive methods of cardiac output measurement, better alternatives than PDD are required. PDD is better suitable for measurement of total blood volume, as our findings indicate. PDD is used also as an indicator for hepatic clearance and hepatic blood flow, especially during liver transplantation.[24-26] The application of PDD for this purpose remains to be validated.

References

1. Fox IJ, Wood EH. Indocyanine green: physical and physiologic properties. Staff Meetings Mayo Clin 1960;35:732-44.
2. Baulig W, Bernhard EO, Bettex D, Schmidlin D, Schmid ER. Cardiac output measurement by pulse dye densitometry in cardiac surgery. Anaesthesia 2005;60:968-73.
3. Hofer CK, Buhlmann S, Klaghofer R, Genoni M, Zollinger A. Pulsed dye densitometry with two different sensor types for cardiac output measurement after cardiac surgery: a comparison with the thermodilution technique. Acta Anaesthesiologica Scandinavica 2004;48:653-7.
4. Bremer F, Schiele A, Sagkob J, Palmaers T, Tschaikowsky K. Perioperative monitoring of circulating and central blood volume in cardiac surgery by pulse dye densitometry. Intensive Care Medicine 2004;30:2053-9.
5. Goy RW, Chiu JW, Loo CC. Pulse dye densitometry: a novel bedside monitor of circulating blood volume. Ann Acad Med Singapore 2001;30:192-8.

6. Haruna M, Kumon K, Yahagi N, Watanabe Y, Ishida Y, Kobayashi N, Aoyagi T. Blood volume measurement at the bedside using ICG pulse spectrophotometry. Anesthesiology 1998;89:1322-8.

7. He YL, Tanigami H, Ueyama H, Mashimo T, Yoshiya I. Measurement of blood volume using indocyanine green measured with pulse- spectrophotometry: its reproducibility and reliability. Crit Care Med 1998;26:1446-51.

8. Henschen S, Busse MW, Zisowsky S, Panning B. Determination of plasma volume and total blood volume using indocyanine green: a short review. J Med 1993;24:10-27.

9. Kanaya N, Iwasaki H, Namiki A. Noninvasive ICG clearance test for estimating hepatic blood flow during halothane and isoflurane anaesthesia. Can J Anaesth 1995;42:209-12.

10. Sakka SG, van HN. Relation between indocyanine green (ICG) plasma disappearance rate and ICG blood clearance in critically ill patients. Intensive Care Med 2006;32:766-9.

11. Soons PA, De Boer A, Cohen AF, Breimer DD. Assessment of hepatic blood flow in healthy subjects by continuous infusion of indocyanine green. Br J Clin Pharmacol 1991;32:697-704.

12. Bertler A, Lewis DH, Lofstrom JB, Post C. In vivo lung uptake of lidocaine in pigs. Acta Anaesthesiol Scand 1978;22:530-6.

13. Iijima T, Aoyagi T, Iwao Y, Masuda J, Fuse M, Kobayashi N, Sankawa H. Cardiac output and circulating blood volume analysis by pulse dye- densitometry. J Clin Monit 1997;13:81-9.

14. Iijima T, Iwao Y, Sankawa H. Circulating blood volume measured by pulse dye-densitometry: comparison with (131)I-HSA analysis. Anesthesiology 1998;89:1329-35.

15. Imai T, Takahashi K, Goto F, Morishita Y. Measurement of blood concentration of indocyanine green by pulse dye densitometry--comparison with the conventional spectrophotometric method. J Clin Monit Comput 1998;14:477-84.

16. Sakka SG, Reinhart K, Wegscheider K, Meier-Hellmann A. Comparison of cardiac output and circulatory blood volumes by transpulmonary thermo-dye dilution and transcutaneous indocyanine green measurement in critically ill patients. Chest 2002;121:559-65.

17. Boer F, Bovill JG, Burm AG, Mooren RA. Uptake of sufentanil, alfentanil and morphine in the lungs of patients about to undergo coronary artery surgery. Br J Anaesth 1992;68:370-5.

18. Bland JM, Altman DG. Statistical methods for assessing agreement between two methods of clinical measurement. Lancet 1986;1:307-10.

19. Bland JM, Altman DG. Agreement between methods of measurement with multiple observations per individual. J Biopharm Stat 2007;17:571-82.

20. Bremer F, Schiele A, Tschaikowsky K. Cardiac output measurement by pulse dye densitometry: a comparison with the Fick's principle and thermodilution method. Intensive Care Med 2002;28:399-405.

21. Imai T, Takahashi K, Fukura H, Morishita Y. Measurement of cardiac output by pulse dye densitometry using indocyanine green: a comparison with the thermodilution method. Anesthesiology 1997;87:816-22.

22. Kroon M, Groeneveld AB, Smulders YM. Cardiac output measurement by pulse dye densitometry: comparison with pulmonary artery thermodilution in post-cardiac surgery patients. J Clin Monit Comput 2005;19:395-9.

23. Sakka SG, Reinhart K, Meier-Hellmann A. Comparison of invasive and noninvasive measurements of indocyanine green plasma disappearance rate in critically ill patients with mechanical ventilation and stable hemodynamics. Intensive Care Medicine 2000;26:1553-6.

24. Okochi O, Kaneko T, Sugimoto H, Inoue S, Takeda S, Nakao A. ICG pulse spectrophotometry for perioperative liver function in hepatectomy. J Surg Res 2002;103:109-13.

25. von Spiegel T, Scholz M, Wietasch G, Hering R, Allen SJ, Wood P, Hoeft A. Perioperative monitoring of indocyanine green clearance and plasma disappearance rate in patients undergoing liver transplantation. Anaesthesist 2002;51:359-66.

26. Hori T, Iida T, Yagi S, Taniguchi K, Yamamoto C, Mizuno S, Yamagiwa K, Isaji S, Uemoto S. K(ICG) value, a reliable real-time estimator of graft function, accurately predicts outcomes in adult living-donor liver transplantation. Liver Transpl 2006;12:605-13.

4

Pulse Dye Densitometry and Indocyanine Green Plasma Disappearance in ASA Physical Status I-II patients

Marije Reekers, Mischa J.G. Simon, Fred Boer, René A.G. Mooren Jack W. van Kleef, Albert Dahan and Jaap Vuyk

Department of Anesthesiology, Leiden University Medical Center, Leiden, The Netherlands

Anesthesia & Analgesia 2010:110:466-72.

Introduction

Indocyanine Green dye (ICG) is extracted from the blood by hepatic parenchymal cells without undergoing enterohepatic circulation.[1] The hepatic clearance of ICG is used for the assessment of hepatic (residual) function.[2-5] The elimination of ICG can be reported as ICG plasma disappearance rate (ICG-PDR), which is the decline in the log-linear elimination curve after the iv administration of a bolus of ICG, expressed as percentage per min. Various reports have been published on the measurement of ICG-PDR for the monitoring of hepatic function during anesthesia and after liver transplantation.[6-9] In addition, ICG-PDR is reported as a prognostic factor in the critically ill.[10-13]

With Pulse Dye Densitometry (PDD), an adaptation of pulse spectrophotometry, it is now possible to measure ICG non-invasively by means of transcutaneous pulse spectrophotometry using a finger or nose probe. Transcutaneously measured ICG concentrations have been shown to correlate very closely to arterial blood ICG concentration measurements in man[14,15] and in a porcine model.[16]

Although the measurement of ICG has been validated properly, the actual mean value and range of ICG disappearance in the healthy population and the cutoff value that discriminates between a normal and impaired hepatic function has not yet been described clearly. Often one refers to a single publication, which is a book chapter that is not readily available.[17] Other publications on the subject date from almost 50 years back and are determined by invasive blood sampling. Nonetheless, information on the range and variability of ICG-PDR in healthy persons is prudent for the interpretation of single or repeated ICG disappearance measurements in the evaluation of liver graft function, hepatic blood flow, or assessment of liver failure in septic shock.

To increase the knowledge of ICG disappearance in a healthy population we evaluated the ICG disappearance rate (ICG-PDR values) in ASA physical status I-II patients not known with hepatic or cardiovascular disease. Measurement of ICG-PDR was performed transcutaneously by Pulse Dye Densitometry using either a finger probe or nose probe. In addition, we compared the transcutaneous measurement of ICG-PDR using PDD to invasive measurement of ICG-PDR in arterial blood.

Methods

Patients

For the determination of the ICG plasma disappearance in an otherwise healthy surgical population, 41 patients were evaluated as they participated in one of two sequential pharmacological studies. In 33 patients, involved in a study on the cardiovascular effects of lumbar epidural anaesthesia with ropivacaine 0.75%, ICG concentrations were measured using the PDD finger probe. Measurements were performed before introduction of epidural anaesthesia. In 8 other patients, involved in a study on pharmacokinetic-pharmacodynamic modeling of propofol, ICG concentrations were measured using the PDD nose probe. To compare transcutaneous measurement of ICG-PDR with invasive measurements, multiple simultaneous ICG measurements in arterial blood were collected in a subset of 10 patients from the first group and all 8 patients from the second group. The studies were performed after obtaining approval from the Medical Ethics Committee of the Leiden University Medical Centre and the patients' written informed consent. The patients were ASA physical status I or II scheduled for elective surgery. Exclusion criteria included a medical history of severe cardiovascular, respiratory, renal, hepatic, neurological or psychiatric disease, use of anti-hypertensive or anti-arrhythmic medication, pregnancy or lactation and a history of hypersensitivity to amide local anesthetics or indocyanine green. In 9 of the 41 patients (22%) chemical testing of liver function had been performed previously by our hospital laboratory and the results were within normal limits.

Procedures

Prior to the ICG clearance measurements a cannula was inserted in a large vein in the fossa cubiti. In 18 patients the radial artery was also cannulated for the collection of arterial blood samples. Pulse Dye Densitometry was performed using the DDG-2001 A/K (Nihon Kohden, Tokyo, Japan). Each session started with the intravenous administration of 10 mg ICG (Infracyanine®), followed by a rapid bolus of 20 ml of saline. In the group of patients in whom arterial blood samples were taken, a computer-controlled syringe pump was programmed to draw up to 33 arterial blood samples of 1.5 ml in the first 2 min after ICG administration. Starting from the second minute a waste sample was drawn first, to avoid mixing within the sampling line. The blood samples were collected in heparinized glass tubes and processed immediately. In the finger probe group, arterial sampling continued up to 15 min following ICG bolus administration. In the nose probe group, arterial blood sampling continued

6-10 min after bolus administration, depending on the return of consciousness, when measurements were terminated. Once complete mixing of the dye was observed, a median number of 7 arterial ICG concentration data points were available for fitting the log-linear elimination curve.

Measurements of ICG in blood

The concentrations of ICG were determined in whole blood using High Performance Liquid Chromatography (Separations analytical instruments, Hendrik-Ido-Ambacht, The Netherlands; column: Ultrasphere ODS 4.6 x 7.5 cm 244254, Beckman Coulter, Mijdrecht, The Netherlands) with ultraviolet and fluorescence detection. The fluorescence settings were as follows: excitation at a wavelength of 780 nm and emission wavelength at 810 nm with a gain of 100. ICG was also measured at 777 nm, its peak in the spectrum. Both ICG and its degradation product were identified by a diode array (Photodiodedetector PDA 100, Dionex, Amsterdam, The Netherlands). The detection limit of the whole blood assay for ICG was at 0.15 or 0.2 $mg.L^{-1}$. The coefficient of variation was less than 6 % over the range from 0.5 to 10.45 $mg.L^{-1}$.

Data collection and processing

ICG-blood concentration data as determined by PDD and from the arterial blood were imported in a spreadsheet program (Excel 2000, Microsoft Corporation, Seattle, U.S.A.). K_{ICG}, the rate constant characterizing the ICG decay curve, was calculated by fitting a semi logarithmic regression curve through the declining part of the ICG concentration curve in the interval of 2-5 min after administration of the bolus ICG. The concentration curve is a monoexponential decay curve,

$$C = C_0 \times e^{(-K \times t)}$$

where C is the ICG concentration, K (min^{-1}) is the elimination constant and t is time in min after administration of the bolus. ICG-PDR ($\%.min^{-1}$) equals Kx100.

Statistical analysis

Comparison of the two methods (non invasive and invasive measurement of ICG) in both groups (finger and nose probe) was done by Bland-Altman analysis, reporting mean difference (bias) and Limits of Agreement (LOA, bias ± 2 SD).[18] Descriptive statistics were generated by the SPSS statistical package (SPSS, version 14.0).

Results

Patients

The characteristics of the 41 patients in which the PDD probes were used for ICG determination, are presented in table 1. In a subset of 10 patients, 4 males and 6 females, 22 dual ICG arterial measurements were taken.

Table 1 Patient characteristics (data presented as median ± SD).

	Finger probe group	Subset for arterial sampling	Nose probe group
Patients (n)	33	10	8
Gender (M/F)	11 / 22	4 / 6	1 / 7
Age (yr)	56.3 ± 18.8	54.2 ± 22.5	42.8 ± 9.6
Weight (kg)	72.8 ± 12.2	70.8 ± 9.2	65.1 ± 6.5
Height (m)	1.71 ± 0.09	1.70 ± 0.10	1.70 ± 0.10
Body mass index (kg m^{-2})	24.9 ± 3.7	24.0 ± 2.5	22.5 ± 2.3

ICG-PDR values in ASA physical status I-II patients

ICG-PDR measured transcutaneously in 41 healthy patients was 23.1 ± 7.9 $\%.min^{-1}$ (n=41; 95% confidence interval 7.4 – 38.8). The range was 9.7 – 43.2 $\%.min^{-1}$. The cumulative frequency distribution and the cumulative normal distribution calculated from the mean and standard deviation of the datasets measured by both PDD probes are presented in figure 1.

Comparison of transcutaneous and invasive ICG-PDR measurements

Bland-Altman analysis showed that with the finger probe, PDD overestimated ICG-PDR by 1.6 $\%.min^{-1}$. The limits of agreement (LOA) were -5.2 to 8.3 $\%.min^{-1}$ (Figure 2, panel A). The relative bias and LOA were 11.6% and -31.5 to 54.7% (Figure 2, panel B). Using the nose probe, PDD underestimated ICG-PDR by -6.0 $\%.min^{-1}$. The limits of agreement were -15.5 to 3.4 $\%.min^{-1}$ (Figure 3, panel A). The relative bias and LOA were -23.1% and -57.2 to 11.0% (Figure 3, panel B).

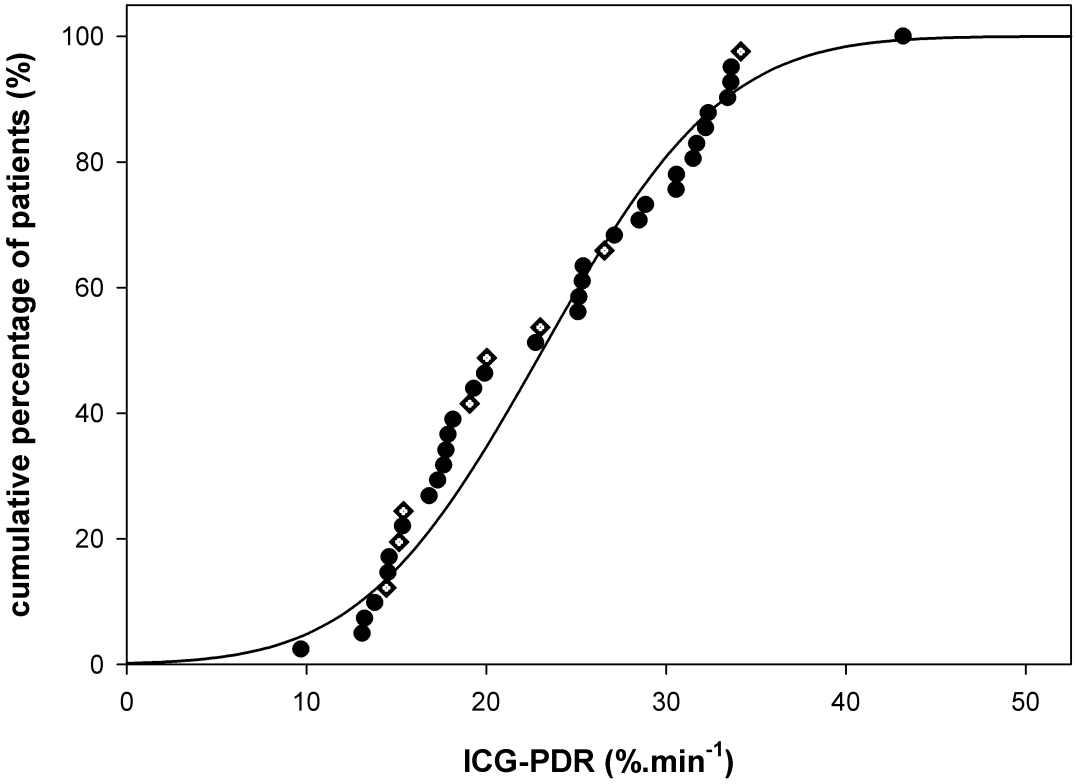

Figure 1 Cumulative frequency distribution of the values found for indocyanine green plasma disappearance rate (ICG-PDR) measured by pulse dye densitometry (PDD) (n=41; bullets for finger probe, open diamonds for nose probe) and cumulative normal distribution function based on the calculated mean and standard deviation (solid line).

Discussion

The most important finding of this study is that in our healthy patient population, combining 41 non-invasive measurements by finger and by nose probes, the mean ICG-PDR was 23.1 %.min^{-1}, with an SD of 7.9 (n=41; 95% confidence interval 7.4 – 38.8). The PDD finger and nose probe both performed adequately in the noninvasive determination of the ICG concentration.

Study limitations

We included otherwise healthy patients (ASA physical status I or II) who were scheduled for elective surgery. Patients with liver disease were excluded from the study based on patient history and physical examination. In 22% of the patients liver function tests (aminotransferases) were available and found to be within normal limits as set by the hospital laboratory.

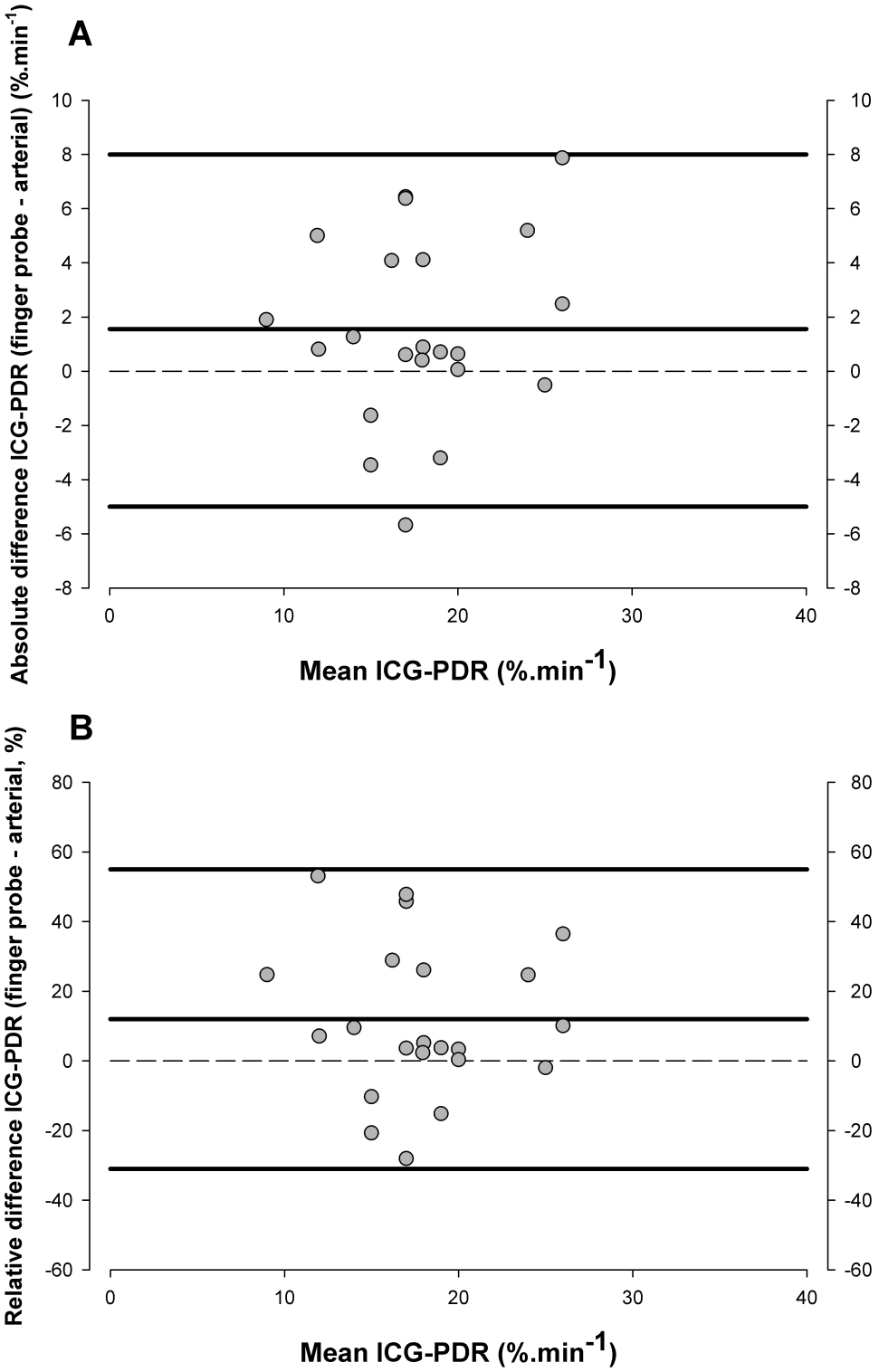

Figure 2 Panel A represents the absolute results (bias and limits of agreement (= ± 2 SD) from the Bland-Altman analysis of indocyanine green plasma disappearance rate (ICG-PDR) measured by the pulse dye densitometry (PDD) finger probe or in an arterial blood sample. Panel B represents the relative difference in ICG-PDR measurement between the PDD finger probe and from arterial blood.

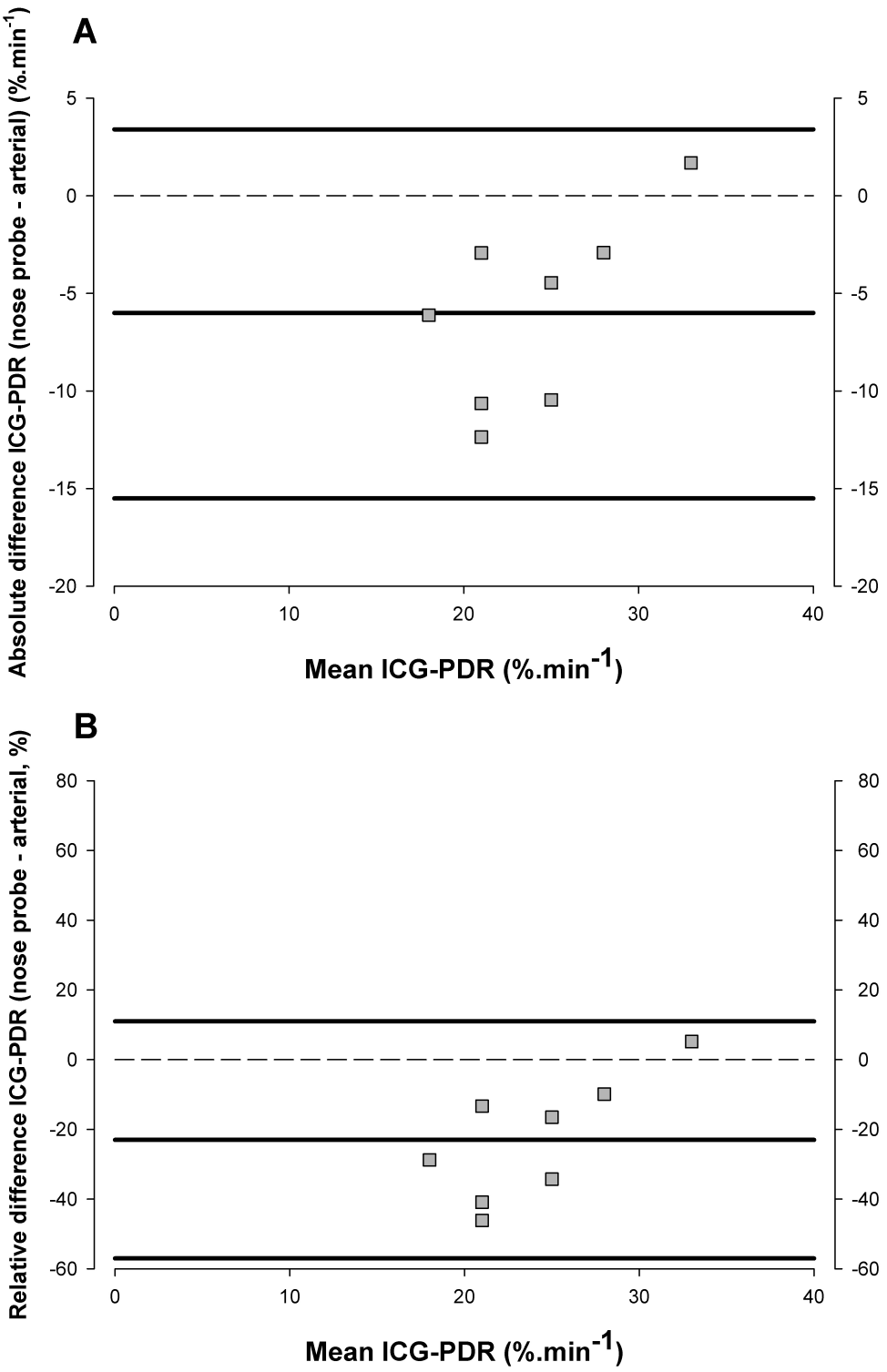

Figure 3 Panel A represents the absolute results (bias and limits of agreement (= ± 2 SD) from the Bland-Altman analysis of indocyanine green plasma disappearance rate (ICG-PDR) measured by the pulse dye densitometry (PDD) nose probe or in arterial blood. Panel B represents the relative difference in ICG-PDR measurement between the PDD nose probe and from arterial blood.

One may argue that ideally hepatic function testing should have been available in all patients. However, none of our patients had a history of hepatic dysfunction, showed any signs of hepatic dysfunction during physical examination or were scheduled for liver related surgery. Furthermore, patients suspected of malnutrition as associated with abnormal body mass index or substance abuse including alcohol abuse or any sign of bleeding disorder were excluded.

It is known that it is not possible to use ICG-disappearance to discriminate between a slight impairment in hepatic cellular function and a change in the hepatic blood flow.[19] For practical purposes, one of these factors is therefore assumed to be constant, in order to interpret changes in ICG-PDR. Changes in the ICG-PDR can be caused by alterations in the excretory function of the liver, even before changes in serum bilirubin levels are observed.[20] A decrease in ICG-PDR appears more sensitive in the detection of early liver failure than an increase in serum bilirubin level[21,22] or critical illness scores like APACHE II.[11] However, generally, changes in ICG-PDR are caused by changes in the splanchnic blood flow and thus result from alterations in hepatic blood flow.[23] In the patients where the nose probe was used, measurements were performed during induction with a bolus dose of propofol. During induction changes in cardiac output, splanchnic blood flow and mean arterial pressure may occur. The results from the nose probe group were evenly distributed among the results from the finger probe group, in which measurements were performed in patients who were awake and under baseline conditions. This might be explained by the fact that the population studied with the nose probe was younger and more homogenous than the finger-probe population. The younger patients may have a more vigorous compensating mechanism to respond to changes in hemodynamics. Since the values found during induction did not compose a separate group, we chose to include the data in the representation of the ICG-PDR values found in healthy patients.

Ideally, repeated measurements would be performed using both the finger and nose probe in the same patient under stable conditions to gather more information on the variability of the measurement. Also, changing of physiological conditions like volume expansion would be nice to investigate further. However, due to the pre-elective surgery setting of the experiments and technical limitations, this was not possible.

Interpretation of the results

We concluded, in agreement with previously published data[16,24,25], that the PDD finger and nose probe noninvasively determine the ICG decay with a relative bias of 12% for the finger probe and -23% for the nose probe. The availability of this noninvasive transcutaneous measurement of ICG by pulse dye densitometry (PDD) makes ICG-PDR a favorable parameter in the evaluation of hepatic flow and/or function. A proper judgment between normal and impaired hepatic function or flow then only is realistic in the presence of a valid description of ICG-PDR in the healthy population. Up until now the normal range of transcutaneously measured ICG-PDR is poorly described[17] as >18 %.min^{-1}.

We report in our study population of 41 patients without liver disease an ICG-PDR of 23.1 (7.9) %.min^{-1}, using noninvasive PDD measurements. Fifteen of our 41 patients (37%) had an ICG-PDR of <18 %.min^{-1}. Ten patients (24%) had an ICG-PDR below 16 %.min^{-1}. According to the study of Sakka and colleagues[11] these persons may have higher mortality. In different studies in critically ill patients, or patient after hepatectomy in whom liver failure may be expected, adjustment of treatment and fluid administration based on a ICG-PDR of <7 %.min^{-1} or <16 %.min^{-1} is recommended.[2,11] In case of liver transplantation, 24 h post-transplantation ICG-PDR values of <18 %.min^{-1} may predict hepatic failure.[7]

All the above mentioned studies illustrate the search for a clinical implementation of ICG-PDR, yet emphasize the difficulties in interpretation. Figure 4 illustrates these interpretation problems. Depicted are the cumulative normal distribution curves calculated from the means and standard deviations of the present surgical study population, the values of a group of patients who underwent major hepatectomy without and with postoperative liver failure as studied by Sugimoto[2] and preoperative patients undergoing liver transplantation studied by Faybik.[9] In all studies PDD was used to measure ICG-PDR. We have chosen these studies as they offer ICG-PDR data from patients with normal hepatic function, and patients with reduced and severely reduced functional liver tissue, respectively. The results in these studies are represented as mean and standard deviation; this is only valid if the results are normally distributed. We assumed the authors tested their data for normal distribution and simulated the data based on the reported mean and standard deviation. As can be observed from figure 4 a decrease in functional liver tissue not only decreases the mean ICG-PDR but also concurs with a decrease in variation around the mean, indicated by an increased steepness of the cumulative distribution curve. As the liver function of the group becomes better,

the distribution curve stretches to the right, but maintains its origin at a value below 10 %.min^{-1}. This has implications for the ability of ICG-PDR to detect differences between patient groups. At any chosen threshold, ICG-PDR value groups will be easier distinguished if the distance between their curves at that value of ICG-PDR is larger. Obviously patients with terminal liver failure or with a decreased but survivable liver function after hepatectomy can be best discriminated from healthy patients around an ICG-PDR of 7.5 %.min^{-1}. Similarly, the reduction in ICG-PDR of surviving post-hepatectomy patients in comparison to healthy patients is best observed around an ICG-PDR of about 20 %.min^{-1}, as the distance between their curves is largest. Since the distance between these curves is diminished their distinction will be hindered by a decreased sensitivity and specificity.

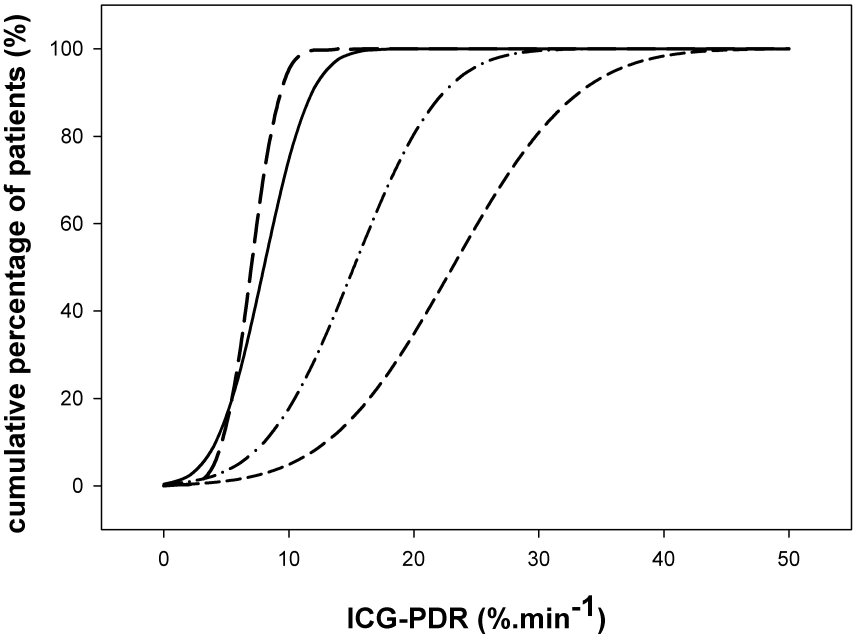

Figure 4 Cumulative frequency curves calculated from the mean and average of the present study (small dash), patient without (dash-dot-dash) and with liver failure (long dash) developing on the first day after major hepatectomy studied by Sugimoto[2] and preoperative patients undergoing liver transplantation surgery (solid line) studied by Faybik [9].

We used receiver operating characteristics (ROCs) to further explore this subject, and this is represented in figure 5. The simulated patient populations from the 2 studies were compared to our healthy population to determine the ICG-PDR cutoff value with the highest sensitivity and specificity to identify the

affected patients. Taking into consideration all noninvasive measurements of ICG-PDR, the patients with liver failure in the study of Faybik would be best identified from our healthy patients, if a cutoff value for ICG-PDR of < 9 $\%.min^{-1}$ would be used, with a sensitivity of 98.5%, a specificity of 96.3%, and an AUC under ROC curve of 0.99 (Figure 5, panel A). Similarly, the patients with terminal liver failure after hepatectomy would be detected with a sensitivity of 98.7% and a specificity of 93.7% if a ICG-PDR value < 11 $\%.min^{-1}$ would be used. The AUC under the ROC curve is 0.99, indicating good accuracy (Figure 5, panel B). To detect decreased liver function of the patient surviving hepatectomy in the study of Sugimoto compared to our healthy patients the detection level would have to be set to ICG-PDR < 19 $\%.min^{-1}$, but the sensitivity would only be 69.8% and the specificity 82.4%. Similarly, the AUC under the ROC curve indicates only moderate accuracy with a value of 0.82 (Figure 5, panel C). Our exploration suggests that terminal liver failure can adequately be detected with ICG-PDR, but non-terminal decrease of liver function is harder to detect. This is supported by the finding of Sugimoto that they were unable to discern patients that would experience liver failure after major hepatectomy using preoperative ICG-PDR values. On the other hand, Hori and co-workers7 were able to detect differences in a homogeneous group of post liver transplant patients as soon as 24 h after transplantation between patients with good outcome (ICG-PDR of 21.0 ± 2.4 $\%.min^{-1}$), (mean ± SD) and bad outcome (ICG-PDR of 16.3 ± 2.1 $\%.min^{-1}$), (mean ± SD). We suggest that this finding is the result of the relative homogeneity of their study group and the accompanying diminished variability of their ICG values.

In conclusion, we evaluated the transcutaneous measurement and defined the absolute value of the ICG-disappearance rate by PDD in an otherwise healthy group of patients scheduled for general non-hepatic surgery. The PDD finger and nose probe showed a relative bias of 12% and -23% respectively, compared to the measurement of ICG-PDR in arterial blood. Within this healthy population the mean ICG-PDR was 23.1 $\%.min^{-1}$ (95% confidence interval 7.4 – 38.8), which is more variable than the value of >18%.min^{-1} which is usually referred to as normal value. Variability in transcutaneous measurement is probably larger than by intravascular fiberoptic measurement. We suggest that a broader evaluation of noninvasive measurement of ICG-PDR in the healthy population is warranted, before this parameter is used as a discriminating tool in the judgment on hepatic function or flow.

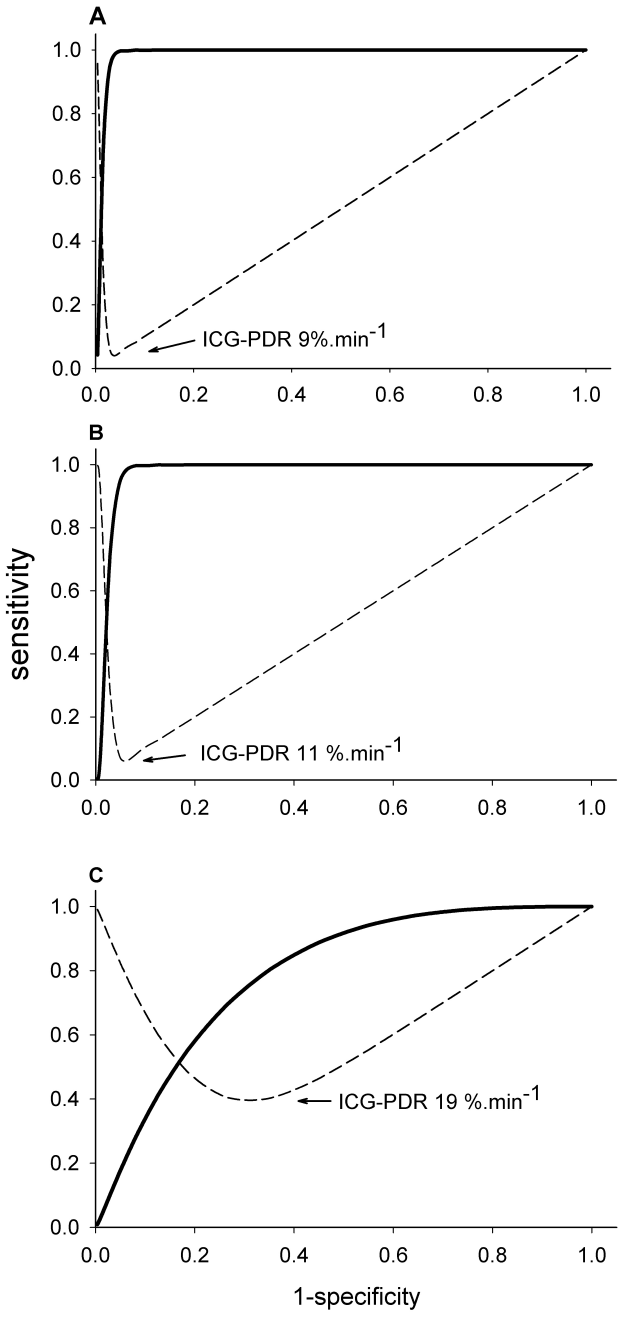

Figure 5 Representation of ROC curves (solid line) and the area under the curve versus the ICG-PDR value (dashed line) of three study populations. In panel A test results for the detection of liver failure in a population undergoing liver transplantation from the study of Faybik[9] are used. An ICG-PDR cut-off value of 9%.min^{-1} generates the optimum sensitivity and specificity in this population. In panel B test results for the detection of liver failure in a population undergoing major hepatectomy from the study of Sugimoto[2] are used.An ICG-PDR cut-off value of 11%.min^{-1} generates the optimum sensitivity and specificity in this population. Panel C represents the results from the population experiencing only decreased liver function after mayor hepatectomy, also from the study by Sugimoto[2]. The cut off value of 19 %.min^{-1} is much less accurate.

References

1. Fox IJ, Wood EH. Indocyanine green: physical and physiologic properties. Staff Meetings Mayo Clin 1960;35:732-44.

2. Sugimoto H, Okochi O, Hirota M, Kanazumi N, Nomoto S, Inoue S, Takeda S, Nakao A. Early detection of liver failure after hepatectomy by indocyanine green elimination rate measured by pulse dye-densitometry. J Hepatobiliary Pancreat Surg 2006;13:543-8.

3. Imamura H, Sano K, Sugawara Y, Kokudo N, Makuuchi M. Assessment of hepatic reserve for indication of hepatic resection: decision tree incorporating indocyanine green test. J Hepatobiliary Pancreat Surg 2005;12:16-22.

4. Lam CM, Fan ST, Lo CM, Wong J. Major hepatectomy for hepatocellular carcinoma in patients with an unsatisfactory indocyanine green clearance test. Br J Surg 1999;86:1012-7.

5. Ohwada S, Kawate S, Hamada K, Yamada T, Sunose Y, Tsutsumi H, Tago K, Okabe T. Perioperative real-time monitoring of indocyanine green clearance by pulse spectrophotometry predicts remnant liver functional reserve in resection of hepatocellular carcinoma. Br J Surg 2006;93:339-46.

6. von Spiegel T, Scholz M, Wietasch G, Hering R, Allen SJ, Wood P, Hoeft A. Perioperative monitoring of indocyanine green clearance and plasma disappearance rate in patients undergoing liver transplantation. Anaesthesist 2002;51:359-66.

7. Hori T, Iida T, Yagi S, Taniguchi K, Yamamoto C, Mizuno S, Yamagiwa K, Isaji S, Uemoto S. K(ICG) value, a reliable real-time estimator of graft function, accurately predicts outcomes in adult living-donor liver transplantation. Liver Transpl 2006;12:605-13.

8. Mandell MS, Wachs M, Niemann CU, Henthorn TK. Elimination of indocyanine green in the perioperative evaluation of donor liver function. Anesth Analg 2002;95:1182-4, table.

9. Faybik P, Krenn CG, Baker A, Lahner D, Berlakovich G, Steltzer H, Hetz H. Comparison of invasive and noninvasive measurement of plasma disappearance rate of indocyanine green in patients undergoing liver transplantation: a prospective investigator-blinded study. Liver Transpl 2004;10:1060-4.

10. Kimura S, Yoshioka T, Shibuya M, Sakano T, Tanaka R, Matsuyama S. Indocyanine green elimination rate detects hepatocellular dysfunction early in septic shock and correlates with survival. Crit Care Med 2001;29:1159-63.

11. Sakka SG, Reinhart K, Meier-Hellmann A. Prognostic value of the indocyanine green plasma disappearance rate in critically ill patients. Chest 2002;122:1715-20.

12. Sakka SG, Reinhart K, Meier-Hellmann A. Comparison of invasive and noninvasive measurements of indocyanine green plasma disappearance rate in critically ill patients with mechanical ventilation and stable hemodynamics. Intensive Care Medicine 2000;26:1553-6.

13. Sakka SG, van HN. Relation between indocyanine green (ICG) plasma disappearance rate and ICG blood clearance in critically ill patients. Intensive Care Med 2006;32:766-9.

14. Iijima T, Aoyagi T, Iwao Y, Masuda J, Fuse M, Kobayashi N, Sankawa H. Cardiac output and circulating blood volume analysis by pulse dye- densitometry. J Clin Monit 1997;13:81-9.

15. Imai T, Takahashi K, Goto F, Morishita Y. Measurement of blood concentration of indocyanine green by pulse dye densitometry--comparison with the conventional spectrophotometric method. J Clin Monit Comput 1998;14:477-84.

16. Kaminski, C, Gratadour, P, Rimmele, T, Goudable, J, Chassard, D. Comparison of measurements of Indocyanine Green Plasma Disappearance Rate between LiMon and Plasmatic Dosages in Septic Pigs. Anesthesiology 101, A720. 2004.

17. Kuntz HD, Schregel W. Indocyanine green: evaluation of liver function; application in intensive care medicine. In: Lewis FR, Pfeiffer U J, eds. Practical Applications of Fiberoptics in Critical Care Monitoring. Berlin Heidelberg New York: Springer, 1990:57-62.

18. Bland JM, Altman DG. Statistical methods for assessing agreement between two methods of clinical measurement. Lancet 1986;1:307-10.

19. Skak C, Keiding S. Methodological problems in the use of indocyanine green to estimate hepatic blood flow and ICG clearance in man. Liver 1987;7:155-62.

20. Sakka SG. Assessing liver function. Curr Opin Crit Care 2007;13:207-14.

21. Hemming AW, Scudamore CH, Shackleton CR, Pudek M, Erb SR. Indocyanine green clearance as a predictor of successful hepatic resection in cirrhotic patients. Am J Surg 1992;163:515-8.

22. Scheingraber S, Richter S, Igna D, Girndt M, Flesch S, Kleinschmidt S, Schilling MK. Indocyanine green elimination but not bilirubin indicates improvement of graft function during MARS therapy. Clin Transplant 2007;21:689-95.

23. Niemann CU, Yost CS, Mandell S, Henthorn TK. Evaluation of the splanchnic circulation with indocyanine green pharmacokinetics in liver transplant patients. Liver Transpl 2002;8:476-81.

24. Tsai, K, Tai, D, Changchien, C, Chen, C. Comparison of ICG Finger Monitor system with conventional blood sampling ICG clearance test in patient with acute severe hepatitis. Gastroenterological Journal of Taiwan 1996;13:186-193.

25. Su, MY, Lin, DY, Sheen, IS, Chu, CM, Chiu, CT, Liaw, YF. Indocyanine green clearence test in non-cirrhotic hepatitis patients: A comparison and analysis between convention blood sampling method and finger piece monitoring method. Chang Gung Medical Journal 1999;22:17-24.

5

Circulatory Model of Vascular and Interstitial Distribution Kinetics of Rocuronium: a Population Analysis in Patients

Michael Weiss[#], Marije Reekers*, Jaap Vuyk* and Fred Boer*

[#] Department of Pharmacology, Martin Luther University Halle-Wittenberg, Halle (Saale), Germany

* Department of Anesthesiology, Leiden University Medical Center, Leiden, The Netherlands

J Pharmacokinet Pharmacodyn 2011;38:165–78.

Introduction

For drugs with rapid onset of action, such as rocuronium, an understanding of the factors governing distribution kinetics is crucial. Although it has been shown in previous studies that rocuronium, like other muscle relaxants, distributes only in the plasma and interstitial fluid volume, the mechanism of the distribution process is not fully understood. One would suggest that the interstitial distribution of rocuronium resembles that of inulin, a marker for extracellular water, but this is not yet clear. Conventional compartmental models are not suitable to answer such questions due to the assumption of instantaneous drug mixing in the compartments. While recirculatory models with compartmental structure characterize the initial phase of vascular mixing well and explain the role of cardiac output as determinant of effect onset [1,2], they are inadequate to directly characterize the tissue diffusion of drugs.

In order to overcome these limitations, a model based on first principles, namely the basic processes of drug distribution in the body, advective transport by blood flow (vascular mixing) and diffusion into extravascular space, has been developed. This minimal physiological model in which the lumped organs of the systemic circulation were described by an axially distributed capillary-tissue exchange model[3] has been applied successfully to analyze the distribution kinetics of inulin, antipyrin[4] and thiopental[5] in dogs. An important feature of this approach is that the use of indocyanine green (ICG) as vascular marker allows a clear distinction between intravascular mixing and tissue diffusion (multiple-indicator method). Analysis of disposition kinetics of rocuronium is based on the information on mixing in the vascular system obtained from the distribution kinetics of ICG. Concomitant injection of a vascular marker (e.g., ICG) with the drug followed by frequent sampling of arterial blood is thus a prerequisite for the application of this modeling approach. The theory of transit time distributions is an adequate mathematical approach because it is independent of a specific model of drug distribution kinetics.

Using the ICG and rocuronium disposition data measured in patients [1], the goal of this study was:

1. to examine vascular mixing in terms of cardiac output and transit time dispersion[6],
2. to model the interstitial distribution kinetics of rocuronium

3. to estimate the parameters with a population approach. The lack of population recirculatory models has been noted in a review on population PK/PD of anesthetics.[7]

Methods

Data and Study Protocol

The experimental protocol, including sampling method, has been described before.[1] To summarize: datasets from ten healthy female patients undergoing eye surgery under general anesthesia after providing written informed consent were evaluated. Premedication, midazolam 7.5 mg orally, was given 60 min prior to induction of anesthesia by target controlled infusion of propofol (target at 4 µg/ml) and remifentanil (adjusted according to the surgical condition). After loss of consciousness, rocuronium 0.35 mg/kg was injected intravenously for muscle relaxation. Rocuronium (10 mg/ml) was injected as a mixture with ICG (25 mg) and autologous blood in a total volume of 10 ml. Of this mixture 9 ml were administered and 1 ml was used for a-posteriori measurement of injectate concentrations.

Blood samples were taken from a cannula in the radial artery. During the first 10 minutes of the experiment, sampling was performed using a custom made computer controlled syringe pump and fraction collector for determination of ICG and rocuronium concentrations. In the first minute, a blood sample was taken every 3 s, followed by sampling every 10 s in the second minute. Consecutive samples were taken at 2.5, 3, 4, 7, and 10 min. Hereafter samples were taken manually at 15, 30, 60, 120, 180, and 240 min for determination of rocuronium concentrations.

Analytical methods

ICG concentrations were measured spectrophotometrically at 850 nm in whole blood. Each patient's whole blank blood with added amounts of ICG was used for construction of a reference line. The measured absorption at 850 nm minus the absorption in the sample taken before the experiment was considered to be caused by ICG. Rocuronium concentrations were measured in whole blood by high-performance liquid chromatography with a fluorescence detector.[1]

Mathematical model

The structure of the circulatory pharmacokinetic model based on advective transport to the organs and diffusion within organs is shown in figure 1. It consists of two heterogeneous subsystems, the pulmonary circulation which includes the lungs and the heart chambers and the systemic circulation where all organs are lumped together. This model has been described in detail previously.[4]

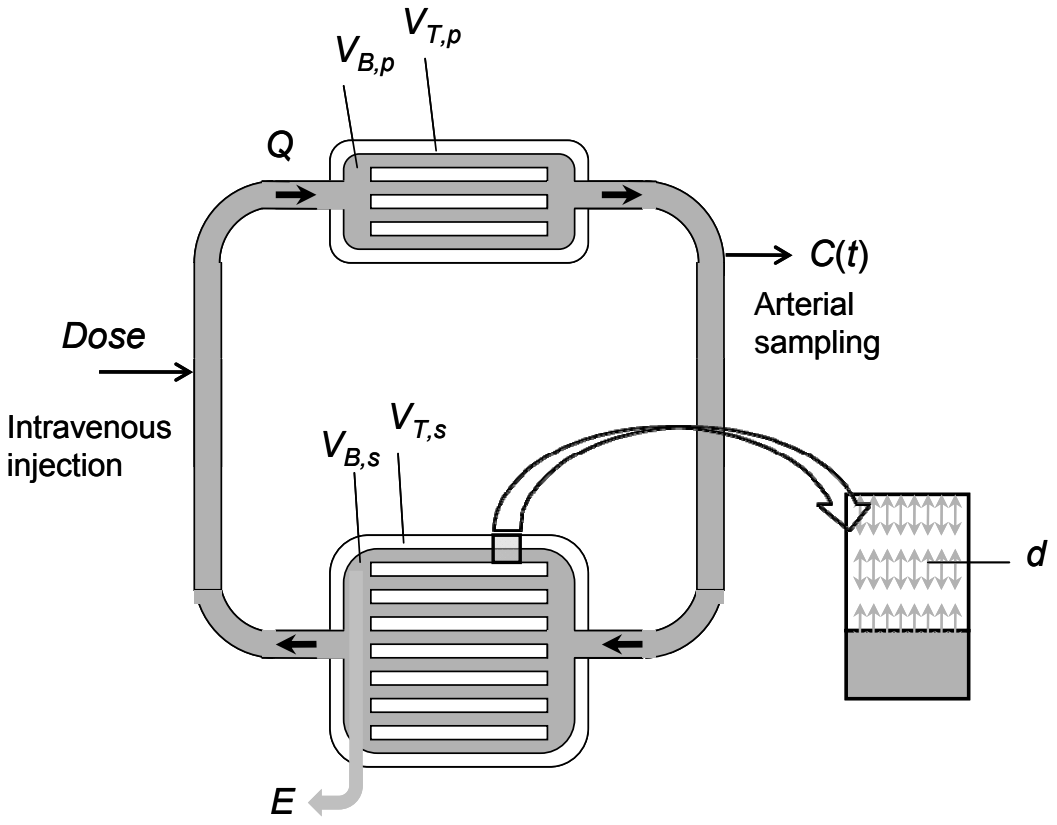

Figure 1 Schematic representation of the circulatory model. The capillary network of organs (indicated by parallel tubes) lead to transit time heterogeneity (dispersion) of vascular marker. All organs of the systemic circulation are lumped together. The blood and tissue volumes of the pulmonary and systemic circulation, respectively, are indicated. Diffusional transport into the tissue space characterized by the diffusional equilibration time *d* is illustrated in an infinitesimal small volume element since the model contains no well mixed spaces. The clearance is defined as product of systemic extraction ratio (E) of the drug and cardiac output (CL= EQ). (For the definition of parameters, see table 1.)

Briefly, the subsystems are characterized by transit time density (TTD) functions and all information on intravascular distribution (mixing) is obtained

from the ICG disposition data. The respective parameters are cardiac output *Q*, the vascular (blood) volumes $V_{B,p}$,$V_{B,s}$ and the relative transit time dispersion $RD^2_{B,p}$, $RD^2_{B,s}$, of each subsystem. (The index i = p and s labels the pulmonary and systemic circulation). A lag-time T_{lag} was introduced to account for the delayed first appearance at the sampling site. These parameters are incorporated into the axially distributed capillary-tissue exchange model, used for diffusion of rocuronium into the extravascular (tissue) space with distribution volumes $V_{T,p}$,$V_{T,s}$ and diffusional equilibration time *d*, the characteristic time constant of the interstitial diffusion process that is determined by the effective tissue diffusion coefficient D_{eff} and the characteristic diffusion path length *L* ($d = L^2/D_{eff}$). The apparent permeability surface area product PS_{diff} , defined as $PS_{diff} = V_{T,s} / d$, is a measure of PS averaged over all organs and combines all of the diffusive transport processes into a single "lumped" parameter. Note that the steady state distribution volume V_{ss} is obtained as the sum of all distribution volumes of rocuronium, $V_{ss}=V_{B,p}+V_{T,p}+V_{B,s}+V_{T,s}$. The model equations fitted to the data are summarized in the Appendix.

For comparison, the rocuronium data were also fitted using the conventional two-compartment-model. On the basis of the parameter estimates V_1 (volume of the central compartment), V_2 (volume of the peripheral compartment), CL_{12} (distribution between V_1 and V_2) and CL_{roc} (clearance), and the distribution (or mixing) clearance CL_M as a model-independent measure of whole body distribution kinetics was calculated as[8]

$$CL_M = CL_{12}\left(1 + V_1 / V_2\right)^2 \qquad (1)$$

Parameter estimation

Population pharmacokinetic analyses were performed with maximum likelihood (ML) estimation (no linearizing approximations) via the expectation maximization algorithm (EM) using the program MLEM implemented in the software package ADAPT 5.[9] The program provides estimates of the population mean inter-subject variability, and standard errors (%RSE) for the maximum likelihood estimates, as well as of the individual subject parameters (conditional means). The residual (error) variance model described the observation standard deviation as linear with the fitted value C(t) as follows: $var[\varepsilon_i(t)] = [\sigma_0 + \sigma_1 C(t_i)]^2$, where σ_0 and σ_1 are the variance parameters. 'Goodness of fit' was assessed using the Akaike Information Criterion and by plotting the predicted versus the measured responses. First, the ICG data were fitted (Appendix, Eq. 2), then the estimates of *Q*, $V_{B,p}$,$V_{B,s}$, τ_{lag}, $RD^2_{B,p}$ and

$RD^2_{B,s}$ for the individual subjects (conditional means) were fixed in fitting the rocuronium data (Appendix, Eqs. 2 and 4). Body weight was investigated as covariate in the analysis. Since compartmental analysis is based on a well-mixed central compartment, only data observed after complete circulatory mixing (t > 1.3 min) were included when applying this model.

The dependencies of parameters from cardiac output were analyzed using least squares linear regression.

Results

The population parameters for ICG are summarized in table 1. That %RSE was not available for ICG parameters is due to the relative large number of adjustable parameters (7) compared to the number of subjects (10) (whereas only 4 parameters were estimated for rocuronium).

The individual fits (based on conditional estimates) are characterized by an R^2 of 0.94 ± 0.03. The observed and predicted pharmacokinetic profiles are depicted in figure 2, panel A for a subject with a R^2 value that was closest to the group median value. The plot of the individual predicted versus observed concentrations (Figure 2, panel B) demonstrates that the data are well fitted by the model.

Systemic transit time heterogeneity ($RD^2_{B,s}$) decreased with increasing cardiac output (Figure 3) and central blood volume ($V_{B,p}$) increased with cardiac output (Figure 4). The clearance of ICG was significantly correlated to cardiac output ($CL_{icg} = 0.144 + 0.15Q$, $R^2 = 0.5$, $p<0.05$).

The rocuronium parameters $V_{T,p}$,$V_{T,s}$, d and CL_{roc} estimated with the circulatory mixing parameters (Q, $V_{B,p}$,$V_{B,s}$, τ_{lag}, $RD^2_{B,p}$ and $RD^2_{B,s}$) held fixed are also depicted in table 1. An individual fit and the goodness-of-fit plot are shown in figures 5, panel A and panel B. The individual fits are characterized by an R^2 of 0.89 ± 0.08.

Although an extension of the model[5] by addition of the pulmonary interstitial space ($V_{T,p}$) improved the fit, it was not estimated as well as the other parameters. Inclusion of weight as covariate did not improve the model in this relatively homogeneous group of 10 subjects.

The parameter estimates for rocuronium obtained using a two-compartment model were: V_{ss} = 20 ± 3 L, CL_{roc} = 0.449 ± 0.023 L.min^{-1} and CL_M = 0.84 ± 0.37 L.min^{-1}. The latter increased significantly with cardiac output (slope = 0.35, $p<0.05$).

Table 1 Patient Parameter estimates for the model of rocuronium distribution kinetics based on circulatory mixing (ICG) in patients under propofol anesthesia (n = 10).

Model parameter, Symbol (unit)	**Population mean (%RSE)**	**Interpatient %CV (%RSE)**
ICG		
Lag time, τ_{lag} (min)*	0.124	9
Cardiac output, Q (L.min^{-1})*	3.52	20
Pulmonary blood volume, $V_{B,p}$ (L)*	1.94	18
Relative dispersion of pulmonary circulation, $RD^2_{B,p}$*	0.090	12
Systemic blood volume $V_{B,s}$ (L)*	1.84	24
Relative dispersion of systemic circulation, $RD^2_{B,s}$*	0.367	21
Clearance, CL_{ICG} (L.min^{-1})	0.669	27
Rocuronium		
Interstitial diffusional equilibration time, d (min)	89.0 (37)	50 (62)
Pulmonary extravascular volume of distribution, $V_{T,p}$ (L)	2.66 (97)	115 (61)
Systemic extravascular volume of distribution $V_{T,s}$ (L)	14.2 (30)	29 (96)
Clearance, CL_{roc} (L.min^{-1})	0.449 (24)	24 (75)
Apparent permeability surface area product $PS_{diff} = V_{T,s}/d$, (L.min^{-1}) †	0.159	92
Steady state volume of distribution, $V_{SS} = V_{B,p} + V_{T,p} + V_{B,s} + V_{T,s}$, (L)†	20.7	24
Distribution clearance (Appendix, Eqs. 5 and 6) CL_M (L.min^{-1}) †	0.63	42
Residual Error, σ_1(%)		
ICG	15.4	
Rocuronium	27.1	

*Corresponding individual estimates were used as fixed parameters in fitting rocuronium data.
†Derived parameters

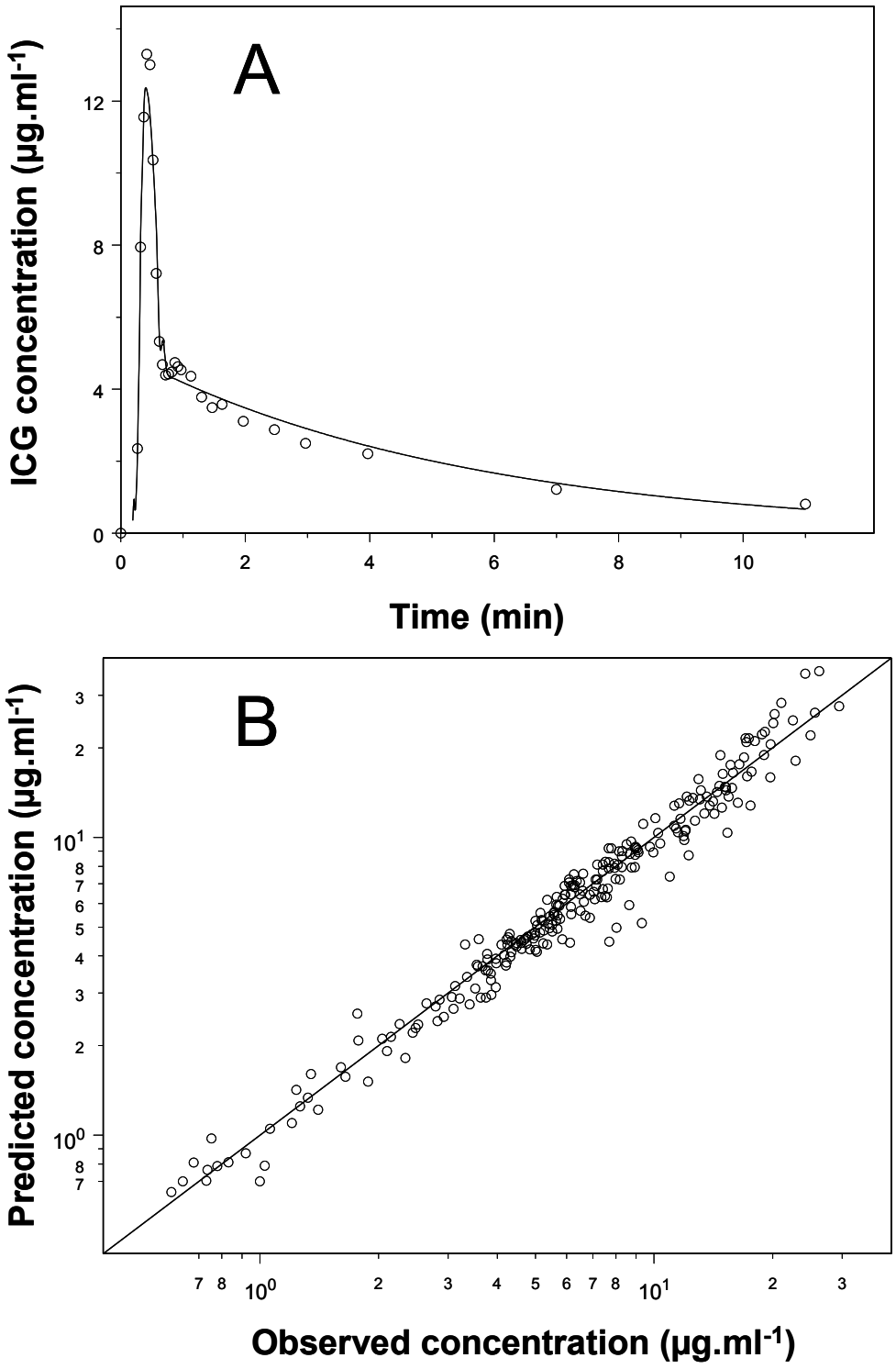

Figure 2 (A) Fit of the time course of arterial ICG concentration in one subject and (B) goodness of fit plot, showing the model-predicted data versus observed data. The solid diagonal line represents the line of identity (predicted concentration = measured concentration).

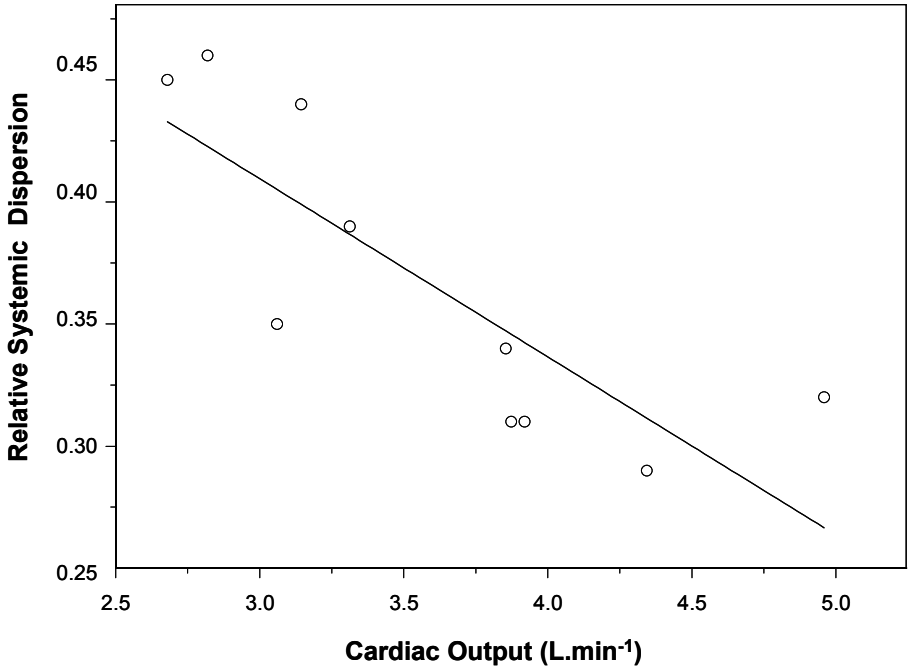

Figure 3 Systemic transit time heterogeneity of ICG ($RD^2_{B,s}$) decreases linearly with cardiac output (Q) with a slope of - 4.1 ($p<0.005$).

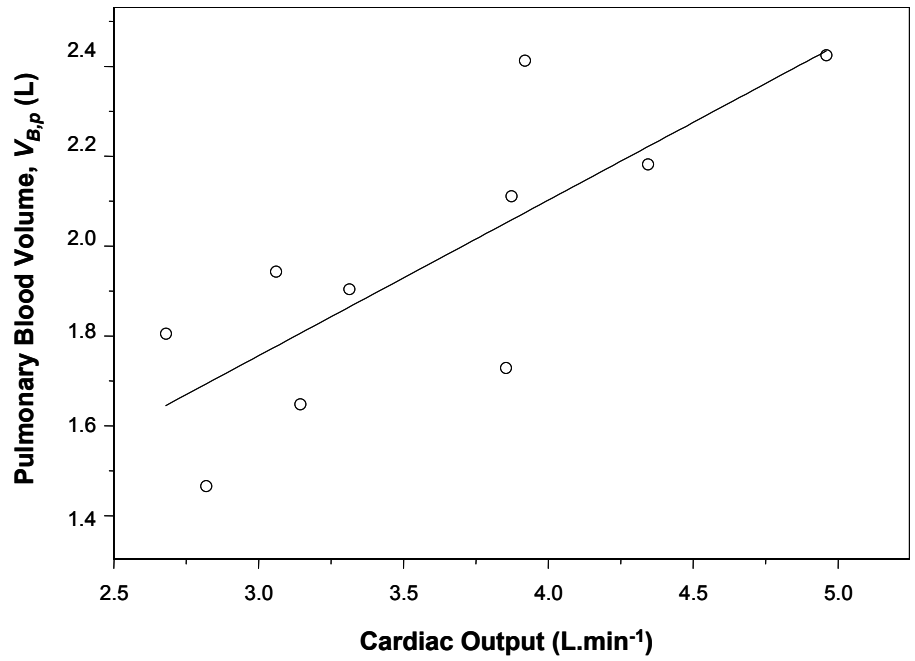

Figure 4 Central blood volume ($V_{B,p}$) increases linearly with cardiac output (Q) with a slope of 3.6 ($p<0.01$).

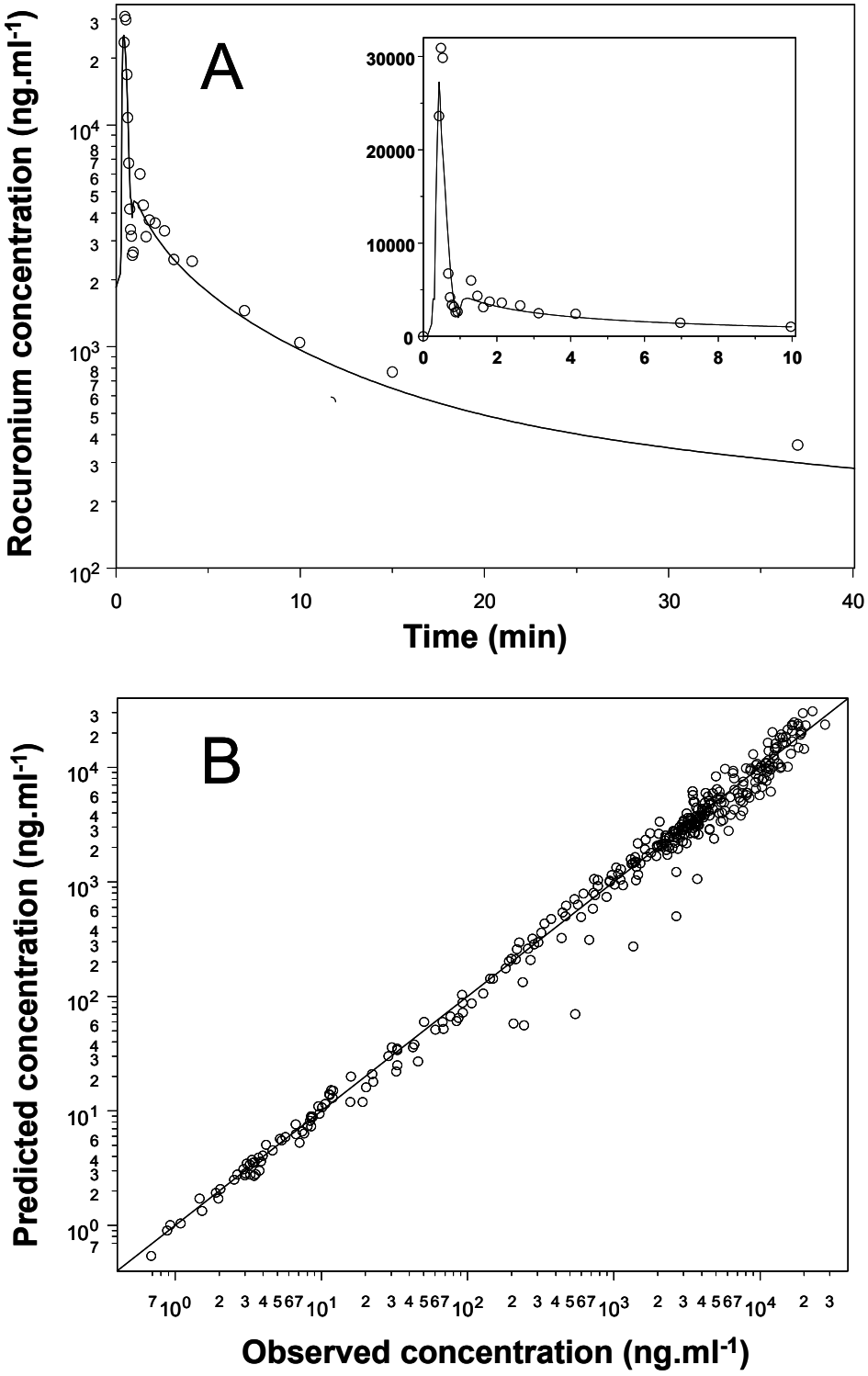

Figure 5 Fit of the time course of arterial rocuronium concentration in one subject (the inset shows the early phase in more detail) (A) and goodness of fit plot (B), showing the model-predicted data versus observed data. The solid diagonal line represents the line of identity (predicted concentration = measured concentration).

Discussion

In order to gain better understanding of the distribution kinetics of drugs with a rapid time-to-onset, a model based on intravascular mixing and capillary-tissue exchange was applied to the muscle relaxant rocuronium. The results show that circulatory models based on transit time theory overcome the structural limitations of compartmental models since no well-mixed spaces are assumed. As expected from previous studies in dogs, vascular mixing of ICG in patients was well described by the recirculatory model based on empirical transit time distributions[10] and the extension of this model to include diffusion into tissue[4] was successfully used to assess the interstitial distribution kinetics of rocuronium.

Vascular mixing

Circulatory mixing is the first step in drug distribution kinetics. Since the parameters of the present model have a definite physiological meaning, the analysis of ICG disposition in patients reveals some interesting insights. First, we found significant correlation between cardiac output and cardiopulmonary volume (Figure 4). This has been observed previously, albeit for a much larger span of cardiac output, including hypertensive patients[11,12] and during exercise in healthy subjects.[13] Apparently the cardiopulmonary volume is a good estimate of cardiac filling and thus correlates with cardiac output.[14]

Second, systemic transit time dispersion decreases with increasing cardiac output (Figure 3). This reduction in heterogeneity of blood transit time through the systemic circulation may result from a redistribution of blood flow to organs and/or a more homogeneous transit time distribution in organs (e.g., skeletal muscle).[10] Note that the heterogeneity of transit time distribution through an organ is based on the fact that some molecules may by random chance traverse the complex capillary network more quickly than others. There are no previous reports about the relationship between systemic transit time dispersion and cardiac output. Interestingly, however, exercise decreased transit time heterogeneity in human skeletal muscle[15] as well as lungs[16] and this effect was explained by vascular recruitment and dilatation. Further clarification of the mechanism underlying the changes in systemic transit time dispersion remains an interesting topic for future studies. The above account shows that our modeling of the ICG data can provide quantitative information on the hemodynamic status of the patient. Our estimate of vascular pulmonary transit times dispersion ($RD^2_{B,p}$ = 0.09) is in good agreement with that of 0.08 estimated using first-pass technetium 99m albumin angiocardiography.[17] While

no estimates of the systemic transit time dispersion of vascular markers are available in the literature, it may be noteworthy that our estimate of $RD^2_{B,s}$ is in the range of 0.2 to 1, where simulation suggests very rapid circulatory mixing.[6]

The estimates reported here for the model-independent parameters ICG distribution volume, clearance and cardiac output are consistent with those obtained previously[1] using a different modeling approach. The finding that clearance of ICG increased significantly with cardiac output can be explained by the relative high hepatic extraction of ICG, which makes clearance highly dependent on hepatic blood flow. Assuming a fractional liver blood flow of 25%, a hepatic extraction ratio of 75 ± 14 % was calculated, which is in accordance with the value of 78% measured in humans.[18]

One should bear in mind that the pharmacokinetics of rocuronium described by this model are derived from data measured in patients under general anesthesia with propofol in a concentration likely to cause vasodilation and cardiodepression. The influence of propofol on the pharmacokinetics of opioids and sedatives has been described before.[19-21] On the other hand, it is not ethical to gather data on muscle relaxants in non-sedated patients.

Interstitial distribution

Permeation across the capillary wall and interstitial diffusion governs extravascular distribution of rocuronium. In the present diffusion-limited model, the parameter *d* defines the rate of distribution (diffusional time constant), and can be interpreted as a phenomenological parameter that takes into account both transcapillary permeability and interstitial diffusivity. It appears that the latter is the rate limiting process.[22] That the value of d = 89 min estimated here for rocuronium in humans, is in the same order of magnitude as that of 51 min for inulin, a prototype of a hydrophilic drug, obtained in dogs[4], indicates that rocuronium distributes into the interstitial space by passive diffusion like inulin. A direct comparison is difficult since apart from the species differences, rocuronium, in contrast to inulin, is plasma-protein bound with a free fraction of 42 % [23] and has an higher apparent diffusion coefficient than inulin.[24,25] However, the much shorter diffusion time *d* of antipyrine compared to inulin (3 vs 51 min) estimated in dogs, which can be explained by the 40-fold higher effective tissue diffusion coefficient of antipyrine[4], suggests that rocuronium undergoes a diffusion limited distribution rather than a flow-limited distribution like antipyrin. The resulting whole-body distribution kinetics of rocuronium is characterized by an apparent permeability surface area product, PS_{diff} = 0.16 L.min^{-1}. While no *PS* values of rocuronium are available in the literature,

the results obtained for inulin and antipyrine in dogs with the same approach[4] speaks for the validity of this estimate. Thus, the apparent PS_{diff} of 0.27 L.min^{-1}, which was estimated for inulin in dogs[4], is quite similar to that of 0.33 L.min^{-1} for inulin measured in human forearm muscle.[26] Furthermore, the interstitial diffusional equilibration time estimated with our modeling approach in vivo appears to be in agreement with in vitro measurements.[27]

The distribution or mixing clearance CL_M, defined as a measure of overall rate of drug mixing into their distribution volumes[8,10]; the values of 0.68 L.min^{-1} obtained from the parameters of the diffusion model (Eq. 6) and of 0.84 L.min^{-1} obtained from the compartmental model (Eq. 1), respectively, are less than cardiac output. The difference can be explained by the fact that the compartmental CL_M (Eq. 1) is defined as distribution out of an empirical central compartment (which has no physiological counterpart), whereas in the present model CL_M characterizes the distribution of rocuronium out of the vascular space in the systemic circulation (Eq. 6). For the latter, no significant correlation with cardiac output was found (in contrast to the compartmental CL_M). The CL_M for unbound rocuronium is quite similar to that of sorbitol, a marker for extracellular water, in humans, for which a correlation with cardiac output was found.[28] Note that an increase of CL_M with a moderate increase in cardiac output would not be in contrast to the assumption of diffusion-limited tissue distribution, since there is a continuous transition from diffusion-limited to flow-limited distribution kinetics.[4]

We found that the volume of distribution of rocuronium (V_{ss} = 20.7 L) was higher than that previously estimated of 17.3 L[1]. This difference may be due to the fact that the present model also accounts for distribution into lung tissue ($V_{T,p}$ = 2.7 L). Since the pulmonary distribution volume of rocuronium is higher than that of ICG, the mean transit time across the lungs is also somewhat higher by 0.8 ± 0.6 s, which is in accordance with the value of 1 s reported in pigs.[29] That the distribution volume of rocuronium (V_{ss}) is similar to that reported for the interstitial space (e.g., Ref. 30) suggests that its tissue binding is of the same degree as the plasma protein binding (with a free fraction of fu = 0.42)[23]. Interestingly, but not unexpected for model-independent parameters, our estimate of rocuronium clearance is nearly identical with that determined previously.[1] The same holds for our estimates of V_{ss} and CL_{roc} (Table 1) and those obtained with the two-compartment model V_{ss} (20 ± 3 L) and CL_{roc} (0.449 ± 0.023 L.min^{-1}). Note that due to the differences between the present and alternative models with respect to model structure, only those parameters could be compared that were independent on the specific structure of the model. For example, there is no counterpart of transit time dispersion

($RD^2_{B,p}$, $RD^2_{B,s}$,) or diffusional equilibration time (*d*) in the other models. Since in the alternative recirculatory model[1,2] the systemic circulation consists of parallel well-mixed compartments, it does not provide direct information on interstitial diffusion.

Finally, it should be recalled that the validity of a model is determined by the modeling objectives. Thus, it was not the goal of this study to improve the fit of the rocuronium data (relative to that obtained in Ref. 1), but rather to understand better the role of vascular mixing (transit time dispersion) and interstitial diffusion. Since the fit of the rocuronium data was already quite optimal in the previous study[1], we did not repeat the PK-PD analysis. Given the fact that the empirical PK-PD link model is based on the time course of plasma concentration, no improvement could be expected. Furthermore, it is obvious that for rocuronium a classical compartmental model is appropriate for estimation of parameters like V_{ss} and CL, which are independent of a specific model structure (only based on the assumption that the rate of drug elimination is proportional to the sampled drug concentration).

Like all models, our approach is based on simplifying assumptions that may lead to certain limitations. Thus, the goodness of fit plots (figures 2 and 5, panels B) are partly non-symmetric around the lines of identity, indicating a non-optimal fit near the recirculation peak. A possible reason for this may be that the systemic transit time distribution (single subsystem), in contrast to parallel channels[1,2,31], does not sufficiently account for a shunt flow. Furthermore, the estimation of clearances is based on the assumption of constant systemic extraction ratios. Since ICG is completely and rocuronium predominantly eliminated by the liver, this implies the assumptions of a constant fractional liver blood flow and a hepatic extraction ratio, which is blood flow independent.

In conclusion, this study demonstrates the applicability of the transit time dispersion based model of vascular mixing and the diffusional tissue distribution model[4] in clinical pharmacokinetics. It accounts for the roles of circulatory mixing and diffusion into the interstitial fluid in determining the distribution kinetics of rocuronium, and thus sheds new light on our understanding of underlying transport physiology. Future applications may include other drugs or reveal the effect of disease states on drug distribution.

Appendix

As derived in Ref. 10, the Laplace transform of the solution to the circulatory model for a vascular indicator $\hat{C}(s)$, i.e. of the concentration-time curve C(t) after injection of dose Div, is

$$\hat{C}(s) = \frac{D_{iv}}{Q} \frac{\hat{f}_{B,p}(s)}{1-(1-CL/Q)\hat{f}_{B,s}(s)\hat{f}_{B,p}(s)} \tag{2}$$

where $\hat{f}_{B,p}(s)$ and $\hat{f}_{B,s}(s)$ are the Laplace transforms of pulmonary and systemic transit time density (TTD), described by the density function of the inverse Gaussian distribution (with index i = s, p)

$$\hat{f}_{B,i}(s) = \exp\left\{\frac{1}{RD^2_{B,i}} - \left[\frac{V_{B,i}/Q}{RD^2_{B,i}/2}\left(s + \frac{1}{2(V_{B,i}/Q)RD^2_{B.i}}\right)\right]^{1/2}\right\} \tag{3}$$

Q and CL denote cardiac output and clearance. The parameters in Eq. 3 are the blood volumes $V_{B,p}$,$V_{B,s}$ and the relative transit time dispersion $RD^2_{B,p}$ $RD^2_{B,s}$, of the pulmonary and systemic circulation. For fitting the C(t) date of a permeating drug like rocuronium also Eq. 2 is used, but s in Eq. 3 is substituted

$$s \rightarrow s + \frac{(V_{T,i}/V_{B,i})}{d}\sqrt{ds}\,\tanh\sqrt{ds} \tag{4}$$

where *d* is the characteristic time constant of the diffusion process[4] .

In other words, $\hat{f}_{B,p}(s)$ and $\hat{f}_s(s)$ in Eq. 2 are replaced by:
the TTDs $\hat{f}_{B,s}(s)$ and $\hat{f}_p(s)$ for rocuronium which are obtained by adding an extra term to *s*, as outlined in Eq. 4. Since the model equations for data fitting are only available in the Laplace domain, we incorporated a method of numerical inverse Laplace transformation[32] into the model file (Fortran) of ADAPT 5.[9]

As secondary parameter the distribution clearance into the tissues of the systemic circulation CL_M was calculated on the basis of the relative dispersion of rocuronium.[3,10]

$$RD_s^2 = RD_{B,s}^2 + \frac{2}{3}\frac{dQ}{V_{B,s}}\frac{(V_{T,s}/V_{B,s})}{(1+V_{T,s}/V_{B,s})^2} \quad (5)$$

according to

$$CL_M = \frac{2Q}{(RD_s^2 - 1)} \quad (6)$$

References

1. Kuipers JA, Boer F, Olofsen E, Bovill JG, Burm AGL. Recirculatory pharmacokinetics and pharmacodynamics of rocuronium in patients: the influence of cardiac output. Anesthesiology 2001;94:47-55.
2. Henthorn TK, Krejcie TC, Avram MJ. Early drug distribution: a generally neglected aspect of pharmacokinetics of particular relevance to intravenously administered anesthetic agents. Clin Pharmacol Ther 2008;84:18-22.
3. Weiss M, Roberts MS. Tissue distribution kinetics as determinant of transit time dispersion of drugs in organs: application of a stochastic model to the rat hindlimb. J Pharmacokin Pharmacodyn 1996;24:173-196.
4. Weiss M, Krejcie TC, Avram MJ. Circulatory transport and capillary-tissue exchange as determinants of the distribution kinetics of inulin and antipyrine in dog. J Pharm Sci 2007;96:913-926.
5. Weiss M, Krejcie TC, Avram MJ. A minimal physiological model of thiopental distribution kinetics based on a multiple indicator approach. Drug MetDispos 2007;35: 1525-1532.
6. Weiss M. Cardiac output and systemic transit time dispersion as determinants of circulatory mixing time: a simulation study. J Appl Physiol 2009;107:445-449.
7. Olofsen E, Dahan A. Population Pharmacokinetics/Pharmacodynamics of Anesthetics. AAPS Journal 2005;7:E383-E389.
8. Weiss M. Residence time dispersion as a general measure of drug distribution kinetics: Estimation and physiological interpretation. Pharm Res 2007;24: 2025-2030.
9. D'Argenio DZ, Schumitzky A, Wang X. ADAPT 5 User's Guide: Pharmacokinetic/ Pharmacodynamic Systems Analysis Software. Biomedical Simulations Resource, Los Angeles. 2009
10. Weiss M, Krejcie TC, Avram MJ. Transit time dispersion in pulmonary and systemic circulation: effects of cardiac output and solute diffusivity. Am J Physiol Heart Circ Physiol 2006;291:H861-870.
11. Messerli FH, De Carvalho JG, Christie B, Frohlich ED. Systemic and regional hemodynamics in low, normal and high cardiac output borderline hypertension. Circulation 1978;58:441-448.

12. Ulrych M, Frohlich ED, Tarazi RC, Dustan HP, Page IH. Cardiac output and distribution of blood volume in central and peripheral circulations in hypertensive and normotensive man. Brit Heart J 1969;31:570-574.

13. Zavorsky GS, Walley KR, Russell JA. Red cell pulmonary transit times through the healthy human lung. Exp Physiol 2003;88:191-200.

14. Rocca GD, Costa MG, Pietropaoli P. How to measure and interpret volumetric measures of preload. Curr Op Crit Care 2007;13:297-302.

15. Heinonen I, Kemppainen J, Kaskinoro K, Peltonen JE, Borra R, Lindroos MM, Oikonen V, Nuutila P, Knuuti J, Hellsten Y, Boushel R, Kalliokoski KK. Comparison of exogenous adenosine and voluntary exercise on human skeletal muscle perfusion and perfusion heterogeneity. J Appl Physiol 2010;108:378-386.

16. Presson Jr RG, Hanger CC, Godbey PS, Graham JA, Lloyd Jr TC, Wagner Jr WW. Effect of increasing flow on distribution of pulmonary capillary transit times. J Appl Physiol 1994;76 :1701-1711.

17. Capderou A, Douguet D, Similowski T, Aurengo A, Zelter M. Non-invasive assessment of technetium-99m albumin transit time distribution in the pulmonary circulation by first-pass angiocardiography. Eur J Nucl Med 1997;24:745-753.

18. Wynne HA, Goudevenos J, Rawlins MD, James OF, Adams PC, Woodhouse KW. Hepatic drug clearance: the effect of age using indocyanine green as a model compound. Brit J Clin Pharmacol 1990;30:634-637.

19. Mertens MJ, Olofsen E, Burm AGL, Bovill JG, Vuyk J. Mixed-effects modeling of the influence of alfentanil on propofol pharmacokinetics. Anesthesiology 2004;100:795-805.

20. Lichtenbelt BJ, Olofsen E, Dahan A, van Kleef JW, Struys M, Vuyk J. Propofol Reduces the Distribution and Clearance of Midazolam. Anesth Analg 2010;110:1597-1606.

21. Bouillon T, Bruhn J, Radu-Radulescu L, Bertaccini E, Park S, Shafer S. Non-steady state analysis of the pharmacokinetic interaction between propofol and remifentanil. Anesthesiology 2002;97:1350-1362.

22. Nara E, Saikawa A, Masegi M, Hashida M, Sezaki H. Contribution of interstitial diffusion in drug absorption from perfused rabbit muscle: effect of hyaluronidase on absorption. Chem Pharm Bull (Tokyo) 1992;40:737-740.

23. Ezzine S, Varin F. Interstitial muscle concentrations of rocuronium under steady-state conditions in anaesthetized dogs: actual versus predicted values. Br J Anaesth 2005;94:49-56.

24. Cameron KS, Fielding L. NMR diffusion coefficient study of steroid-cyclodextrin inclusion complexes. Magn Reson in Chem 2002;40:S106-S109.

25. Paaske WP, Sejrsen P. Transcapillary exchange of 14C-inulin by free diffusion in channels of fused vesicles. Acta Physiol Scand 1977;100:437-445.

26. Keiding S, Henriksen O, Sejrsen P. Muscle capillary permeability for [14C] inulin and [51Cr] EDTA in human forearm. Acta Physiol Scand 1988;133:335-342.

27. Law RO, Phelps CF The size of the sucrose, raffinose, and inulin spaces in the gastrocnemius muscle in the rat. J Physiol 1966;186:547-557.

28. Weiss M, Hübner GH, Hübner IG, Teichmann W. Effects of cardiac output on disposition kinetics of sorbitol: recirculatory modelling. Br J Clin Pharmacol 1996;41:261-268.

29. Beaufort TM, Proost JH, Houwertjes MC, Roggeveld J, Wierda J. The pulmonary first-pass uptake of five nondepolarizing muscle relaxants in the pig. Anesthesiology 1999;90:477-483.

30. Levitt DG. The pharmacokinetics of the interstitial space in humans. Clin Pharmacol 2003;3: 3.

31. Avram MJ, Krejcie TC, Henthorn TK, Niemann CU. Beta-adrenergic blockade affects initial drug distribution due to decreased cardiac output and altered blood flow distribution. J Pharmacol Exp Ther 2004;311: 617-624.

32. Schalla M, Weiss M. Pharmacokinetic curve fitting using numerical inverse Laplace transformation. Eur J Pharm Sci 1999;7:305-309.

6

Early Phase Pharmacokinetics of Propofol in Humans: the Role of the Lung Explored by Recirculatory Modeling

Marije Reekers, Fred Boer, Erik Olofsen, René A.G. Mooren, Albert Dahan, and Jaap Vuyk

Department of Anesthesiology, Leiden University Medical Center, Leiden, The Netherlands

Anesthesia & Analgesia: submitted.

Introduction

The pharmacology of the induction of anesthesia is still poorly understood and often roughly described using compartmental modeling. The inability to describe and predict the plasma concentration of a drug like propofol during induction of anesthesia may lead to under- or overdosing in various patient groups, leading to insufficient anesthetic effect or undesired side effects and is a problem that has been recognized in the anesthetic field.[1]

In contrast to compartmental modeling, the early disposition of induction agents may be better described using physiological based modeling techniques like recirculatory modeling, as is described in chapter 2 of this thesis. Unfortunately, for intravenous anesthetics data on this type of modeling are still scarce. Within the short timeframe of the induction of anesthesia the importance of cardiac output as driving force of drug distribution is generally accepted, while the role of the lung as a modulator of the peaks and troughs in blood drug concentration is still poorly understood. This is especially the case for the disposition of anesthetic agents in humans.

The role of the lung as a pharmacological entity that modulates drug disposition, biotransformation and elimination can be studied in vivo by inclusion of the lung as a separate compartment within the central blood compartment.[2] The central blood compartment includes the intravascular volume of the heart and the lungs combined, as well as that of the central arteries. Ideally, the characteristics of such a compartment are best studied when the drug concentrations (and metabolites) are measured in the volumes before, after and from the compartment itself.

The fast-acting intravenous hypnotic agent propofol is known to be primarily cleared and metabolized in the liver, but is also known to undergo renal metabolism and excretion.[3-5] The lungs play a significant role in the uptake of propofol, but so far, discrepancy[6-8] remains on the significance of metabolism of propofol in, or excretion from, the lungs. Because propofol is a volatile and highly lipophilic agent, diffusion into the alveoli after disposition in the pulmonary tissues is likely. This assumption has proven realistic[9-13], now that propofol is detected in the expired air, although the actual expired propofol concentration still remains difficult to quantify.

The scarcity of recirculatory data on propofol in humans and the uncertainty of the role of the lung in its pharmacokinetics has led us to study the early-phase

pharmacokinetics of propofol in healthy patients during induction of anesthesia. The aim of this study was 3-fold:

1. To describe the early-phase pharmacokinetics of propofol in humans.
2. To determine the role of the lung in the clearance and distribution of propofol.
3. To compare the predictive accuracy of a recirculatory pharmacokinetic model for propofol with compartmental models from the literature, which are used in daily practice to predict the blood propofol concentration during induction of anesthesia.

Methods

Patients

The study was performed after approval of the Medical Ethics Committee of the Leiden University Medical Centre and written informed consent. Ten patients, ASA status I or II scheduled for elective surgery were included in the study. Exclusion criteria included a BMI>30, a medical history of severe cardiovascular, respiratory, renal, hepatic, neurological or psychiatric disease, use of anti-hypertensive or anti-arrhythmic medication, pregnancy or lactation and a history of hypersensitivity to ICG.

Procedures

Prior to the study a cannula was inserted in a large vein in the fossa cubiti for fluid and drug administration. The radial artery was cannulated for the collection of arterial blood samples and intra-arterial blood pressure measurement and cardiac output monitoring through arterial pulse contour analysis with the LiDCO (LiDCO plus, LiDCO Ltd, Cambridge, UK). At every heart beat the arterial systolic blood pressure (SBP), diastolic blood pressure (DBP), mean arterial pressure, heart rate, cardiac output and stroke volume were gathered, provided the arterial cannula was not used for blood sampling. Peripheral oxygen saturation and pulse rate was measured using a finger probe. A second finger probe was applied for the transcutaneous measurement of ICG (DDG 2001, Nihon Kohden, Japan). Sedative data were gathered using the bispectral index score (BIS) (A-2000, Aspect Medical Systems, USA); the raw and processed electroencephalogram (EEG) data were transferred to a laptop computer every second. ECG monitoring was applied as well. Control blood samples were taken for the construction of reference aliquots and

determination of the hemoglobin level and sodium content, needed for the calibration of the LiDCO and DDG monitor. The LiDCO monitor was calibrated before each experiment by intravenous administration of 0.2 mmol lithium. The LiDCO monitor calibration was based on the non-invasive online determined arterial lithium concentration-time curve and the cardiac output calculated. The LiDCO has been studied and found acceptably reliable in cardiac output monitoring, when compared with traditional thermodilution cardiac output monitoring for up to 8 h after calibration (LidCO versus thermodilution: r = 0.86).[14,15]

Before the start of each experiment, baseline measurements of the arterial blood pressure, heart rate (HR), cardiac output (CO) and BIS were recorded for at least 15 min. After 3 min of preoxygenation with 100% O_2, each session started with the rapid intravenous administration of propofol 3 $mg.kg^{-1}$, mixed with 10 mg of ICG (Infracyanine®, Laboratoire SERB, France). The propofol/ICG bolus was immediately followed by a rapid bolus of 20 ml of NaCl 0.9%. A computer-controlled syringe pump combined with a fraction collector was programmed to draw 37 arterial blood samples in the first 2.5 min after propofol administration at 0, 3, 6, 9, 12, 15, 18, 21, 24, 27, 30, 33, 36, 39, 42, 45, 48, 51, 54, 57, 60, 63, 66, 69, 72, 75, 78, 81, 84, 87, 90, 100, 110, 120, 130, 140, and 150 sec. Due to the construction of the sampling device, no mixing in the tubing could occur, as has been described before[16] (Figure 1). Five more blood samples were drawn manually at 3, 4, 5, 7.5 and 10 min after administration of the ICG bolus dose. During manual sampling, a waste sample was drawn first. The blood samples were collected in heparinized glass tubes and processed immediately.

Measurements of ICG and propofol in blood

The concentrations of ICG and propofol were determined in series in heparin whole blood using High Performance Liquid Chromatography (HPLC) (Separations analytical instruments, Hendrik-Ido-Ambacht, The Netherlands; column: Ultrasphere ODS 4,6 x 7.5 cm 244254, Beckman Coulter, Mijdrecht, The Netherlands) with ultraviolet and fluorescence detection for respectively ICG and propofol. Thymol was used as the internal standard for both compounds and was measured by fluorescence detection. For each patient a calibration curve was constructed, using the patients own blood prior to injection of ICG and propofol. The blood was deproteinized with acetonitril and the supernatance was injected on the HPLC. The fluorescence settings were as follows; excitation at a wavelength of 275 nm and the emission wavelength at 310 nm with a gain of 10 to measure propofol. ICG was measured at

785 nm, its peak in the spectrum, on the PDA 100. Both ICG and its degradation product were identified by this diode array (Photodiodedetector PDA 100, Dionex, Amsterdam, The Netherlands). The detection limit of the whole blood assay for ICG was at 0.2 $mg.L^{-1}$ and at 0.5 $mg.L^{-1}$ for propofol. The coefficient of variation was less than 8 % over the range from 0.5 to 10.45 $mg.L^{-1}$ for ICG and less than 4 % in the range of 1 to 90 $mg.L^{-1}$ for propofol.

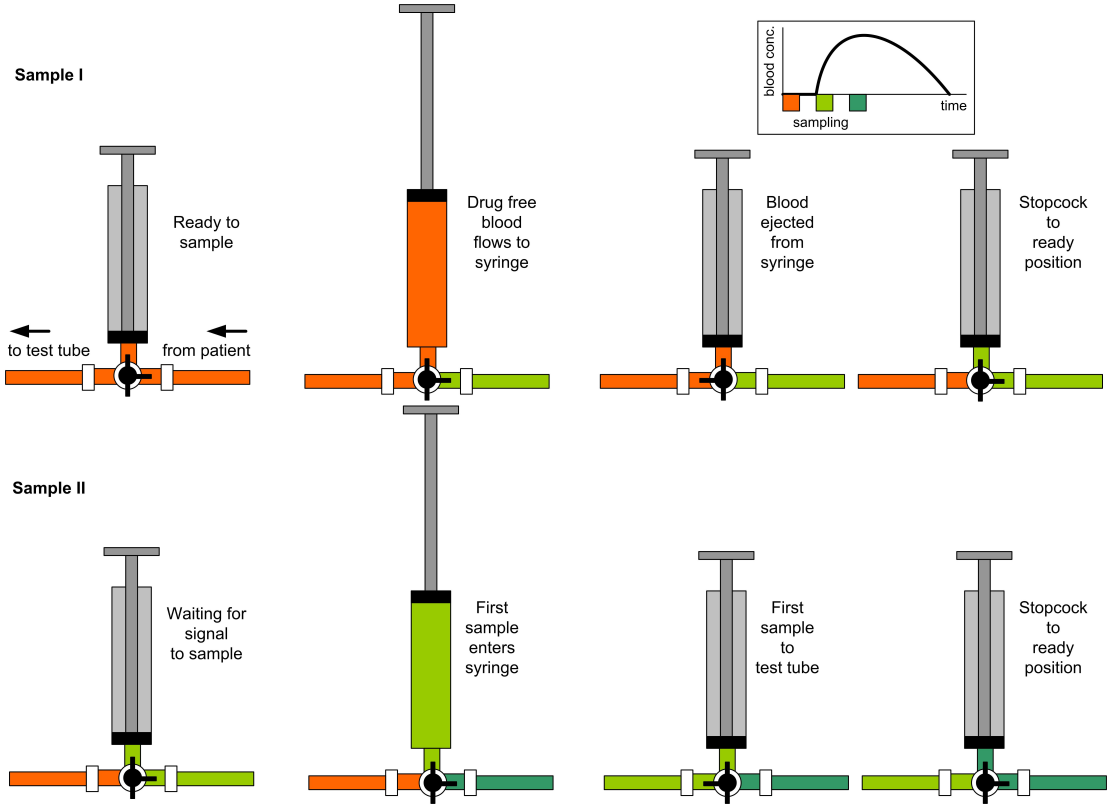

Figure 1 Schematic representation of the syringepump, in which the tubing and stopcock construction is represented. Since the volume that is aspirated by the syringe equals the volume in the tubing, no mixing of the blood samples can occur.

Data collection and processing

BIS and raw EEG data were transferred to a laptop and imported into a spreadsheet program (Excel 2000, Microsoft Corporation, Seattle, U.S.A.). The same applied for the hemodynamic data derived from the LiDCO monitor, including arterial blood pressure and cardiac output, as well as for arterial blood ICG-concentrations, to undergo further analysis.

Pharmacokinetic modeling

A recirculatory model, in analogy to the model described for determination of lung uptake and pulmonary clearance of propofol in sheep[17]and explained in chapter 2 of this thesis, was constructed using the indicator ICG to estimate the intravascular compartment. The model for ICG contained a central part, consisting of two parallel pathways, modeled by n tanks-in-series (Figure 1). To account for the delay observed between injection of the bolus ICG and the detection of any amount of ICG, a lag-time was incorporated into the model as an extra delay element: T_{lag}. Cardiac output was calculated by dividing the administered ICG dose by the area under the first pass concentration-time curve (A_1+A_2; see below). The shape of the first pass concentration-time curve, including all data before evidence of ICG recirculation, was described by the sum of two Erlang functions, each representing the convolution of n 1-compartment models connected in series[18]

$$C(t) = A_1 * \frac{k_1^{n_1} t^{n_1-1}}{(n_1-1)!} + A_2 * \frac{k_2^{n_2} t^{n_2-1}}{(n_2-1)!}$$

where n_1 and n_2 are the number of compartments in series in the central delay elements; k_1 and k_2 are the rate constants between the compartments in series; n_1/k_1 and n_2/k_2 are the mean transit times of the central delay elements; A_1 and A_2 are the areas under the first pass concentration-time curves. The two Erlang functions were fitted to the data using the solver function in Excel (Microsoft Corporation, Seattle, U.S.A.), whereby data were uniformly weighted. The lag-time and parameters simulating the first-pass curve (T_{lag}, $V_{C(f+s)}$ and $MTT_{C(f+s)}$) were then transferred to the SAAM program (SAAM II, version 1.1.1, SAAM Institute, University of Washington, USA) to further analyze the peripheral part of the systemic circulation, including recirculation. This part consisted of two parallel pathways as well, defined by their respective volumes ($V_{ND(f+s)}$) and clearances ($Cl_{ND(f+s)}$). Combined with the elimination clearance Cl_{EL} the summed clearances equaled the cardiac output.

The model for propofol was constructed in a similar way, meaning that the data before recirculation of ICG were fitted by two Erlang-functions. The lag-time was fixed from the ICG data. Then, the parameters were transferred to the SAAM program. For the model of propofol a single tissue compartment was added, in analogy to drug modeling described by Henthorn et al.[19], since only a short period after recirculation was studied (Figure 2). The ratio between the peripheral systemic circulation pathways (ND-f and ND-s) was kept identical to

this ratio determined for ICG. Lung retention at first-pass was determined as described before.[20,21]

Comparison to other pharmacokinetic datasets

For comparison of the accuracy of the pharmacokinetic parameters found in this study in relation to the pharmacokinetic parameter sets reported in literature, the 2 parameter sets were selected that are clinically used in the target controlled infusion (TCI) systems for propofol and are commercially available. These are the parameter set described by Marsh[23], which is incorporated in the Diprifusor® system (AstraZeneca), and the parameter set described by Schnider[24], which is incorporated in the Orchestra Base Primea® system (Fresenius Kabi ltd). For both pharmacokinetic parameter sets the predicted plasma concentration-time curve of propofol was simulated, based on the administration of an instantaneous bolus of 201.3 mg of propofol to a woman of 42 years of age, weighing 67 kg, and with a length of 1.72 m (our average patient with the average dose administered). Simulation was performed using the Tivatrainer©(F.H.M. Engbers, LUMC, Leiden, the Netherlands).

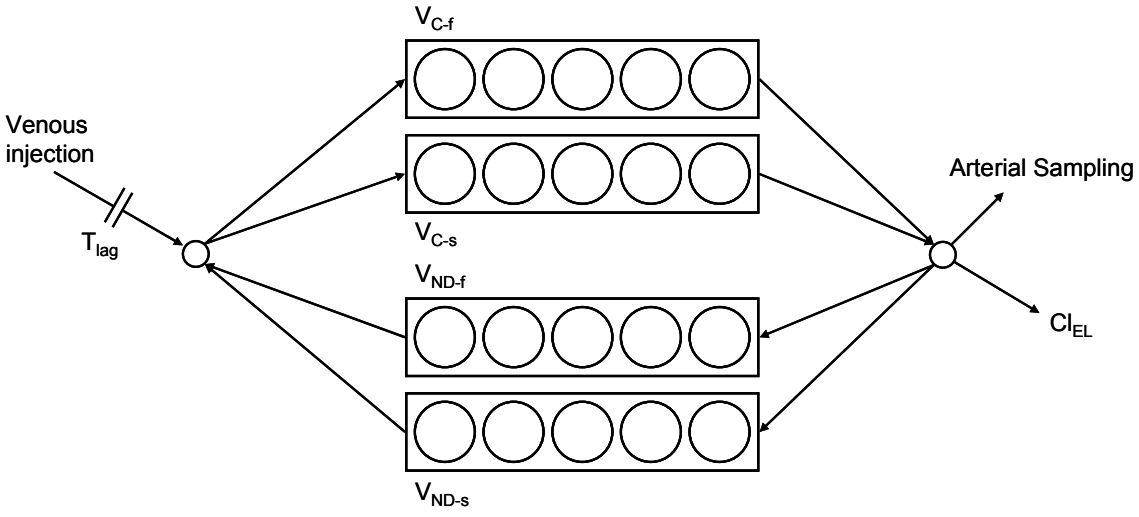

Figure 2 Intravascular part of the recirculatory model, used to fit the ICG data. The model consists of a delay element representing the venous lag time (T_{lag}), two parallel central pathways represented by a varying number of tanks-in-series (a fast $V_{C\text{-}f}$ and slow $V_{C\text{-}s}$) and two parallel non-distributive peripheral compartments (a fast $V_{ND\text{-}f}$ and slow $V_{ND\text{-}s}$). Cl_{EL} is the elimination clearance.

Statistical analysis

Descriptive statistics were generated by the SPSS statistical package (SPSS, version 17). Parameters were tested for normality using the Kolmogorov-Smirnov test. Any parameter that was not normally distributed was tested for normal distribution after log transformation. If the log transformed parameters proved to be normally distributed, the mean and standard error of the mean (SEM) were thereafter transformed back using the following equations: mean = $e^{\mu+\sigma\text{^}2/2n}$ and SEM = $\sqrt{((e^{\sigma\text{^}2/n}-1)e^{2\mu+\sigma\text{^}2/n})}$. Linear regression analysis was performed using the same statistical package. Statistical significance was assumed at $p<0.05$. Data are described as mean ± SD, unless reported otherwise.

Results

Patients

The 10 patients included were 2 males and 8 females, who were aged 42.2 ± 8.7 yr, weighed 67.1 ± 11.8 kg, were 1.72 ± 0.1 m with a body mass index of 22.5 ± 2.2 $kg.m^{-2}$. The induction of anesthesia with the intravenous bolus dose of propofol (3 $mg.kg^{-1}$) resulted in a rapid loss of consciousness in all patients with a lowest BIS of 24 ± 9, measured at 75 (60-115) seconds (median and range) after the intravenous administration of propofol. All patients had to be ventilated by mask. With again decreasing blood propofol concentrations and sedative levels, BIS reached a mean of 72 before the data collection was terminated. Data collection was terminated after sufficient data was gathered to allow recirculatory modeling of propofol pharmacokinetics but before return to consciousness. After termination of the study, anesthesia was continued with propofol, remifentanil and atracurium and the trachea was intubated. The patients then were ready for their scheduled surgical procedure. The study was completed without any adverse event. No patients reported any signs of awareness. All blood samples were analyzed within 12 weeks.

The mean peak arterial plasma ICG and peak arterial blood propofol concentration occurred at 18 and 21 sec past administration, respectively, reflecting the equally rapid distribution of ICG and propofol. Examination of the propofol-concentration time data revealed that the peak arterial blood propofol concentration, with an average of 88 ± 17 $\mu g.ml^{-1}$, profoundly exceeded that generally considered sufficient for surgical anesthesia (EC_{50} for loss of consciousness 3.4 $\mu g.ml^{-1}$)[25], reflecting the poor initial mixing of propofol in the

vascular compartment. The pharmacokinetic parameters of ICG are displayed in Table 1. The cardiac output in these healthy volunteers was close to 7 $L.min^{-1}$, equivalent to the sum of clearances of ICG. Furthermore, ICG elimination clearance was 1.19 $L.min^{-1}$, smaller but close to the assumed hepatic blood flow of 1.35 $L.min^{-1}$, reflecting the sole elimination of ICG through hepatic elimination.

Recirculatory modeling

The concentration-time data for ICG were modeled by the classic recirculatory model for the central circulation as discussed in chapter 2 of this thesis, with the addition of a venous lag time (T_{lag}) to correct for the delay of the drug transfer from the venous injection point to the right atrium. The parameters determined for ICG are represented in table 1. All parameters were distributed normally or lognormally. Parameters that were transformed back from logtransformation were V_{ND-s}, V_{SS}, MTT_C and MTT_{ND-f}. The model for the central compartment is represented in figure 2.

For the modeling of the propofol concentration-time data, the recirculatory model that provided the best fit was selected following visual inspection and application of the Akaike criterion. The resulting recirculatory model consisted of two parallel tanks-in-series representing the central compartment including the lungs. The propofol concentration-time data before recirculation of propofol was observed, were analyzed separately using Erlang functions. This procedure is similar as is described for the modeling of the central compartment for ICG. The cardiac output and venous lag time were fixed according to the ICG model for each patient. No elimination from the pulmonary compartment could be determined. As a consequence, the pulmonary volume acted as a distribution volume and was determined as the difference in volumes of the central compartments determined for ICG and propofol. The peripheral part of the model consists of two parallel non-distributive pathways, a slow (ND-s) and a fast one (ND-f), defined by their volumes and clearances, and is completed by a peripheral distributive tissue compartment as can be seen in figure 3.

The non-distributive compartments represent the part of the intravascular compartment outside the thorax and may represent vascular beds like the great vessels and the splanchnic vascular bed. The ratio between the fast and the slow intravascular pathway was kept equal for the ICG and the propofol model. The parameters for the recirculatory propofol model are presented in table 1 as well. All parameters were distributed normally or lognormally (Cl_{ND-f}). The

parameter Cl_{ND-f} was transformed back after logtransformation. The individual fits for the ICG and propofol concentration-time curves for the 10 patients show that the predicted ICG and propofol concentrations very closely correspond to those actually measured (Figure 4). Linear regression analysis showed good correlation between the measured and predicted blood propofol concentrations (R^2 = 0.959; p<0.001, Figure 5).

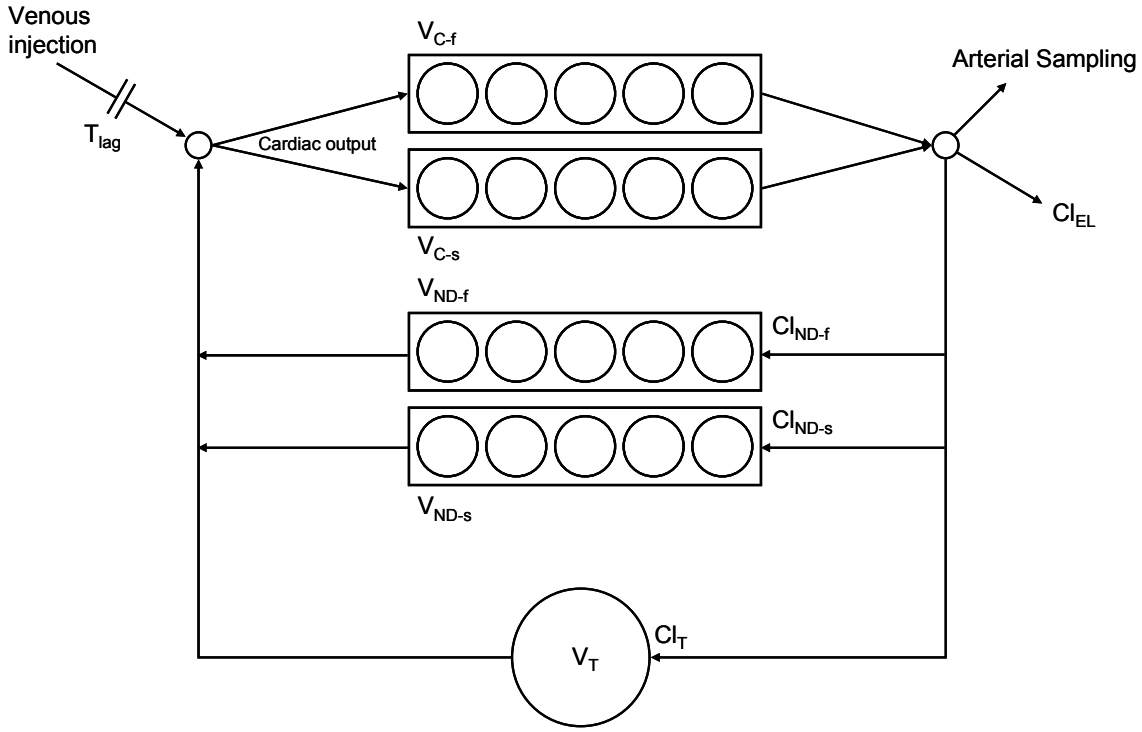

Figure 3 Representation of the recirculatory model used to fit the propofol concentration data. The intravascular compartment as described for ICG in figure 1 is extended with a peripheral tissue compartment V_T. The ratio between the flows (Cl_{ND-f} and Cl_{ND-s}) to the non-distributive compartments V_{ND-f} and V_{ND-s} is kept equal to that determined for ICG. The total of all clearances equals the cardiac output.

The propofol concentrations predicted by the pharmacokinetic models as described by Marsh[23] and Schnider[24], based on the simulated administration of a bolus propofol dose, are represented in figure 6. Plasma concentrations were simulated for the average bolus administered to a female patient with the average characteristics from our study population. The simulated plasma concentration curves are plotted against all plasma concentrations determined in our study. The curve constructed from the recirculatory pharmacokinetic parameters in our study is represented by the solid line in figure 6. The peak

blood propofol concentrations detected in our study by rapid sampling were almost 10 times higher as predicted by the Marsh model and twice as high as predicted by the Schnider model.

Table 1 Pharmacokinetic parameters found for the ICG and propofol model, stating volumes (V) in L, clearances (Cl) in $L.min^{-1}$ and mean transit times (MTT) in min for the central ($_C$), non-distributive fast ($_{ND-f}$), non-distributive slow ($_{ND-s}$), tissue ($_T$) and pulmonary ($_P$) compartment, as well as the steady state volume (V_{SS}) and the elimination clearance (Cl_{EL}) and cumulative clearance ($\sum Cl$), which equals the cardiac output. T_{lag} represents the venous lag time. At the bottom row the lung retention in represented in %. Parameters are stated as mean with their standard error of the mean (SEM).

	ICG		**propofol**	
parameter	**mean**	**SEM**	**mean**	**SEM**
V_C	1.71	0.20	2.31	0.17
V_{ND-f}	0.88	0.09	0.28	0.07
V_{ND-s}	1.68	0.18	0.22	0.05
V_P			0.60	0.11
V_T			9.90	1.39
V_{SS}	4.22	0.35	12.71	1.41
Cl_{EL}	1.19	0.11	3.38	0.23
Cl_{ND-f}	4.67	0.52	0.89	0.14
Cl_{ND-s}	1.12	0.15	0.25	0.05
Cl_T			2.33	0.21
$\sum Cl$	6.98	0.47	6.98	0.47
MTT_C	0.24	0.03	0.34	0.03
MTT_{ND-f}	0.19	0.03	0.30	0.05
MTT_{ND-s}	1.78	0.26	0.93	0.11
MTT_T			4.29	0.54
T_{lag}	0.13	0.02	0.08	0.02
lungretention(%)			25.68	2.06

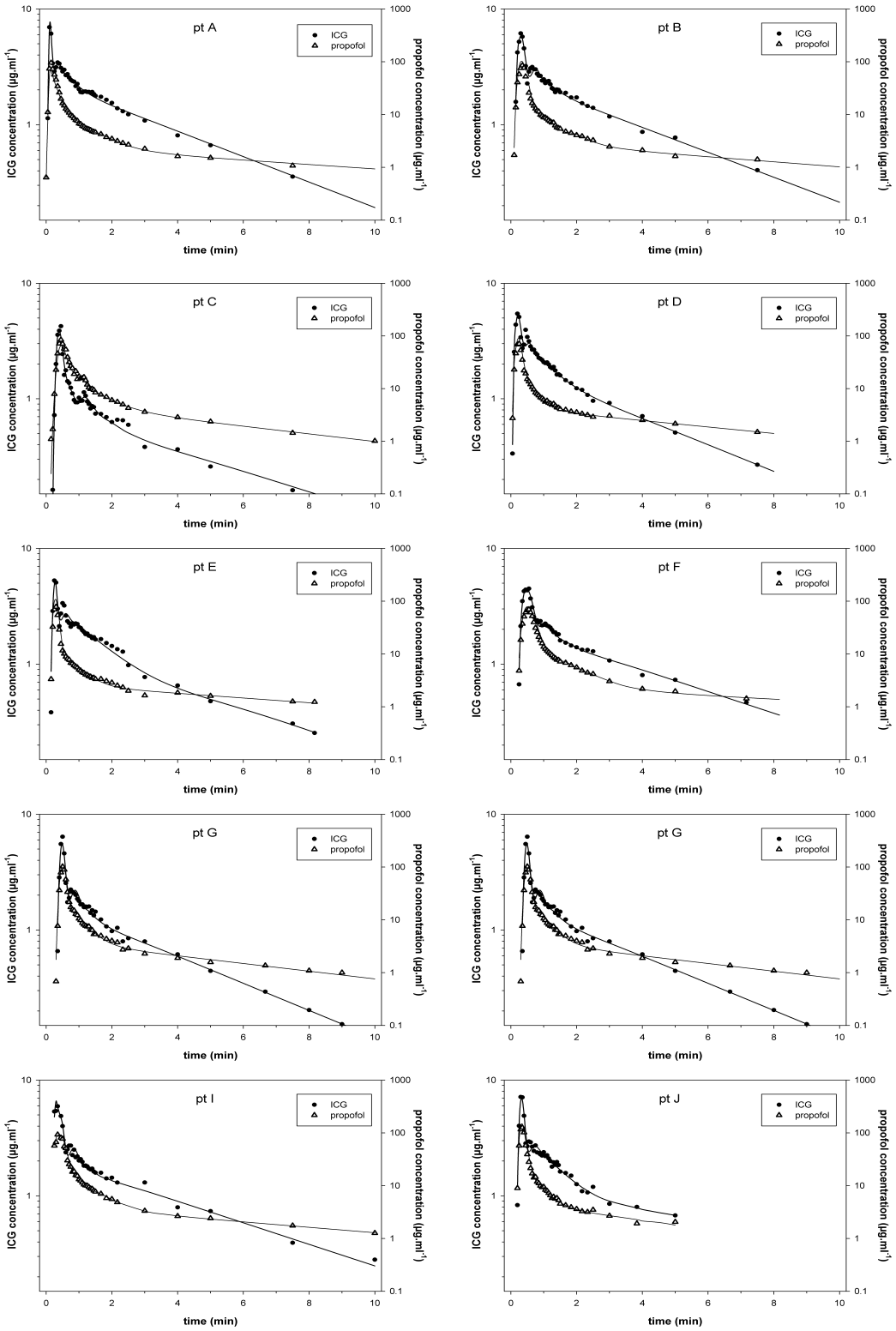

Figure 4 Individual fits of the blood concentration data of Indocyanine Green (●) and propofol(Δ) in each patient. On the horizontal axis the time in min, on the vertical left axis the ICG concentration and on the right vertical axis the propofol concentration in $\mu g.ml^{-1}$.

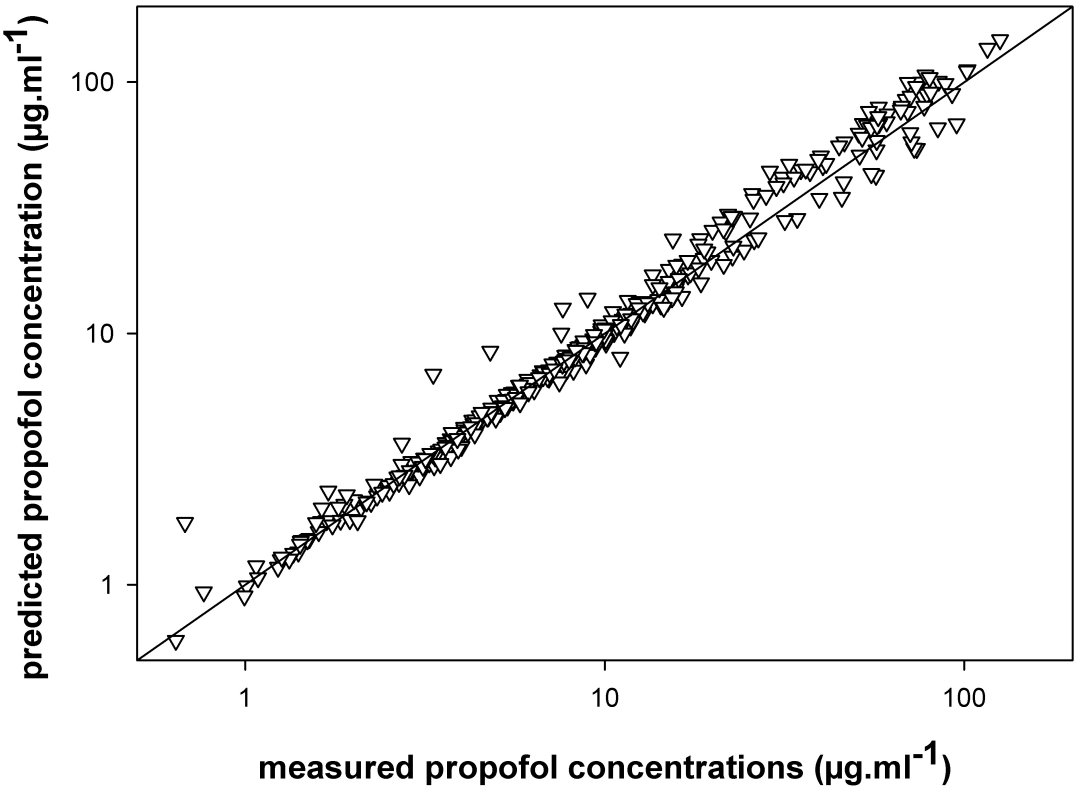

Figure 5 Correlation of the measured versus predicted data for propofol. The regression formula is prop predicted= -424.7 + (1.112 * prop measured). The R^2 equals 0.959; p<0.001. The line in the graph is the line of equality (y=x).

Discussion

We studied the recirculatory pharmacokinetics of propofol with the aims to:

1. Closely evaluate the early-phase concentration-time relationship of propofol during induction of anesthesia.
2. To determine the role of the lung in the clearance and distribution of propofol.
3. To compare the predictive accuracy of a recirculatory propofol pharmacokinetic model with compartmental models from the literature.

We conclude that propofol, after bolus administration, exhibits blood concentrations that profoundly exceed those related to the hypnotic effect reflecting its poor initial mixing. We conclude that propofol shows no clinical relevant clearance from the lung. Lastly, we demonstrate that compartmental models, now widely used in anesthetic practice in target controlled infusion

pumps, significantly underestimate the actual blood propofol concentration in the first minutes after induction of anesthesia.

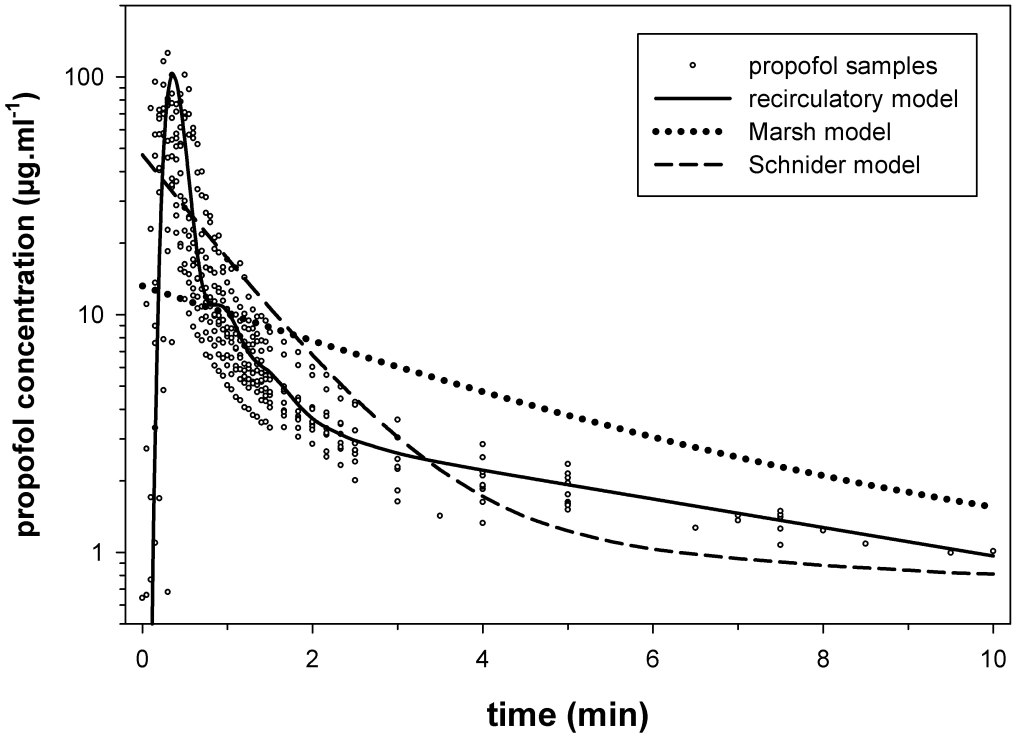

Figure 6 Simulations of the concentration-time curves of propofol after administration of an intravenous bolus of 201 mg to a female of 42 yrs, weight 67 kg and height 1.72 m (averages in our study population) based on different pharmacokinetic models. The open circles represent all propofol blood samples in our study. The dotted curve is a simulation based on pharmacokinetics from the Marsh[23] model; the propofol concentrations are underestimated in the peak and overestimated in the elimination phase. The striped curve is a simulation based on the pharmacokinetic model by Schnider[24], which performs better, but still underestimates peak concentrations and those in the elimination phase. The solid line represents the simulation based on our average pharmacokinetic parameters from the recirculatory model.

This recirculatory model compared to existing model.

So far, the only recirculatory pharmacokinetic model for propofol in humans available was that by Upton et al.[26], who gathered data from various sources to describe and model the distribution and elimination of propofol. Although we acknowledge the uniqueness of this model, various assumptions and estimates were necessary to develop this model that was accomplished after combining the data of many authors. In particular, not all parameters were determined

based on the available data but some parameters had to be estimated based on "known physiology". In addition to the uncertainty involved with combining data from various sources, also the results presented by Upton, though very worthy form a physiological point of view, offer little clues to be implemented directly and associated to the clinical dose-concentration-effect relationship of propofol. Because, apart from Upton et al., only animal data were available on the recirculatory pharmacokinetics of propofol we studied the recirculatory pharmacokinetics in humans.

Modeling of the pulmonary compartment

The role of the lungs in the early phase of mixing and distribution of propofol into deeper tissue compartments remained yet not fully understood. Consensus exists in that the liver is the main organ of biotransformation and elimination of propofol, partly due to its high extraction ratio of up to 0.9. However, during the anhepatic phase in liver transplantations, extrahepatic clearance of propofol has been demonstrated. Also total body clearance exceeds the hepatic blood flow. To explore the role of the lung, recirculatory modeling of our data for propofol was initiated in analogy to the model described by Kuipers et al.[17] regarding the propofol recirculatory pharmacokinetics in sheep. In the sheep model pulmonary uptake was modeled by a distribution compartment placed in series with the tanks-in-series. For the description of lung uptake in our patients the addition of a distribution compartment, either parallel or in series, did not result in an adequate description of the concentration time curves for propofol. Yet, these curves of propofol and ICG were different, indicating a delay of propofol in the lungs. Pulmonary elimination could not be discerned from distribution or central elimination. Therefore a model for propofol was constructed in which pulmonary distribution was described by tanks-in-series only (Figure 1) to indicate a delay in the appearance of drug molecules at the effluent side of the organ. This delay is inhomogeneous compared to a fixed delay (expressed in sec). The pulmonary volume was determined as the difference between the combined volumes of the fast and slow central compartments for ICG and propofol.[19] Also the mean transit times for ICG and propofol through the central compartment differed.

The pulmonary first-pass uptake of propofol in our patients of 25.7 ± 6.5% is in agreement with the 28% reported earlier by He et al.[27], however small compared to other intravenous drugs used in anesthesia, such as fentanyl, sufentanil or other basic amines.[28] Despite the fact that propofol is highly lipophilic, the first pass lung uptake is relatively low. To be retained in the lungs, the drug in the lung tissue must be bound or otherwise hindered in the back

release to the blood. One mechanism that may be involved in this, is that the drug is ionized. This mechanism probably plays a significant role for basic amines, in which cellular depots possibly play a role.[29,30] Despite the fact that propofol is highly lipophilic, its pKa of 11 makes it more ionized than the basic amines, resulting in less retention in the lungs. That propofol can penetrate in due time in deeper compartments has been shown by Grossherr and co-workers, who could detect propofol in epithelial line fluid.[31]

Propofol lung uptake has been described in cats[32], sheep[17] and goats and pigs.[33] Pulmonary uptake and more importantly clearance is disputed in humans.[6,27,34] The lungs have been viewed as a possible site of clearance because propofol is detectable in exhaled air.[9-11,13] Yet, the quantities exhaled by the lungs are expressed in parts per billion that are detected by very sensitive equipment. These quantities multiplied by the exhaled minute volume embody a very small amount compared to the quantities delivered by the venous blood through the cardiac output. In mechanically ventilated patients undergoing cardiac surgery, Grossherr and coworkers [12] measured 2.8 and 22.5 ppb in exhaled air while the concurrent blood concentrations were 0.3 and 3.3 µg/ml. From these and our data we conclude that propofol clearance by exhaling air is clinically insignificant. We assume that propofol is bound to the vascular tissues (endothelial lining) but that propofol does not transfer to “deep” compartments in the lungs. This would explain that a distribution compartment cannot be fitted and that propofol is better described using a dispersion model (tanks-in-series). We suspect that other sites of extrahepatic clearance are more important than the lungs and especially the kidneys are good candidates. Renal excretion of propofol and its metabolites has been demonstrated with a high renal extraction ratio of 0.6 to 0.7[3,4], leading to a renal clearance of almost up to 30% of the total body clearance.

This recirculatory model compared to compartmental models

The comparison of the predicted propofol concentrations based on the recirculatory pharmacokinetic model, with those predicted as based on the compartmental models by Marsh and Schnider, revealed a significant underestimation of the peak concentrations and an overestimation of the plasma concentration around the time of recirculation by compartmental models, as seen in figure 6. The fact that standard compartmental models poorly predict early-phase kinetics has been recognized before.[19,35] Recently, an adaptation of a compartmental model by inclusion of a lag time and transit elements was introduced by Masui et al.[36] Although this model performed better than the ones tested here, underestimation of the peak concentration

remained. These misrepresentations may have clinical implications indeed. Underestimation of the propofol blood concentration may result in unnecessary overdosing of propofol and aggravated hemodynamic depression when propofol is administered by TCI based on compartmental pharmacokinetic models. On the other hand can an overestimation of the propofol blood concentration lead to insufficient sedation and increase the chance of awareness of the patient.

In conclusion, we successfully described the pharmacokinetics of propofol by recirculatory modeling. After bolus administration, propofol exhibits blood concentrations that greatly exceed those related to hypnotic effect, reflecting its poor initial mixing. We conclude that propofol shows no clinical relevant clearance from the lung. Lastly, we demonstrated that compartmental models, now widely used in anesthetic practice in target controlled infusion pumps, significantly underestimate the actual blood propofol concentration in the first minutes after induction of anesthesia.

References

1. Avram MJ, Krejcie TC. Using front-end kinetics to optimize target-controlled drug infusions. Anesthesiology 2003;99:1078-86.
2. Krejcie TC, Henthorn TK, Niemann CU, et al. Recirculatory pharmacokinetic models of markers of blood, extracellular fluid and total body water administered concomitantly. J Pharmacol Exp Ther 1996;278:1050-7.
3. Hiraoka H, Yamamoto K, Miyoshi S, et al. Kidneys contribute to the extrahepatic clearance of propofol in humans, but not lungs and brain. Br J Clin Pharmacol 2005;60:176-82.
4. Takizawa D, Hiraoka H, Goto F, et al. Human kidneys play an important role in the elimination of propofol. Anesthesiology 2005;102:327-30.
5. Bleeker C, Vree T, Lagerwerf A, Willems-van BE. Recovery and long-term renal excretion of propofol, its glucuronide, and two di-isopropylquinol glucuronides after propofol infusion during surgery. Br J Anaesth 2008;101:207-12.
6. Chen YZ, Zhu SM, He HL, et al. Do the lungs contribute to propofol elimination in patients during orthotopic liver transplantation without veno-venous bypass? Hepatobiliary Pancreat Dis Int 2006;5:511-4.
7. Dawidowicz AL, Fornal E, Mardarowicz M, Fijalkowska A. The role of human lungs in the biotransformation of propofol. Anesthesiology 2000;93:992-7.
8. He YL, Ueyama H, Tashiro C, et al. Pulmonary disposition of propofol in surgical patients. Anesthesiology 2000;93:986-91.

9. Hornuss C, Praun S, Villinger J, et al. Real-time monitoring of propofol in expired air in humans undergoing total intravenous anesthesia. Anesthesiology 2007;106:665-74.

10. Takita A, Masui K, Kazama T. On-line monitoring of end-tidal propofol concentration in anesthetized patients. Anesthesiology 2007;106:659-64.

11. Harrison GR, Critchley AD, Mayhew CA, Thompson JM. Real-time breath monitoring of propofol and its volatile metabolites during surgery using a novel mass spectrometric technique: a feasibility study. Br J Anaesth 2003;91:797-9.

12. Grossherr M, Hengstenberg A, Meier T, et al. Propofol concentration in exhaled air and arterial plasma in mechanically ventilated patients undergoing cardiac surgery. Br J Anaesth 2009;102:608-13.

13. Perl T, Carstens E, Hirn A, et al. Determination of serum propofol concentrations by breath analysis using ion mobility spectrometry. Br J Anaesth 2009;103:822-7.

14. Hamilton TT, Huber LM, Jessen ME. PulseCO: a less-invasive method to monitor cardiac output from arterial pressure after cardiac surgery. Ann Thorac Surg 2002;74:S1408-S1412.

15. Jonas MM, Tanser SJ. Lithium dilution measurement of cardiac output and arterial pulse waveform analysis: an indicator dilution calibrated beat-by-beat system for continuous estimation of cardiac output. Curr Opin Crit Care 2002;8:257-61.

16. Reekers M, Simon MJ, Boer F, et al. Cardiovascular monitoring by pulse dye densitometry or arterial indocyanine green dilution. Anesth Analg 2009;109:441-6.

17. Kuipers JA, Boer F, Olieman W, et al. First-pass lung uptake and pulmonary clearance of propofol: assessment with a recirculatory indocyanine green pharmacokinetic model. Anesthesiology 1999;91:1780-7.

18. Avram MJ, Krejcie TC, Niemann CU, et al. The effect of halothane on the recirculatory pharmacokinetics of physiologic markers. Anesthesiology 1997;87:1381-93.

19. Henthorn TK, Krejcie TC, Avram MJ. Early drug distribution: a generally neglected aspect of pharmacokinetics of particular relevance to intravenously administered anesthetic agents. Clin Pharmacol Ther 2008;84:18-22.

20. Jorfeldt L, Lewis DH, Lofstrom JB, Post C. Lung uptake of lidocaine in healthy volunteers. Acta Anaesthesiol Scand 1979;23:567-74.

21. Geddes DM, Nesbitt K, Traill T, Blackburn JP. First pass uptake of 14C-propranolol by the lung. Thorax 1979;34:810-3.

22. Boer F, Bovill JG, Burm AG, Mooren RA. Uptake of sufentanil, alfentanil and morphine in the lungs of patients about to undergo coronary artery surgery. Br J Anaesth 1992;68:370-5.

23. Marsh B, White M, Morton N, Kenny GN. Pharmacokinetic model driven infusion of propofol in children. Br J Anaesth 1991;67:41-8.

24. Schnider TW, Minto CF, Gambus PL, et al. The influence of method of administration and covariates on the pharmacokinetics of propofol in adult volunteers. Anesthesiology 1998;88:1170-82.

25. Vuyk J, Engbers FH, Lemmens HJ, et al. Pharmacodynamics of propofol in female patients. Anesthesiology 1992;77:3-9.

26. Upton RN, Ludbrook G. A physiologically based, recirculatory model of the kinetics and dynamics of propofol in man. Anesthesiology 2005;103:344-52.

27. He YL, Ueyama H, Tashiro C, et al. Pulmonary disposition of propofol in surgical patients. Anesthesiology 2000;93:986-91.

28. Boer F. Drug handling by the lungs. Br J Anaesth 2003;91:50-60.

29. Upton RN, Doolette DJ. Kinetic aspects of drug disposition in the lungs. Clin Exp Pharmacol Physiol 1999;26:381-91.

30. MacIntyre AC, Cutler DJ. The potential role of lysosomes in tissue distribution of weak bases. Biopharm Drug Dispos 1988;9:513-26.

31. Grossherr M, Hengstenberg A, Meier T, et al. Discontinuous monitoring of propofol concentrations in expired alveolar gas and in arterial and venous plasma during artificial ventilation. Anesthesiology 2006;104:786-90.

32. Matot I, Neely CF, Katz RY, Neufeld GR. Pulmonary uptake of propofol in cats. Effect of fentanyl and halothane. Anesthesiology 1993;78:1157-65.

33. Grossherr M, Hengstenberg A, Dibbelt L, et al. Blood gas partition coefficient and pulmonary extraction ratio for propofol in goats and pigs. Xenobiotica 2009;39:782-7.

34. Dawidowicz AL, Fornal E, Mardarowicz M, Fijalkowska A. The role of human lungs in the biotransformation of propofol. Anesthesiology 2000;93:992-7.

35. Krejcie TC, Avram MJ. What determines anesthetic induction dose? It's the front-end kinetics, doctor! Anesth Analg 1999;89:541-4.

36. Masui K, Kira M, Kazama T, et al. Early phase pharmacokinetics but not pharmacodynamics are influenced by propofol infusion rate. Anesthesiology 2009;111:805-17.

7

Recirculatory Pharmacokinetic-Pharmacodynamic Modeling of Propofol in Man

Marije Reekers, Fred Boer, Erik Olofsen, René A.G. Mooren, Albert Dahan, and Jaap Vuyk

Department of Anesthesiology, Leiden University Medical Center, Leiden, The Netherlands

Introduction

Induction of anesthesia with an intravenous hypnotic agent like propofol can be achieved by administration of a manual bolus followed by a continuous infusion, with an infusion rate based on (lean) body weight, age and/or sex, or by using a computer controlled infusions systems for Target Controlled Infusion (TCI). In everyday practice a large interindividual variability in the induction phase can be observed, with variation in time to loss of consciousness, depth of sedation, and incidence and magnitude of respiratory and hemodynamic side effects, as has been reviewed in the Cochrane review by Leslie et al.[1] This variation is explained by the interindividual variability in pharmacokinetics and pharmacodynamics within the population. The origin of variability lies in the influence of age, weight, body composition, gender, comorbidities, hemodynamic variability like cardiac output, but also pharmacogenomics.[2] During induction or maintenance of anesthesia, interaction with co-administered drugs like opioids, is evident.[3,4] Opioids increase the blood concentration of co-administered hypnotic agents and shift the dose-reponse relationship of hypnotic agents to the left via pharmacodynamic interaction.[5,6]

With the introduction of PK-PD modeling by Sheiner and colleagues[7], the concept of the effect-site has been introduced: a virtual compartment that is coupled to the intravascular compartment via the transfer constant k_{e0} since the effect compartment has no apparent volume. Conventional 3-compartment models generally underpredict the intravascular drug concentration following a bolus induction dose of fast acting drugs like propofol see also chapter 2. In the study on early-phase pharmacokinetics of propofol described in chapter 6 of this thesis, we presented a recirculatory pharmacokinetic model for propofol in humans. In that study we simulated the blood concentration-time curve of a propofol bolus dose of 3 mg/kg as based on 2 pharmacokinetic parameter sets that are implemented in the commercially available TCI systems for propofol: the parameter set of Marsh[8] in the Diprifusor™ by AstraZeneca and the parameter set of Schnider[9] in the Orchestra Base Primea™ by Fresenius Kabi. Through these simulations we demonstrated that the peak concentrations of propofol after the administration of a bolus of 3 $mg.kg^{-1}$ could be well predicted by our recirculatory model, but were significantly underestimated by the other PK sets.

During TCI both the effect-site concentration may be targeted, as well as the plasma site, depending on the PK-PD parameter sets available in the device. When applying effect site concentration as the target concentration, ideally, the

implemented effect site equilibration half-life is determined in the same population as the pharmacokinetic parameters are, as is the case for the Schnider effect site TCI (k_{e0} of 0.456 min^{-1}).[9] This is not the case for the Marsh-effect site TCI (k_{e0} of 0.26 min^{-1})[10], as is used in the Diprifusor™. In targeting the effect-site concentration, the pharmacodynamic variability is superimposed upon the pharmacokinetic variability and/or inaccuracy of the pharmacokinetic model.

Knowing the poor prediction of the blood drug concentration by compartmental models in the early-phase after a bolus drug dosing, we explored the effect-site equilibration of propofol as based on recirculatory modeling with the bispectral index (BIS) as effect parameter and compared this to the effect-site equilibration of propofol as described by the compartmental models of Marsh and Schnider et al.

Methods

Patients and Procedures

The concentration-time-effect data used in this study were gathered during the study on early-phase pharmacokinetics of propofol as described in chapter 6. In this study, with approval of the Medical Ethics Committee of the Leiden University Medical Centre and written informed consent, the propofol dose-concentration-effect data of 10 patients, ASA physical status I or II scheduled for elective surgery, were studied. Based on highly frequent arterial blood sampling during the first minutes after administration of an iv bolus of 3 $mg.kg^{-1}$ of propofol, we developed a recirculatory model, using indocyanine green as a marker for the intravascular compartment.

Data collection

Prior to the study a cannula was inserted in a large vein in the fossa cubiti for fluid and drug administration. The radial artery was cannulated for the collection of arterial blood samples and hemodynamic monitoring. At every heart beat the arterial systolic blood pressure (SBP), diastolic blood pressure (DBP), mean arterial pressure, heart rate, cardiac output and stoke volume were gathered, provided the arterial cannula was not used for blood sampling. ECG monitoring was applied as well. Peripheral oxygen saturation and pulse rate were measured using a finger probe. Sedative data were gathered using the bispectral index (BIS) (A-2000, Aspect Medical Systems, USA); the raw and

processed electroencephalogram (EEG) data were transferred to a laptop computer every second. Control blood samples were taken for the construction of reference aliquots. Before the start of each experiment, baseline measurements of the arterial blood pressure, heart rate (HR), cardiac output (CO) and BIS were recorded for at least 15 min. After 3 min of preoxygenation with 100% O_2, each session started with the rapid intravenous administration of propofol 3 $mg.kg^{-1}$, mixed with ICG 10 mg (Infracyanine®, Laboratoire SERB, France) as described before.[11] The propofol/ICG bolus was immediately followed by a rapid bolus of 20 ml of NaCl 0.9%. A computer-controlled syringe pump combined with a fraction collector was programmed to draw 37 arterial blood samples in the first 2.5 min after propofol administration at 3 sec apart for the first 1.5 min, then at every 10 sec for the remaining min. Due to the construction of the sampling device, no mixing in the tubing could occur, as has been described before.[11] Five more samples were drawn manually up to 10 min after administration of the propofol bolus dose, at 3, 4, 5, 7.5 and 10 min. During manual sampling, a waste sample was drawn first. The blood samples were collected in heparinized glass tubes and processed immediately by HPLC as described in chapter 6. The study ended when the patient showed clear signs of arousal, if the BIS reached 80 or after 10 minutes.

Data processing

BIS and raw EEG data were transferred from the A-2000 monitor to a laptop and imported into a spreadsheet program (Excel 2000, Microsoft Corporation, Seattle, U.S.A.). The A-2000 calculated the BIS and other processed EEG variables based on artefact-free epochs of data, where each epoch is 2 seconds. Each calculated value was based on an average of the last n epochs, where n represents approximately 60 seconds of data (A-2000 manual).

Pharmacokinetic modeling

A recirculatory PK model was constructed for propofol, using the indicator ICG to estimate the intravascular compartment, as is described in chapter 6. A recirculatory model consisting of central and non-distributive delay compartments for the intravascular compartment, combined with a single tissue compartment and a venous lag-time, described the propofol blood concentrations best. The parameters found for propofol included a steady-state volume of 12.7 ± 1.4 L, a pulmonary volume of 0.6 ± 0.1 L, a tissue volume of 9.9 ± 1.4 L, an elimination clearance of 3.4 ± 0.2 $L.min^{-1}$ and a venous lag time of 0.08 ± 0.02 min. The mean cardiac output was 7.0 ± 0.5 $L.min^{-1}$. For the other defining parameters is referred to table 1 in chapter 6.

Pharmacodynamic modeling

The relationship between the propofol blood concentrations and the hypnotic effect measured by BIS was analyzed by coupling an effect compartment to the pharmacokinetic model via a link parameter (Figure 1). As the effect compartment is assumed to have an infinitively small volume, the link parameter is reported as k_{e0}.[7] This parameter is also reported as the equilibration half-time ($t_{1/2}k_{e0}$ = ln2/k).

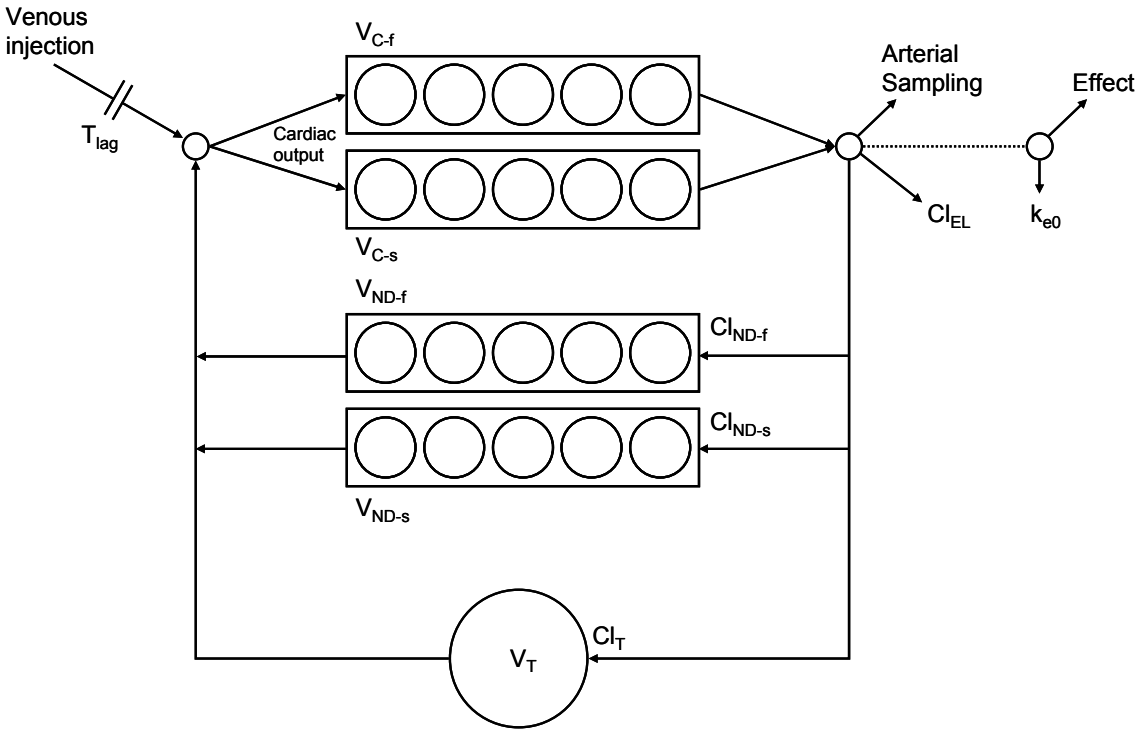

Figure 1 Representation of the recirculatory model used to fit the propofol concentration data. The pharmacokinetic recirculatory model for propofol in chapter 6 is extended with an effect compartment. The effect compartment is coupled to the blood compartment via the first order rate constant k_{e0}.

The BIS data were transferred to the SAAM program (SAAM II, version 1.1.1, SAAM Institute, University of Washington, USA) and fitted to a sigmoid E_{max} model using the Hill equation, which is defined by E_{max}, slope gamma and the EC_{50} (the concentration at which 50% of the effect is achieved). Two types of the effect model were analyzed: the classic form, which is called model 1 and an alternative model in which a pharmacodynamic lag time $T_{lag\text{-}PD}$ was added to partially account for the delay in onset of the effect. This is defined as model 2 and is comparable to the pharmacodynamic modeling of the effect on BIS of propofol by Struys et al.[5,6,12]

Pharmacodynamic simulations

Using the pharmacodynamic parameter sets determined for model 1 and 2 as described above, the effect site concentration was calculated. The effect site concentration was also simulated for the pharmacokinetic parameter sets described by Schnider and Marsh, combined with their respective k_{e0} of 0.456 and 0.26 min^{-1}, as implemented in TCI systems for effect-site targeted infusion of propofol. The input for the simulation was a bolus of 201 mg of propofol administered to a female weighing 67 kg and with a length of 1.72 m, the average of our study population.

Statistical Analysis

Descriptive statistics were generated by the SPSS statistical package (SPSS, version 17). Parameters were tested for normality using the Kolmogorov-Smirnov test. Parameters that were not normally distributed were tested for normal distribution after log transformation. If log transformation then revealed a normal distribution, the mean and standard error of the mean (SEM) were transformed back using the following equations:

$$mean = e^{\mu+\sigma^2/2n}$$

and

$$SEM = \sqrt{\left(\left(e^{\sigma^2/n}-1\right)e^{2\mu+\sigma^2/n}\right)}$$

where μ and σ represent the mean and SD in the log transformed dataset. Linear regression analysis was performed using the same statistical package. Means of the parameters between groups and the squared residuals of the measured versus the predicted effect data were tested for difference using the Paired Samples T-Test. Difference in goodness of fit between model 1 and 2 for each patient was tested using the F-test. Statistical significance was assumed at $p<0.05$. Data are reported as mean ± standard deviation (SD), unless stated otherwise.

Results

Patients

The 10 patients included were 2 males and 8 females, who were aged 42.2 ± 8.7 yr, weighed 67.1 ± 11.8 kg, were 1.72 ± 0.1 m with a body mass index of 22.5 ± 2.2 $kg.m^{-2}$.

The induction of anesthesia with the intravenous bolus dose of propofol (3 $mg.kg^{-1}$) resulted in a rapid loss of consciousness in all patients with a lowest BIS of 24 ± 9, measured at 75 (60-115) sec (median and range) after the intravenous administration of propofol. All patients had to be ventilated by mask to maintain oxygenation. When the blood propofol concentration decreased after the bolus dose administration and BIS levels increased again to a mean BIS of 72 ± 9, the data collection was terminated to assure that patients remained unconscious. The study was then terminated and anesthesia continued with propofol, remifentanil and atracurium and the trachea was intubated. The patients then were ready for their scheduled surgical procedure. The study was completed without any adverse event. No patients reported any signs of awareness.

PK-PD model

Via a data transfer protocol the raw and processed EEG variables were registered from the A-2000 monitor. A BIS value was generated every second. In order to capture the rapid change in levels of hypnosis, no averaging was performed on the generated BIS data. The data sets therefore contained 270 - 600 data points for the BIS effect measurement. Firstly, the BIS data were analyzed using a classic sigmoid E_{max} model, coupled to the blood concentration of propofol via k_{e0} (Figure 1). This was defined as model 1. Visual inspection of the BIS data over time revealed a varying time to onset of the effect (BIS drop), after which in most patients the BIS decreased rapidly, to consequently regain higher BIS values in a slower manner. This effect pattern was only poorly reflected by the parameters k_{e0} and γ in the classical model 1. To improve the quality of fit of model 1 a modification was made to the pharmacodynamic model by introducing a pharmacodynamic lag time $T_{lag\text{-}PD}$. This improved the fit of the PD data and was defined as model 2. The parameters determined by fitting model 1 and model 2 are represented in table 1. The parameters determined by model 1 showed a normal distribution. The parameters determined by model 2 showed a normal or lognormal

(EC_{50} and k_{e0}) distribution. All parameters differed significantly between the models according to the Paired Samples T-test ($p<0.05$).

Table 1 Parameters describing the pharmacodynamics of propofol based on recirculatory pharmacokinetics, determined by two different pharmacodynamic models. In model 1 a standard sigmoid Emax model is coupled to the blood concentration via a single transfer constant k_{e0}. In model 2 the sigmoid E_{max} model is linked via a pharmacodynamic lag time combined with the transfer constant k_{e0}.

Parameter	**Model 1**		**Model 2**	
	Mean	**SEM**	**Mean**	**SEM**
EC_{50} ($\mu g.ml^{-1}$)	2.79	0.12	3.82	0.35
E_{max}	97.7	0.5	96.5	0.5
gamma	14.67	2.71	3.69	0.75
$t_{1/2}k_{e0}$ (min)	7.33	0.56	3.82	0.65
$T_{lag\text{-}PD}$ (min)			0.47	0.06

For an illustrative patient the PK-PD model fitted to the BIS data using model 1 (panel A) or model 2 (panel B) is presented in figure 2. Improvement of fit of the induction phase with model 2, when a pharmacological lag time was introduced, is clearly visible.

Linear regression analysis of the predicted versus measured effect data showed a better correlation for model 2 than for model 1 (R^2 of 0.940 vs 0.883, both $p<0.0001$, Figure 3). The residuals of the measured versus predicted effect for all data points in all patients are represented in time in figure 4. The squared residuals of model 1 differed significantly from those of model 2 ($p<0.001$), as determined by the Paired T-test. The F test provided further evidence that model 2 fitted the data significantly better than model 1 ($p<0.0001$). The fitted curve based on the pharmacodynamic parameters for model 2 in reference to the measured BIS curves of all patients is represented in figure 5.

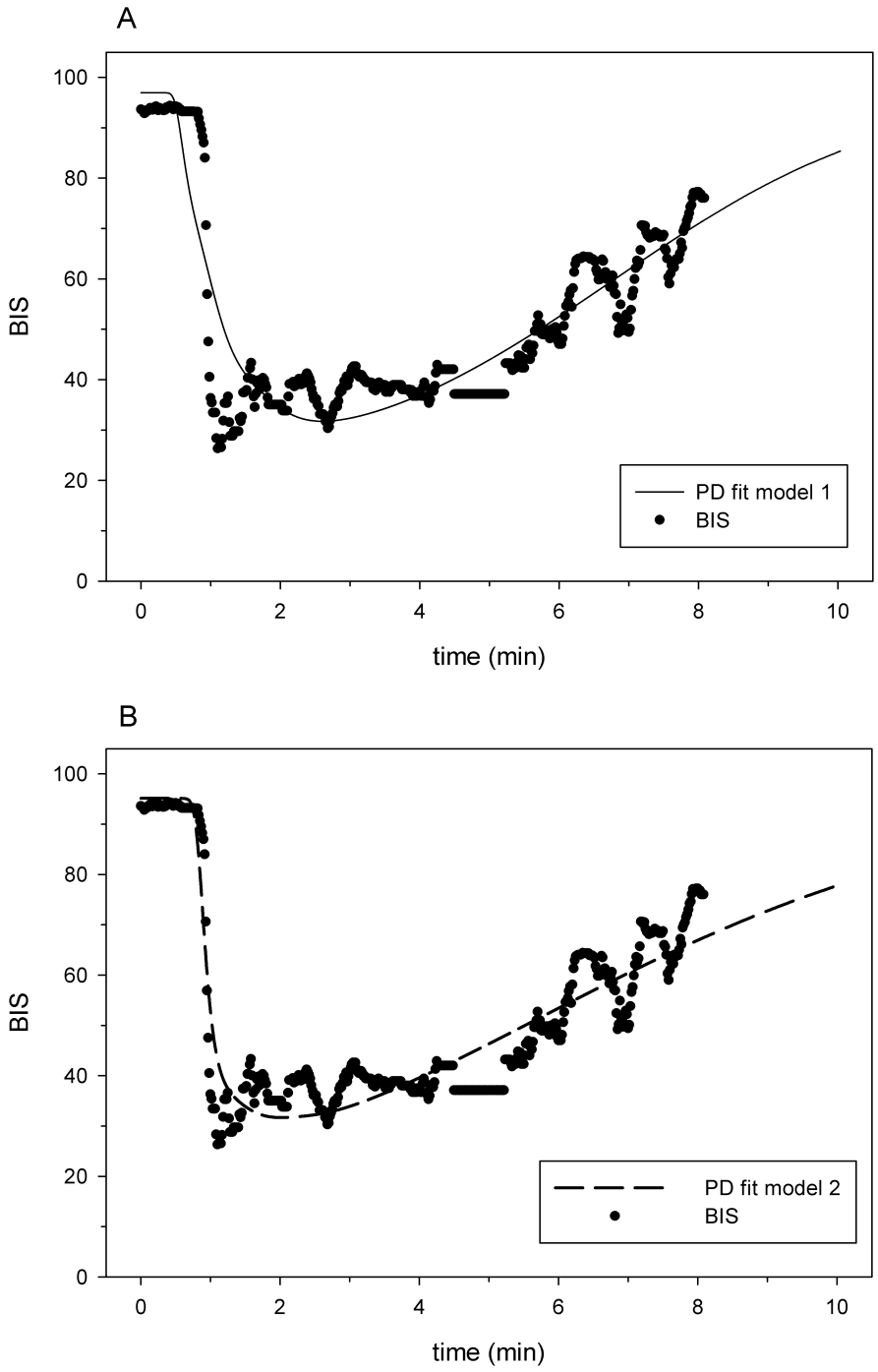

Figure 2 Fit of the pharmacodynamic data of propofol in a representative patient, using two PK-PD models: in panel A the effect is directly coupled to the central blood compartment via k_{e0} (R^2=0.84), in panel B a pharmacodynamic lag time ($T_{lag\text{-}PD}$) is added to the model (R^2=0.90). The F test showed that model 2 fitted the data better than model 1 ($p<0.0001$).

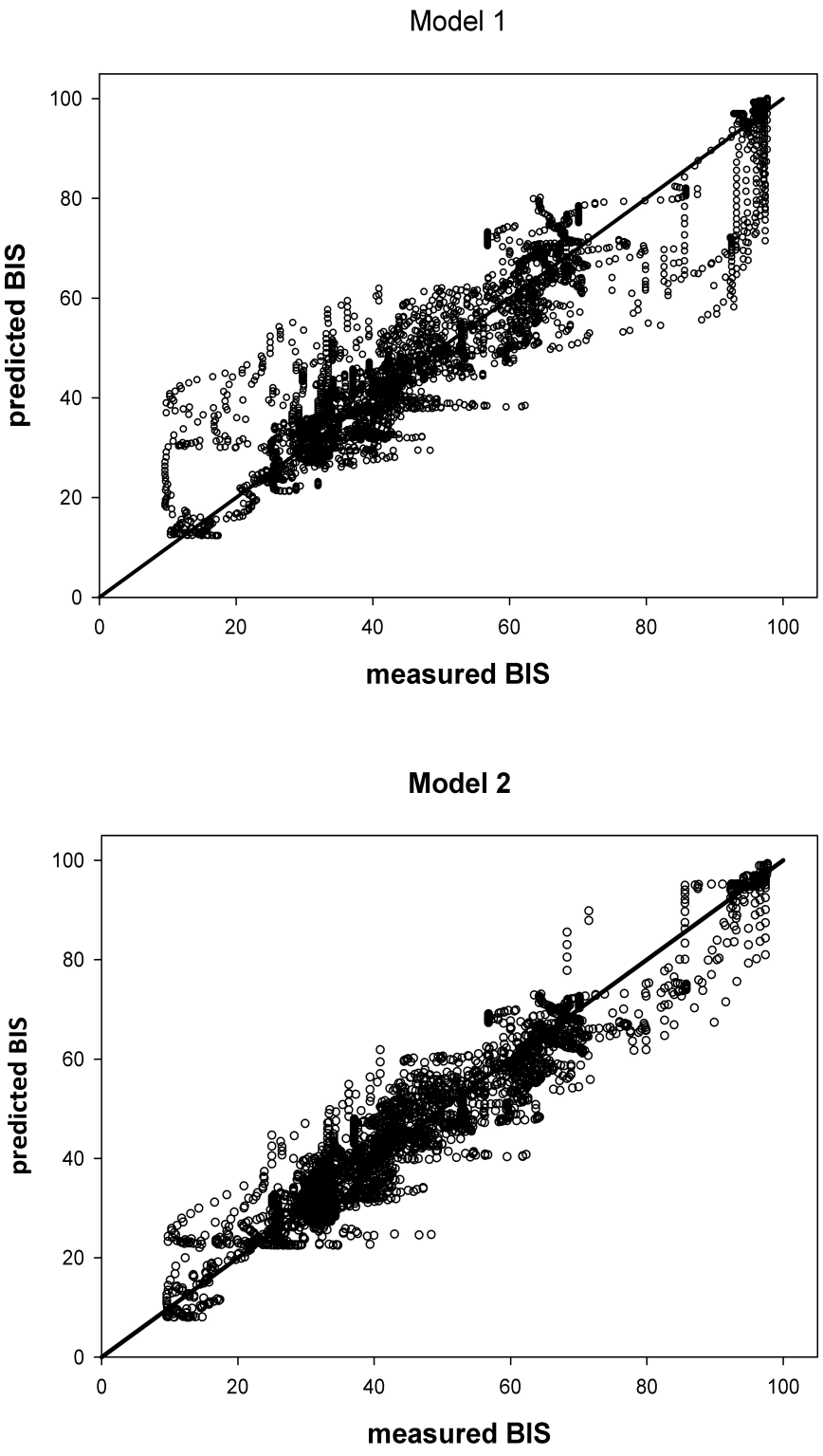

Figure 3 Measured versus predicted BIS effect data, fitted with model 1 (R^2=0.883) and model 2 (R^2=0.940, for all data points. The solid line is the line of identity (y=x).

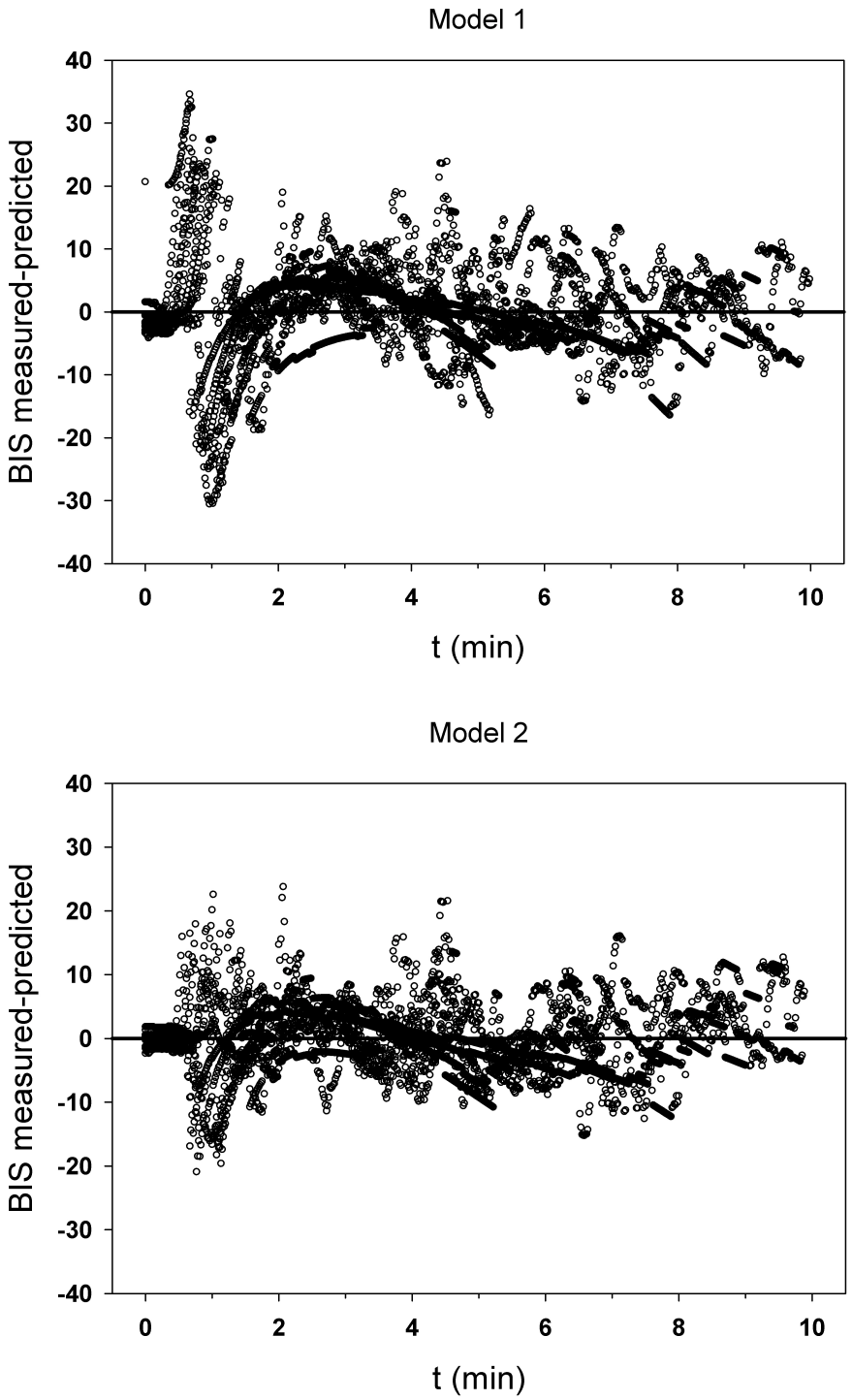

Figure 4 Residuals of the measured versus predicted BIS values for all datasets, fitted with model 1 (classical model) and model 2 (model including a pharmacodynamic lag time). The squared residuals differed significantly for the 2 models ($p<0.05$).

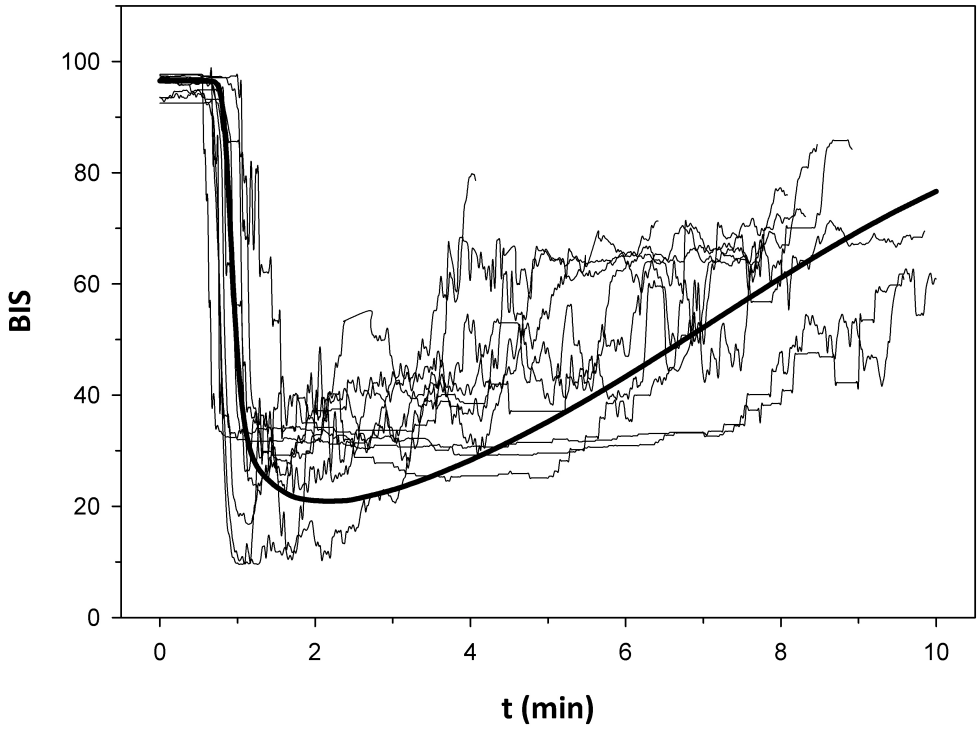

Figure 5 The fitted pharmacodynamic model for BIS based on the parameters derived with model 2, including a pharmacological lag time (thick solid line) amid the measured effect curves of all 10 patients.

Discussion

Compartmental modeling poorly describes propofol concentrations during the initial mixing phase and thus may misjudge the blood-effect site disequilibrium. We explored the effect-site equilibration of an induction bolus of propofol by recirculatory pharmacokinetic modeling combined with BIS as effect parameter, and compared this to the k_{e0} as based on compartmental modeling. We successfully defined the recirculatory equilibration constant (k_{e0}) for the effect of propofol on BIS in 2 ways. The k_{e0} determined by the first, classic recirculatory PK-PD model was about 50% of the ke_0 reported in literature as determined by compartmental PK-PD modeling. This is in analogy with similar recirculatory-compartmental ke_0 comparisons e.g. for rocuronium (0.13 versus 0.24).[13] The equilibration half-life $t_{1/2}k_{e0}$ determined by the second model, in which a variable pharmacodynamic lag time was included, generated a better fit of the median time to peak effect that was observed at 1.25 min. Compartmental pharmacokinetic models underestimate the blood propofol concentration. When modeling the effect in relation to a compartmental

pharmacokinetic model this PK-underestimation is compensated for by a consecutive overestimation of the effect-site equilibration time. With this notice we demonstrate that a reported k_{e0} can only be interpreted in context with its PK-PD model.

Limitations of the study

Pharmacodynamic modeling of the sedative effect of propofol has been performed using multiple effect parameters like the mid-latency auditory evoked potentials[14], spectral edge frequency[10], bispectral index score[15], CUP[9] and permutation entropy[16], which are all EEG derived effect parameters. These effect parameters are derived, scaled and averaged in different ways, often undisclosed to the public. Albeit the fact that BIS is subject to a moving average (which can be adjusted from 30 to 15 sec on the monitor) and therefore shows an implicit delay, the method is widely available and has been incorporated into the standard OR equipment. Uncertainty on the mathematics by which the BIS is calculated did not outweigh the practical benefits of the BIS as effect parameter. By downloading the raw EEG data from the A-2000 monitor, we attempted to construct the fast reacting parameter permutation entropy. However, this was hampered by the occurrence of burst suppression after administration of the induction bolus of 3 $mg.kg^{-1}$ of propofol. The way that BIS handles artifacts (which can be any rapid change in the signal) by maintaining its former level, combined with the fact that excitation which is observed in the EEG at the start of induction and cannot be reflected by BIS, may account for the delay we observed in our effect measurements.[17] This phenomenon has been solved before by constructing a biphasic[18] or 2-compartment effect model for EEG.[19] Addition of a fixed lag time of 0.1 min has been described by Struys et al.[12] To deal with comparable problems, Kazama and colleagues did not start fitting the k_{e0} until 1.25 min after adjusting the targeted propofol concentration in their TCI system and measuring EEG with the A-1000.[20]

In our model we chose to introduce a variable pharmacodynamic lag time to account for delay in effect on mathematical grounds. However, considering the high blood peak concentrations we detected by rapid sampling, it may also reflect other phenomena like the transport through the microcirculation[21,22] and diffusion kinetics[23] that influence the equilibration ratio from the blood to the effect compartment. The $T_{lag\text{-}PD}$ showed correlation with the cardiac output (R^2=0.524, $p<0.02$).

The number of patients enrolled in this study is relatively small. However, the vast amount of data generated by the high sampling frequency of blood

concentrations as well as effect measurements, allowed for accurate fitting and less need for interpolation. The variability on the pharmacodynamic parameters is therefore not due to a large variability in the pharmacokinetics.

The real k_{e0}?

The findings in this study once more demonstrate that no such parameter as the real k_{e0} for propofol exists. Up to now a number of studies have been performed, generating various values for the k_{e0} (and its equilibration halftime) for propofol. Billard et al. reported a k_{e0} of 0.20 ($t_{1/2}k_{e0}$: 3.5 min);[10] Schnider et al. reported a k_{e0} of 0.456 ($t_{1/2}k_{e0}$: 1.51 min)[9] and Struys et al. of 1.21 ($t_{1/2}k_{e0}$: 0.57 min)[24] and later of 0.58 ($t_{1/2}k_{e0}$: 1.2 min) for a bolus and 0.32 ($t_{1/2}k_{e0}$: 2.2)[12] for infusion based on BIS, whereas a k_{e0} of 0.26 ($t_{1/2}k_{e0}$: 2.6 min) based on auditory evoked potentials is incorporated in the Diprifusor (preliminary results presented by M. White).[25] Kazama et al. compared 4 age groups, receiving a step-up schedule of propofol TCI. For each age group a different k_{e0} could be determined, even with or without taking EEG activation into account. Values for $t_{1/2}k_{e0}$ varied between 2.29 and 4.33 min.[20] The implications of combining different PK data sets with various k_{e0} values is clearly described by Glen.[25] Misinterpretation may lead to underdosing with the risk of awareness, or overdosing with the possibility of eliciting side effects like hemodynamic and cardiac depression. To illustrate this we simulated the calculated effect-site concentration, based on our recirculatory pharmacokinetic model that is presented in chapter 6. We compared this to the calculated effect-site concentrations produced by the PK-PD model described by Schnider and by Marsh (Figure 6).

Due to lack of information on the complete pharmacodynamic model on which the k_{e0} of Schnider (0.456) and Marsh (0.26) are based, we could not simulate the BIS effect which would be expected at the calculated effect site concentration. Both the Marsh and Schnider models are implemented in commercially available TCI systems.

The simulations of the effect-site concentration show the influence of the parameter sets on the calculated effect-site concentration and its time-course. Interpretation of the effect-site concentration involves knowledge of the EC_{50} which determines the desired target concentration. Furthermore, the k_{e0} is influenced by the mode of administration, i.e. bolus or infusion[12]. In our study k_{e0} showed correlation with cardiac output as well (R^2 =0.600; $p<0.01$).

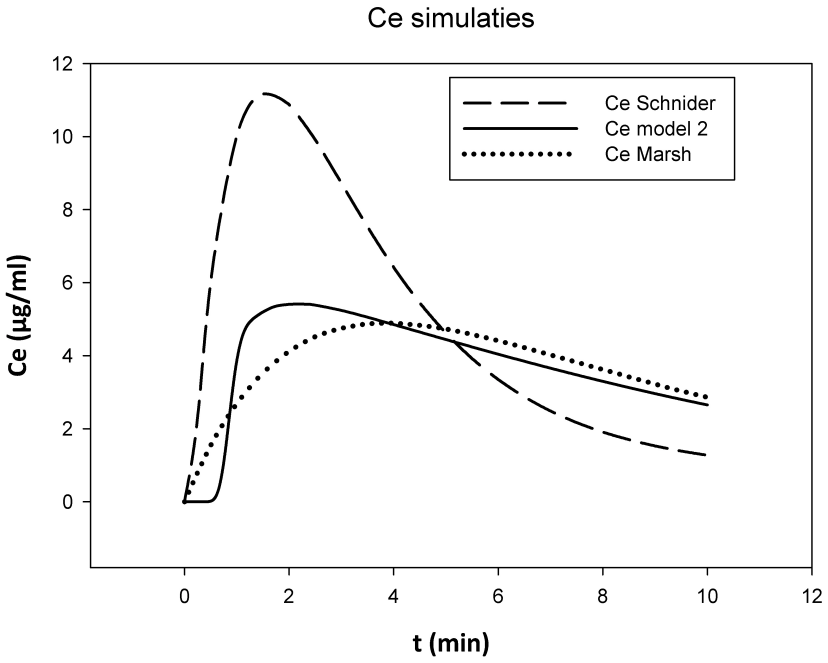

Figure 6 Simulations of the effect-site concentrations calculated from the PK-PD models described by Marsh[25], Schnider[9] and model 2 presented in this study. Note the high Ce from the Schnider model and the delay in time to peak effect (max Ce) with the Marsh model. The mean time to peak effect measured in our study was 1.2 min.

Conclusion

We explored the effect-site equilibration of an induction bolus of propofol by recirculatory pharmacokinetic modeling combined with BIS as effect parameter, and compared this to the k_{e0} as based on compartmental modeling. We successfully defined the recirculatory equilibration constant (k_{e0}) for the effect of propofol on BIS. The classically determined k_{e0} was about 50% of the k_{e0} reported in literature as determined by compartmental PK-PD modeling. Effect data were best fitted after inclusion of a variable pharmacodynamic lag time.

Compartmental pharmacokinetic models underestimate the blood propofol concentration after induction of anesthesia. When modeling the effect in relation to a compartmental pharmacokinetic model this PK-underestimation is compensated for by a consecutive PD-overestimation of the effect-site equilibration constant (k_{e0}). With this we draw attention to the fact that a k_{e0} may only be implemented within the context of the pharmacokinetic model used and the effect parameter studied.

References

1. Leslie K, Clavisi O, Hargrove J. Target-controlled infusion versus manually-controlled infusion of propofol for general anaesthesia or sedation in adults. Cochrane Database Syst Rev 2008;CD006059.

2. Levy G. Predicting effective drug concentrations for individual patients. Determinants of pharmacodynamic variability. Clin Pharmacokinet 1998;34:323-33.

3. Struys MM, Vereecke H, Moerman A, et al. Ability of the bispectral index, autoregressive modelling with exogenous input-derived auditory evoked potentials, and predicted propofol concentrations to measure patient responsiveness during anesthesia with propofol and remifentanil. Anesthesiology 2003;99:802-12.

4. Vuyk J. TCI: supplementation and drug interactions. Anaesthesia 1998;53 Suppl 1:35-41.

5. Vuyk J, Mertens MJ, Olofsen E, et al. Propofol anesthesia and rational opioid selection: determination of optimal EC50-EC95 propofol-opioid concentrations that assure adequate anesthesia and a rapid return of consciousness. Anesthesiology 1997;87:1549-62.

6. Lichtenbelt BJ, Mertens M, Vuyk J. Strategies to optimise propofol-opioid anaesthesia. Clin Pharmacokinet 2004;43:577-93.

7. Sheiner LB, Stanski DR, Vozeh S, et al. Simultaneous modeling of pharmacokinetics and pharmacodynamics: application to d-tubocurarine. Clin Pharmacol Ther 1979;25:358-71.

8. Marsh B, White M, Morton N, Kenny GN. Pharmacokinetic model driven infusion of propofol in children. Br J Anaesth 1991;67:41-8.

9. Schnider TW, Minto CF, Gambus PL, et al. The influence of method of administration and covariates on the pharmacokinetics of propofol in adult volunteers. Anesthesiology 1998;88:1170-82.

10. Billard V, Gambus PL, Chamoun N, et al. A comparison of spectral edge, delta power, and bispectral index as EEG measures of alfentanil, propofol, and midazolam drug effect. Clin Pharmacol Ther 1997;61:45-58.

11. Reekers M, Simon MJ, Boer F, et al. Cardiovascular monitoring by pulse dye densitometry or arterial indocyanine green dilution. Anesth Analg 2009;109:441-6.

12. Struys MM, Coppens MJ, De NN, et al. Influence of administration rate on propofol plasma-effect site equilibration. Anesthesiology 2007;107:386-96.

13. Kuipers JA, Boer F, Olofsen E, et al. Recirculatory pharmacokinetics and pharmacodynamics of rocuronium in patients: the influence of cardiac output. Anesthesiology 2001;94:47-55.

14. White M, Schenkels MJ, Engbers FH, et al. Effect-site modelling of propofol using auditory evoked potentials. Br J Anaesth 1999;82:333-9.

15. Schraag S, Bothner U, Gajraj R, et al. The performance of electroencephalogram bispectral index and auditory evoked potential index to predict loss of consciousness during propofol infusion. Anesth Analg 1999;89:1311-5.

16. Olofsen E, Sleigh JW, Dahan A. Permutation entropy of the electroencephalogram: a measure of anaesthetic drug effect. Br J Anaesth 2008;101:810-21.

17. Pilge S, Zanner R, Schneider G, et al. Time delay of index calculation: analysis of cerebral state, bispectral, and narcotrend indices. Anesthesiology 2006;104:488-94.

18. Gregg KM, Varvel JR, Shafer SL. Application of semilinear canonical correlation to the measurement of opioid drug effect. J Pharmacokinet Biopharm 1992;20:611-35.

19. Kuizenga K, Wierda JM, Kalkman CJ. Biphasic EEG changes in relation to loss of consciousness during induction with thiopental, propofol, etomidate, midazolam or sevoflurane. Br J Anaesth 2001;86:354-60.

20. Kazama T, Ikeda K, Morita K, et al. Comparison of the effect-site k(eO)s of propofol for blood pressure and EEG bispectral index in elderly and younger patients. Anesthesiology 1999;90:1517-27.

21. Bassingthwaighte JB, Warner HR. Indicator dispersion in the circulation. Am Heart J 1965;69:838-41.

22. Fallon MS, Howell BA, Chauhan A. Importance of Taylor dispersion in pharmacokinetic and multiple indicator dilution modelling. Math Med Biol 2009;26:263-96.

23. Bassingthwaighte JB, Raymond GM, Butterworth E, et al. Multiscale modeling of metabolism, flows, and exchanges in heterogeneous organs. Ann N Y Acad Sci 2010;1188:111-20.

24. Struys MM, De ST, Depoorter B, et al. Comparison of plasma compartment versus two methods for effect compartment--controlled target-controlled infusion for propofol. Anesthesiology 2000;92:399-406.

25. Glen JB. The development and future of target controlled infusion. Adv Exp Med Biol 2003;523:123-33.

8

Summary, Conclusions and Future Perspectives

Summary

The pharmacology of the induction of anesthesia is still poorly understood. As a consequence, the onset of anesthesia is often associated with hemodynamic and respiratory depression resulting from a relative anesthetic overdose, while at other times patients receive an insufficient dose and suffer from inadequate analgesia or awareness. The pharmacology of the induction of anesthesia is regularly described using compartmental modeling, although this method is generally known to predict drug concentrations during induction inaccurately. This inaccuracy, as well as the clinical importance of proper induction dosing, elicited the studies in this thesis. Our aim was to better describe the early phase pharmacokinetics and pharmacodynamics of anesthetic agents through recirculatory modeling. Because indocyanine green (ICG) plays an important role in recirculatory modeling, the first part of this thesis deals with the analysis and modeling of ICG in blood.

In **chapter 2** a general overview of the various methods of pharmacokinetic modeling is given. The pros and cons of compartmental and more physiologically-based analytical methods of defining the dose-concentration-effect relationship of anesthetic agents, are described. The recirculatory model described by Kuipers et al. for the muscle relaxant rocuronium, using ICG as intravascular marker, is discussed in detail.

In **chapter 3** we evaluated the accuracy of the noninvasive transcutaneous measurement of ICG by the DDG-2001. Two different probes were used to determine transcutaneously the concentration of ICG in blood and the derived hemodynamic parameters cardiac output, central blood volume and total blood volume. These measurements were compared to the simultaneous measurements of ICG in arterial blood, and the derived hemodynamic parameters based on arterial measurements, acquired by rapid sampling. The results of this study seriously question the reliability of the noninvasive measurement of cardiac output and central blood volume in the individual patient as measured by pulse-dye densitometry with the DDG-2001. Both the finger and nose probe proved equally unreliable. The overall conclusion of this study is that, although total blood volume is measured relatively better, the DDG-2001 is not accurate enough for noninvasive cardiac output measurement to be clinically useful in hemodynamic monitoring.

In **chapter 4** we studied the accuracy of the noninvasive measurement of the Indocyanine Green Plasma Disappearance Rate (ICG-PDR) versus arterial

measurement of ICG, in the population described in chapter 3. ICG-PDR is used clinically as a measure of hepatic failure, for example in patients directly after liver transplantation. As data on transcutaneously measured ICG-PDR in patients without liver failure is scarce, this was explored. Respectively, the Pulse Dye Densitometry (PDD) finger and nose probe showed a relative bias of 12% and -23%, compared to arterial ICG measurements. The mean ICG-PDR was 23.1 $\%.min^{-1}$, comparable to previously published data. However, the ICG-PDR variability in this healthy population proved much larger than previously described (95% CI: 7.4-38.8$\%.min^{-1}$). Patients with an ICG-PDR of 8 $\%.min^{-1}$ may thus exhibit normal liver function in contrast to the former cited cut off value of 18 $\%.min^{-1}$, indicating liver failure. Further evaluation of ICG-PDR in the healthy population may improve our insight in the value of this parameter in patients suffering from hepatic failure or post liver transplantation.

In **chapter 5** we evaluated a circulatory pharmacokinetic model for rocuronium, based on intravascular and diffusion kinetics. The data upon which this model is based were the same as those described in chapter 2 by Kuipers et al. It was not the goal of this study to improve the fit of the rocuronium data relative to that already obtained, but rather to better understand the role of vascular mixing (transit time dispersion) and interstitial diffusion. The study demonstrated the applicability of the transit time dispersion based model of vascular mixing and the diffusional tissue distribution model in clinical pharmacokinetics. It accounts for the importance of the roles of circulatory mixing and diffusion into the interstitial fluid in determining the distribution kinetics of rocuronium, and thus sheds new light on our understanding of underlying transport physiology. The importance of flow is stressed by the significant correlation between cardiac output and cardiopulmonary volume described in this study and by the fact that systemic transit time dispersion decreased with increasing cardiac output. Future applications may include other drugs or reveal the effect of disease states on drug distribution.

In **chapter 6** a recirculatory pharmacokinetic model for propofol in humans is presented. The model describes the distribution, recirculation and elimination of propofol after the administration of an induction bolus dose, based on ICG pharmacokinetics. The role of the lung in the distribution and elimination of propofol is discussed. We successfully described the pharmacokinetics of propofol by recirculatory modeling. After bolus administration, propofol exhibits blood concentrations that exceed by 10-30 fold those related to hypnotic effect, reflecting its poor initial mixing. We conclude that propofol shows no clinically relevant clearance from the lung. Lastly, through computer simulation we demonstrated that compartmental models, now widely used in anesthetic

practice in target controlled infusion pumps, significantly underestimate the actual blood propofol concentration in the first minutes after induction of anesthesia.

In **chapter 7** the recirculatory pharmacokinetic model for propofol was implemented in a pharmacokinetic-pharmacodynamic model for propofol. The effect was measured by the bispectral index score (BIS). We explored the effect-site equilibration of an induction bolus of propofol by recirculatory pharmacokinetic modeling combined with BIS as effect parameter, and compared this to the k_{e0} as based on compartmental modeling. We successfully defined the recirculatory equilibration constant (k_{e0}) for the effect of propofol on BIS. The k_{e0} determined by the classically based, recirculatory PK-PD model was about 50% of the k_{e0} reported in literature as determined by compartmental PK-PD modeling. However, effect data were best fitted after inclusion of a variable pharmacodynamic lag time of approximately 0.5 min. Compartmental pharmacokinetic models underestimate the blood propofol concentration after induction of anesthesia. When modeling the effect in relation to a compartmental pharmacokinetic model this PK-underestimation is compensated for by a consecutive PD-overestimation of the effect-site equilibration constant (k_{e0}). With this we draw attention to the fact that a k_{e0} may only be implemented within the context of the pharmacokinetic model used and the effect parameter studied.

Conclusions and Future Perspectives

Titration to effect is the most important action anesthesiologists use to assure adequacy of anesthesia and safeguard their patients from serious side effects. For a proper titration to effect the anesthesiologist takes into consideration the historical response to a given dose to estimate the response to a future dose. During induction of anesthesia the anesthesiologist is still unaware of the dose-response relationship of the patient and titration is therefore impossible. As a result population PK-PD data are of great importance during induction of anesthesia. Because for many agents the knowledge of the covariates of influence on the induction dose-response relationship is lacking, many patients experience serious side effects during induction of anesthesia, often in the form of hemodynamic depression.

In this thesis light is shed on the pharmacology of induction of anesthesia. The front-end kinetics are complex and often flow dependent. The observations in

this thesis teach us that the modeling of the dose-concentration-effect relation is insufficiently described by compartmental modeling and improves by applying recirculatory PK-PD modeling. (Non)invasive ICG measurement is used extensively in recirculatory modeling but is less well suited for hemodynamic monitoring.

We started this work with the idea that with the noninvasive measurement of ICG and the derived hemodynamic parameters like cardiac output, at the bedside before induction, we would be able to identify the relevant parameters of the recirculatory model of ICG and of the drug used for induction of anesthesia. This result has not been reached in this thesis and requires further study. Future research may aim at clarification of the influence of various covariates on the recirculatory PK-PD in the induction phase, the relationship between the high peak concentrations in blood after bolus administration and the hemodynamic depression, and at the influence of co-administered opioids or hypnotic agents used as premedication drugs on the dose-concentration-effect relationship of propofol. Inclusion of subjects with differing physiology based on age, weight or illness, will extend the knowledge on the impact of recirculatory modeling in these patient groups. The need for a fast responding and predictive effect parameter to measure rapidly changing states of consciousness remains. With the application of sampling at high frequency of both blood and effect, new phenomena may be revealed which will necessitate other forms of modeling.

9

Samenvatting, Conclusies en Toekomstperspectieven

Samenvatting

De farmacologie van de inductie van anesthesie, het in slaap maken, is nog steeds moeilijk te doorgronden. Dit heeft onder andere nog steeds tot gevolg dat de aanvang van anesthesie enerzijds veelal geassocieerd is met hemodynamische instabiliteit en ademhalingsdepressie ten gevolge van een relatieve overdosering van anesthetica, terwijl anderzijds patiënten door een ondermaatse dosering het slachtoffer kunnen worden van inadequate pijnstilling of het optreden van awareness. De farmacokinetiek van de inductie van anesthesie wordt veelal beschreven met behulp van compartimentele modellen, hoewel het bekend is dat via deze methode de geneesmiddelconcentratie tijdens de inductiefase onnauwkeurig wordt voorspeld. Deze onnauwkeurigheid, naast het klinische belang van het adequaat doseren tijdens de inductiefase, zijn de aanleiding geweest tot het opzetten van de onderzoeken beschreven in dit proefschrift. Het was ons doel de vroege fase farmacokinetiek en farmacodynamiek van anesthetica te beschrijven met behulp van een recirculatoir model. Aangezien de kleurstof indocyanine groen (ICG) een belangrijke rol speelt bij recirculatoir modelleren, zijn de eerste hoofdstukken van dit proefschrift gewijd aan de bepaling en het modelleren van ICG concentraties in bloed.

In **hoofdstuk 2** wordt een overzicht gegeven van de verschillende methoden van farmacokinetisch modelleren. De voors en tegens worden beschreven van compartimentele- en meer fysiologisch gestoelde analytische methoden voor het beschrijven van de dosis-concentratie-effect relatie van anesthetica. Het recirculatoire model zoals beschreven door Kuipers et al. voor de spierverslapper rocuronium, waarbij ICG is gebruikt als intravasculaire marker, wordt uitgebreid besproken.

In **hoofdstuk 3** wordt de nauwkeurigheid van de niet-invasieve transcutane meting van ICG met behulp van de DDG-2001 geëvalueerd. Twee verschillende detectoren zijn gebruikt om door de huid de concentratie van ICG in het bloed te meten en hieruit de hemodynamische parameters hartminuutvolume, centraal bloed volume en totaal bloed volume te berekenen. Deze transcutane metingen zijn vergeleken met metingen in simultaan afgenomen arteriële bloedmonsters. De hemodynamische parameters zijn ook vergeleken met de berekeningen, afgeleid uit hoog frequente arteriële bloedmonsters. De resultaten gevonden in dit onderzoek trekken de betrouwbaarheid van de niet-invasieve meting van het hartminuutvolume en het centraal bloedvolume ernstig in twijfel, wat betreft de meting in de

individuele patiënt zoals uitgevoerd via pulse-dye-densitometrie met de DDG-2001. Zowel de neus- als de vingerdetector bleken even onbetrouwbaar. De algemene conclusie van dit onderzoek is dat, hoewel de meting van het totale bloedvolume betere resultaten liet zien, de DDG-2001 niet nauwkeurig genoeg is in het niet-invasief meten van het hartminuutvolume, om klinisch toepasbaar te zijn als hemodynamische bewaking.

In **hoofdstuk 4** wordt het onderzoek gepresenteerd naar de nauwkeurigheid van de niet-invasieve meting van de indocyanine groen plasma verdwijnings ratio (ICG-PDR), vergeleken met deze meting in slagaderlijk bloed. Deze vergelijking is bestudeerd in dezelfde patiëntengroep als beschreven in hoofdstuk 3. ICG-PDR is klinisch in gebruik als maat voor leverfalen, bijvoorbeeld bij patiënten na levertransplantatie. Aangezien er weinig gegevens beschikbaar zijn betreffende de transcutane meting van ICG-PDR in patiënten zonder leverfalen, hebben wij hier nader onderzoek naar gedaan. De Pulse Dye Densitometrie (PDD) vinger- en neusdetector lieten een relatieve bias zien van respectievelijk 12% en -23%, wanneer vergeleken met metingen van ICG in arterieel bloed. De gemiddelde ICG-PDR was 23,1 $\%.min^{-1}$, vergelijkbaar met eerder gepubliceerde gegevens. Echter, de spreiding in deze gezonde populatie bleek veel groter te zijn dan eerder was beschreven (95% betrouwbaarheidsinterval: 7,4 – 38,8 $\%.min^{-1}$). Patiënten met een ICG-PDR van 8 $\%.min^{-1}$ kunnen dus een normale leverfunctie hebben, in tegenstelling tot de eerder beschreven onderwaarde van 18 $\%.min^{-1}$, welke leverfalen zou indiceren. Een verdere evaluatie van ICG-PDR in de gezonde populatie kan onze inzichten in de waarde van deze meting bij patiënten met leverfalen of na levertransplantatie vergroten.

In **hoofdstuk 5** wordt een circulatoir farmacokinetisch model voor rocuronium beschreven, dat gebaseerd is op intravasculaire– en diffusie kinetica. De gegevens waar dit model op is gebaseerd, zijn dezelfde als welke zijn gebruikt voor het model beschreven in hoofdstuk 2 door Kuipers et al. Het doel van deze studie was niet het verbeteren van de fit van de rocuronium data ten opzichte van het eerder beschreven model, maar om een beter inzicht te krijgen in de rol van menging in het vaatbed (transit tijd dispersie) en de rol van diffusie naar het interstitium. Dit onderzoek toonde aan dat het model, dat gebaseerd is op de transit tijd dispersie van intravasculaire menging en diffusie naar het interstitium, goed toepasbaar is op farmacokinetische data uit de klinische praktijk. Het geeft hiermee het belang weer van circulatoire mixing en diffusie naar de interstitiële vloeistof, bij het bepalen van de distributie kinetiek van rocuronium. Hiermee is ons inzicht in de fysiologie van geneesmiddelen transport toegenomen. De belangrijke rol van stroomsnelheid wordt benadrukt

door de significante correlatie tussen hartminuutvolume en cardiopulmonale volumina beschreven in deze studie. Tevens neemt de systemische transit tijd dispersie af bij een toename van het hartminuutvolume. In de toekomst zal dit model toegepast kunnen worden op andere geneesmiddelen. Daarnaast kan het beter inzicht geven in de rol van ziekte op de verspreiding van geneesmiddelen in het lichaam.

In **hoofdstuk 6** wordt een recirculatoir farmacokinetisch model voor propofol in mensen gepresenteerd. Dit model beschrijft de verdeling, recirculatie en uitscheiding van propofol na het toedienen van een standaard bolus inductie dosis, gebaseerd op de farmacokinetiek van ICG. De rol van de long in de verdeling en uitscheiding van propofol wordt nader belicht. Op succesvolle wijze hebben wij de farmacokinetiek van propofol beschreven met behulp van een recirculatoir model. Na een bolus toediening van propofol worden concentraties gevonden die 10-30 keer de concentratie overtreffen, die gerelateerd is aan hypnotisch effect. Dit illustreert de slechte mixing in de initiële fase. Verder concluderen wij dat klaring van propofol door de long niet in klinische relevante mate aanwezig is. Tenslotte maken we door computer simulaties duidelijk dat compartimentele modellen de werkelijke concentratie van propofol in het bloed direct na de inductie van anesthesie, significant onderschatten. Dergelijke modellen worden in de klinische praktijk via doel gestuurde infusie pompen veelvuldig gebruikt.

In **hoofdstuk 7** is het recirculatoire farmacokinetische model voor propofol geïmplementeerd in een farmacokinetisch-farmacodynamisch (PK-PD) model voor propofol. Het effect van de anesthesie is gemeten met de bispectrale index score (BIS). Het bereiken van het evenwicht tussen de concentratie van propofol in het bloed en het effect compartiment, na het toedienen van een bolus propofol, is onderzocht door middel van het combineren van het recirculatoire farmacokinetische model voor propofol met BIS als effect parameter. De effect compartiment equilibratie constante k_{e0} is vergeleken met die, zoals bekend bij compartimentele modellen. Met succes hebben wij de recirculatoire equilibratie constante k_{e0} kunnen bepalen voor het effect van propofol op de BIS in twee verschillende modellen. De k_{e0} bepaald uit het klassiek gestoelde recirculatoire PK-PD model, was ongeveer 50% van de k_{e0} zoals gerapporteerd in de literatuur, op basis van compartimentele modellen. De effect data konden echter het beste gefit worden na toevoeging van een variabele farmacodynamische vertragingstijd van ongeveer een halve minuut. Compartimentele farmacokinetische modellen onderschatten de concentraties van propofol in het bloed na de inductie van anesthesie. Tijdens het modelleren van het effect, gekoppeld aan een compartimenteel farmacokinetisch model,

wordt de farmacokinetische onderschatting blijkbaar gecompenseerd door een daaropvolgende farmacodynamische overschatting in de effect compartiment equilibratie constante k_{e0}. Hiermee benadrukken wij dat een k_{e0} altijd beschouwd moet worden in de context van het farmacokinetische model dat is gebruikt en de effect parameter die is gemeten.

Conclusies en toekomstperspectieven

Titreren op effect is de belangrijkste vaardigheid die anesthesiologen gebruiken om een adequate anesthesie te waarborgen en hun patiënten te behoeden voor ernstige bijwerkingen. Om goed te kunnen titreren op effect, is een eerdere reactie op een toegediende dosis maatgevend voor de grootte van de volgende dosis. Tijdens de inductie van anesthesie is de anesthesioloog nog onkundig van de individuele dosis-respons relatie voor de betreffende patiënt, en is titreren dus niet mogelijk. Dit verklaart het belang van populatie PK-PD gegevens voor de inductie van anesthesie. Aangezien van veel geneesmiddelen niet bekend is wat de invloed is van verschillende variabelen op de inductie dosis-respons relatie, gaat de inductie van anesthesie bij veel patiënten gepaard met ernstige bijwerkingen, hoofdzakelijk hemodynamische instabiliteit.

In dit proefschrift wordt de farmacologie van de inductie van anesthesie nader belicht. Vroege-fase kinetiek is complex en veelal afhankelijk van de bloedstroomsnelheid. De bevindingen in dit proefschrift tonen aan dat tijdens het modelleren van de dosis-concentratie-effect relatie de vroege fase gebrekkig beschreven wordt door compartimentele modellen. De toepassing van een recirculatoir PK-PD model leidt tot een grote verbetering hierin. De (niet)invasieve meting van ICG is onontbeerlijk bij recirculatoir modelleren. Deze meting van ICG is minder geschikt voor hemodynamische bewaking in de klinische praktijk.

Bij aanvang van dit project gingen we uit van de hypothese dat het mogelijk zou moeten zijn om, aan het bed van de patiënt, op basis van een niet-invasieve ICG meting, de relevante factoren van invloed voor de individuele patiënt te kunnen bepalen. De bepaling van het hartminuutvolume zou, op gelijke wijze, hier deel van uitmaken. Op basis van deze factoren zou het dan mogelijk zijn, met behulp van een recirculatoir model, een adequate en veilige inductie te bewerkstelligen met een anestheticum naar keuze. Deze doelstellingen zijn nog niet bereikt en vragen verder onderzoek. Toekomstig

onderzoek zou zich moeten richten op het verhelderen van de invloed van verschillende covariaten op het recirculatoire model. Tevens zou gekeken moeten worden naar de relatie tussen de hoge piekconcentraties die gemeten worden na een bolus toediening en de hemodynamische depressie die optreedt tijdens inductie. Een ander onderwerp voor verder onderzoek is de invloed van comedicatie, zoals premedicatie in de vorm van opiaten of benzodiazepines, op de dosis-concentratie-effect relatie van propofol tijdens de inductiefase. Overigens zou het includeren in het onderzoek van patiëntengroepen met een andere fysiologie op basis van leeftijd, gewicht of bijkomende ziekte, ook meer informatie geven over de toepasbaarheid van het recirculatoire model in deze populaties. Daarnaast blijft de noodzaak bestaan tot het ontwikkelen van een snel reagerende en beter voorspellende meetwaarde van het anesthetische effect op het brein, in snel wisselende fases van het bewustzijn. Door het met hoge frequentie meten van geneesmiddelen concentraties en effect kunnen nog andere fenomenen onthuld worden, welke weer andere vormen van modelleren noodzakelijk maken.

Curriculum Vitae

Marije Reekers was born on the 20th of July, 1971 in Oegstgeest. After completing secondary school, the Nijmeegse Scholengemeenschap, in 1989, she spent a year at high school in Maryland, USA. In 1990 the study of Biomedical Sciences was started at Leiden University, which from 1992 was combined with the study of Medicine. Research projects were performed at the department of Clinical Oncology, supervised by P. Schrier, and the department of Anesthesiology, supervised by F.H.M. Engbers, both at the Leiden University Medical Centre. She performed her graduation project at the department of Pharmacology at the Erasmus Medical Centre under supervision of dr. A. Maassen van den Brink and professor P.R. Saxena of the Erasmus University in Rotterdam, and professor M.D. Ferrari of the department of Neurology at the Leiden University Medical Centre. Graduation in Biomedical Sciences and Medicine was in 1996. After obtaining the medical degree in 1998, she was employed for two years as a clinical trial investigator and gynecological trial consultant, conducting phase II and III pharmaceutical trials. Clinical experience was gained as a resident at the department of Internal Medicine and Cardiology in the Groene Hart Hospital in Gouda. In 2001 she started a residency program under supervision of professor J.W. van Kleef, combined with a PhD program under supervision of professor A.G.L. Burm, dr. F. Boer and dr. J. Vuyk at the department of Anesthesiology at the Leiden University Medical Centre. After the sad passing of professor Burm, supervision was transferred to professor A. Dahan.

Following her registration as Anesthesiologist in 2009, she has been working as a staff member at the department of Anesthesiology at the Leiden University Medical Centre, chaired by professor L.P.H.J. Aarts.

Marije lives together with Paul J. Aleman and has a daughter Birgit and a son Floris.

List of Publications

MaassenVanDenBrink A, Reekers M, Bax WA, Ferrari MD, Saxena PR. Coronary side-effect potential of current and prospective antimigraine drugs. Circulation 1998;98:25-30.
www.ncbi.nlm.nih.gov/pubmed/9665056

MaassenVanDenBrink A, Reekers M, Bax WA, Saxena PR. Human isolated coronary artery contraction to sumatriptan characterised by the selective 5-HT1B/1D receptor antagonist GR55562. Pharmacol Toxicol 2000;86:287-90.
www.ncbi.nlm.nih.gov/pubmed/10895993

Reekers M, Boer F, Vuyk J. Basic concepts of recirculatory pharmacokinetic modelling. Adv Exp Med Biol 2003;523:19-26.
www.ncbi.nlm.nih.gov/pubmed/15088836

Simon MJ, Reekers M, Veering BT, Boer F, Burm AG, van Kleef JW, Vuyk J. Cardiovascular parameters and liver blood flow after infusion of a colloid solution and epidural administration of ropivacaine 0.75%: the influence of age and level of analgesia. Eur J Anaesthesiol 2009;26:166-74.
www.ncbi.nlm.nih.gov/pubmed/19142093

Reekers M, Simon MJ, Boer F, Mooren RA, van Kleef JW, Dahan A, Vuyk J. Cardiovascular monitoring by pulse dye densitometry or arterial indocyanine green dilution. Anesth Analg 2009;109:441-6.
www.ncbi.nlm.nih.gov/pubmed/19608815

Reekers M, Simon MJ, Boer F, Mooren RA, van Kleef JW, Dahan A, Vuyk J. Pulse dye densitometry and indocyanine green plasma disappearance in ASA physical status I-II patients. Anesth Analg 2010;110:466-72.
www.ncbi.nlm.nih.gov/pubmed/20081133

Reekers M, Boer F, Vuyk J. In response. Anesth Analg 2010;111:1076-1077.
DOI:10.1213/ANE.0b013e3181ef35e7

Weiss M, Reekers M, Vuyk J, Boer F. Circulatory model of vascular and interstitial distribution kinetics of rocuronium: a population analysis in patients. J Pharmacokinet Pharmacodyn 2011;38:165-78.
The original publication is available at www.springerlink.com
www.ncbi.nlm.nih.gov/pubmed/21125318